LBL-10096

Lawrence Berkeley Laboratory
UNIVERSITY OF CALIFORNIA

CHEMICAL BIODYNAMICS DIVISION

INTERACTION OF BENZO[a]PYRENE-7,8-DIHYDRODIOL-9,10-OXIDE WITH SIMIAN VIRUS 40 DNA AND CHROMATIN

Howard Byron Gamper, Jr.
(Ph.D. thesis)

November 1979

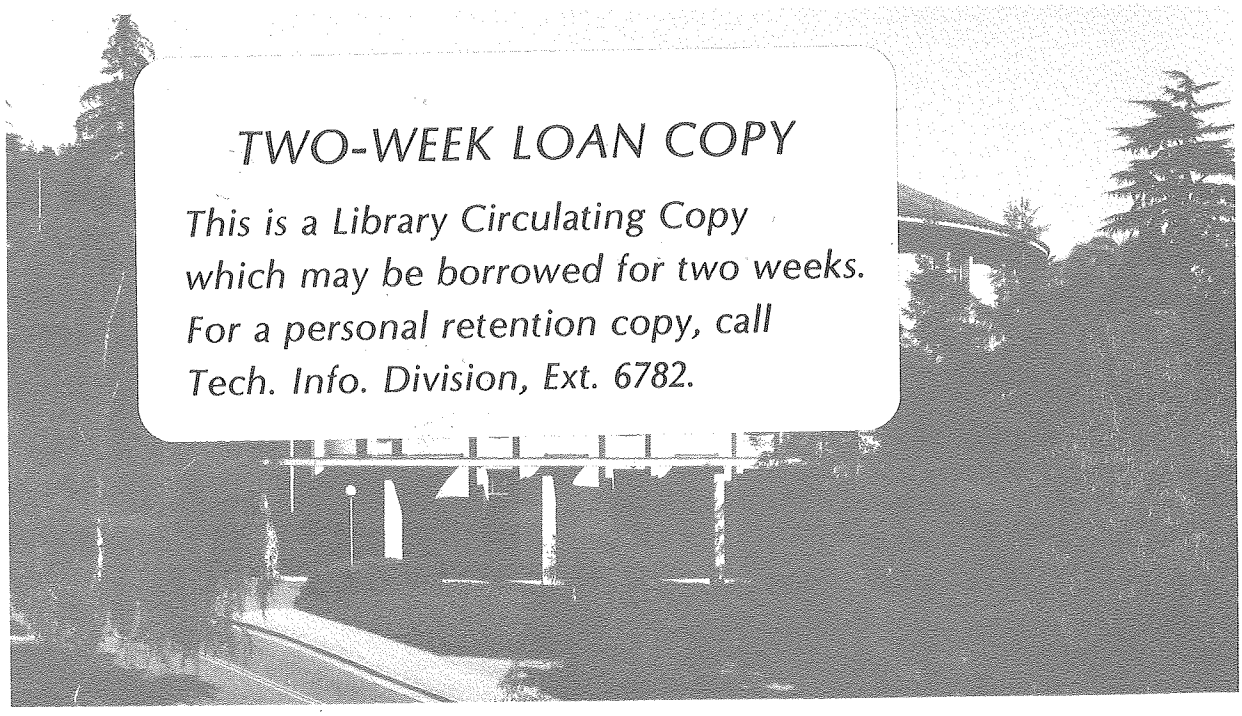

Prepared for the U.S. Department of Energy under Contract W-7405-ENG-48

DISCLAIMER

Interaction of Benzo[a]pyrene-7,8-dihydrodiol-9,10-Oxide
with Simian Virus 40 DNA and Chromatin

By

Howard Byron Gamper, Jr.

ABSTRACT

Benzo[a]pyrene (BaP) is a widespread environmental pollutant and a potent carcinogen. In mammalian cells it undergoes metabolic activation to the ultimate carcinogen benzo[a]pyrene-7,8-dihydrodiol-9,10-oxide (BaP diol epoxide). This metabolite is responsible for the majority of BaP-originated DNA and RNA alkylation events. The primary adduct present in both macromolecules consists of a linkage between the C-10 position of the hydrocarbon and the exocyclic amino group of guanine.

The work described in this thesis involved a study of the conformation of simian virus 40 (SV40) DNA and chromatin reacted in vitro with BaP diol epoxide. The topological constraints in superhelical SV40 DNA permitted a detailed study of BaP diol epoxide induced DNA strand scission and helix unwinding. The modulation of DNA alkylation and strand scission by histones and the effect of these phenomena on the integrity of the chromatin repeat unit structure was investigated using BaP diol epoxide modified SV40 minichromosomes.

Nicking of superhelical SV40 DNA was monitored by agarose gel electrophoresis or alkaline sucrose gradient centrifugation. Approximately 1% of the initial BaP diol epoxide alkylation sites rearranged with strand scission after 24 hr at 37^{o} and pH 8.0. Since the hydrocarbon N^{2} guanine adduct is not expected to nick the DNA backbone at neutrality, strand scission was due to one or more minor alkylation products.

The kinetics of nicking were characteristic of a multistep rearrangement terminating in strand scission. Alkaline catalysis of this process and recognition of the modified DNA by apurinic endonuclease were taken as evidence for a depurination strand scission mechanism. No evidence was obtained for nicking proceeding through a phosphotriester mechanism; thus BaP diol epoxide did not degrade TMV RNA and poly(dT) or form a reaction product with dibutyl phosphate.

The superhelical density of BaP diol epoxide modified superhelical and partially relaxed SV40 DNA was determined electrophoretically and an unwinding angle for the hydrocarbon guanine adduct was calculated. The angle was dependent upon the torsional strain of the molecule and ranged from 330^{o} to 30^{o}. This data indicated that the modified G-C base pair was disrupted and, in the presence of torsional strain, led to the further denaturation of up to 8 adjacent base pairs. In the absence of such strain the alkylation sites had an ordered structure with the hydrocarbon oriented in the minor or major groove of the helix.

Although BaP diol epoxide adducts were externally bound, the hydrocarbon appeared to intercalate prior to reaction with the exocyclic amino group of guanine. Thus, covalent binding was modulated by helix stability. Counterions inhibited alkylation by up to 90%, Mg^{2+} being 50 fold more effective than Na^{+}, and superhelical SV40 DNA was more susceptible to modification than partially relaxed viral DNA.

The alkylation of SV40 minichromosomes was also investigated. Low levels of modification (< 5 DNA adducts/minichromosome) did not alter the structure of these molecules. Relative to protein-free SV40 DNA, minichromosomal DNA was 1.5X less susceptible to alkylation but 2X more prone to strand scission. The alkylation of minichromosomal DNA, as

probed by staphylococcal nuclease, was random.

M. Calvin

DEDICATION

To my parents Howard and Pauline.

ACKNOWLEDGEMENTS

I express my deepest gratitude to the following individuals who have helped make this thesis a reality:

Dr. J. Bartholomew for invaluable support and guidance;

Prof. M. Calvin for many insightful and enthusiastic discussions;

My friends S. Platt, A. Tung, W. Vaughan, and T. Yamamoto for much appreciated scientific as well as personal interaction;

Colleagues at L. C. B. including J. Becker, T. Meehan, K. Straub, and H. Yokota for generous assistance and many stimulating conversations;

An excellent support staff including R. Ajemian, W. Erwin, B. Gordon, P. Hayes, B. Klingel, W. McAllister, M. Press, and M. Taylor whose expertise made research and publication easier.

Special thanks are extended to A. Tung for several creative suggestions which have emerged in this thesis, S. Platt for a conscientious and critical editing of the first draft, and C. Gamper for excellent typing of the dissertation.

This work was supported by the Department of Energy, Office of Health and Environmental Research, under contract # W-7405-ENG-48 and by the National Cancer Institute under contract # YO1-CP 50203.

TABLE OF CONTENTS

ABBREVIATIONS

AAAF	N-acetoxy-2-acetylaminofluorene
AES	automatic external standardization
AHH	aryl hydrocarbon hydroxylase
A-T	adenine-thymine
BaP	benzo[a]pyrene
BaP diol epoxide	(±) 7β,8α-dihydroxy-9α,10α-epoxy-7,8,9,10-tetrahydrobenzo[a]pyrene
BaP tetraol	7,8,9,10-tetrahydroxy-7,8,9,10-tetrahydrobenzo-[a]pyrene
C_i	curie
cpm	counts per minute
DMSO	dimethyl sulfoxide
DNA	deoxyribonucleic acid
DNase	deoxyribonuclease
dpm	disintegrations per minute
EDTA	ethylenedinitrilotetraacetic acid
E.U.	enzyme unit
G-C	guanine-cytosine
HPLC	high pressure liquid chromatography
MW	molecular weight
NADPH	nicotinamide adenine dinucleotide phosphate (reduced)
PAH	polycyclic aromatic hydrocarbon
PFU	plaque forming unit
RF	replicative form
RNA	ribonucleic acid

RNase	ribonuclease
rpm	revolutions per minute
SDS	sodium dodecyl sulfate
S_N1	substitution nucleophilic unimolecular
SV40	simian virus 40
TD	Tris-diluent; 0.137 M NaCl, 5 mM KCl, 5 mM Na_2HPO_4, 25 mM Tris-HCl, pH 7.5
TEMED	N,N,N',N'-tetramethylethylenediamine
TLC	thin layer chromatography
T_m	melting point
TMV	tobacco mosaic virus
Tris	tris(hydroxymethyl)aminomethane
uv	ultraviolet

Chapter 1: Introduction

Epidemiological studies indicate that 80% of human cancer originates from exposure to environmental agents (1). One such agent is the ubiquitous pollutant benzo[a]pyrene. Metabolic activation of this polycyclic aromatic hydrocarbon (PAH) generates the ultimate carcinogen benzo[a]pyrene-7,8-diol-9,10-oxide (BaP diol epoxide), a highly reactive electrophile which covalently binds to cellular macromolecules (2). The interaction of BaP diol epoxide with DNA is of particular interest, since a preponderance of evidence indicates that carcinogen modification of DNA initiates the transformation process (3-5). A prerequisite to understanding this process is a knowledge of the chemical as well as physical structure of the modified DNA. During the past three years several groups have elucidated the chemical structures of the major BaP diol epoxide-DNA adducts (6-17). An equally important consideration, which has intrigued me during this period, has been the microenvironment of the alkylation sites. Towards that end I have investigated the conformation of BaP diol epoxide modified simian virus 40 DNA (SV40 DNA). This small superhelical DNA is an ideal substrate for studying BaP diol epoxide induced DNA strand scission and helix unwinding. Furthermore, with the availability of a chromatin analog, i.e. the SV40 minichromosome, I have investigated the effect of nucleosome structure on the interaction of BaP diol epoxide with DNA.

The PAHs are widespread environmental pollutants which arise from the incomplete burning or pyrolysis of organic material (18). These

compounds are relatively unreactive and highly lipophilic. Yet several are strong carcinogens including BaP, dibenz[a,h]anthracene, 7,12-dimethylbenz[a]anthracene, and 3-methylcholanthrene. Early investigators noted that these and other carcinogenic hydrocarbons were planar, asymmetric, and limited in size to 4-6 fused rings, suggesting the existence of a cellular receptor of similar size and shape (19). Furthermore, a fundamental structural unit present in these hydrocarbons was the phenanthrene nucleus and, in particular, the meso-phenanthrenic or K-region double bond. Molecular orbital calculations showed this region to be relatively electron rich and nucleophilic.

Correlation of PAH carcinogenicity with empirical molecular orbital indices of K-region reactivity for a large number of PAHs generated considerable interest and led the Pullmans (20) to propose the K-region theory, which held that physical or covalent interaction of the K-region of PAHs with critical cellular receptors was involved in the initiation of carcinogenesis. During the past decade this theory has been discredited and replaced by the more general electrophilic reactant theory formulated by the Millers (21). Extensive research on the metabolism of a wide number of structurally diverse carcinogens led them to propose that highly reactive electrophiles are the active or ultimate forms of chemical carcinogens. These ultimate carcinogens are formed from the parent compounds through chemical decomposition or metabolic activation. Their covalent linkage to cellular macromolecules is a necessary, although not always sufficient, event in chemical carcinogenesis.

Most mammalian cells oxidize PAHs to more polar water soluble metabolites which can be excreted (22). In lieu of this metabolism the PAHs would accumulate within the cell and disrupt normal biochemical

functions. The overall detoxification sequence is depicted in Figure 1 for the weak carcinogen benz[a]anthracene. The initial oxidation is catalyzed by the relatively nonspecific, often highly inducible microsomal mixed function monooxygenase system, referred to here as aryl hydrocarbon hydroxylase (AHH). This enxyme complex is composed of the flavoprotein NADPH cytochrome P450 reductase and the terminal monooxygenase cytochrome P450 (or P448) embedded in a phospholipid matrix (23). Several isozymes of the cytochrome exist and in saturating CO they absorb maximally at 448 or 450 nm (24,25). The intact complex splits molecular oxygen forming water and oxene; the latter high energy oxygen adds to the hydrocarbon nucleus forming an epoxide. The location of the oxirane ring is determined by the PAH and by the cytochrome P450 isozyme. With methylated hydrocarbons oxene can also insert into the methyl group forming an alcohol. There are several modes by which the reactive hydrocarbon epoxides are detoxified within a cell. The more labile epoxides nonenzymatically rearrange to phenols or hydrolyze to dihydrodiols. Epoxide hydrase, a microsomal enzyme which partially copurifies with cytochrome P450, catalyzes the hydrolysis of epoxides to trans-dihydrodiols (26). Both the phenols and the dihydrodiols are conjugated to glucuronic acid or sulfate by cytoplasmic enzymes (27,28). Glutathione S-transferase catalyzes the nucleophilic addition of glutathione to the oxirane ring (29). Further enzymatic modification generates premercapturic acids which at low pH dehydrate to form mercapturic acids.

The oxidation of PAHs by AHH accomplishes their activation. Most hydrocarbon epoxides are highly reactive electrophiles which can covalently add to nucleophilic centers on DNA, RNA, and protein. Boyland (30) first proposed the existence of hydrocarbon epoxides as ultimate

Figure 1.

Generalized metabolic scheme for polycyclic aromatic hydrocarbons. AHH = aryl hydrocarbon hydroxylase, EH = epoxide hydrase, and Transferase = glutathione S-transferase.

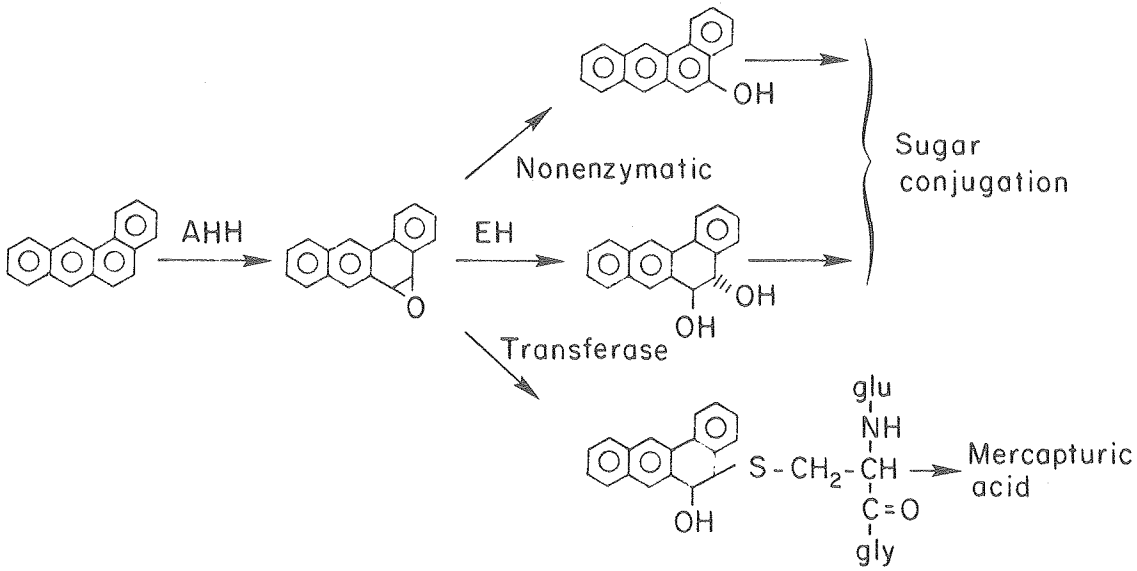
AHH
EH
Nonenzymatic
Transferase
OH
OH
OH
O
Sugar
conjugation
glu
NH
S-CH2-CH
C=O
gly
Mercapturic
acid

XBL798-4977

carcinogens nearly 30 years ago, but only recently has this proposal been conclusively demonstrated for two PAHs, BaP and benz[a]anthracene (31). The biological fate of a given epoxide is clearly dependent upon the relative balance of macromolecular alkylation versus detoxification.

The most intensively studied PAH is BaP. Over 1300 tons of this potent carcinogen are released into the atmosphere of the United States annually (32). It is found in cigarette smoke, automobile exhausts, and industrial emissions and is strongly suspect in the etiology of human lung and skin cancers (33). The liver, where systemic metabolism of this and other PAHs occurs, is refractile to BaP (34). Other tissues, however, possess AHH activity and an altered metabolic pattern may render them more susceptible to neoplastic transformation. The two-stage metabolic activation of BaP to BaP diol epoxide was elucidated by Borgen *et al.* (35) and Sims *et al.* (36) and is presented in Figure 2. The 7,8-dihydrodiol, formed by sequential action of AHH and epoxide hydrase on BaP, is stereoselectively oxidized by AHH at the 9,10 double bond to the (+) *anti* and (+) *syn* isomers of BaP diol epoxide (14,37).

BaP diol epoxide is a very biologically active xenobiotic. It is extremely cytotoxic (38) and highly mutagenic (39-43) as well as being carcinogenic (44-47). These properties are believed to arise from the ability of the epoxide to alkylate cellular macromolecules. *In vivo* (14) and in tissue culture (34) this particular metabolite is responsible for the majority of BaP-originated DNA and RNA alkylation events and for a minor fraction of the protein alkylation events. The extensive modification by BaP diol epoxide is understandable given that it is a poor substrate for epoxide hydrase (48) and possibly glutathione S-transferase (36) and that it has a sufficiently long half-life to

Figure 2.

Metabolic activation of benzo[a]pyrene. The formation of (+) anti-BaP diol epoxide is shown. The corresponding (+) syn isomer is formed from the (+) trans-7,8-diol.

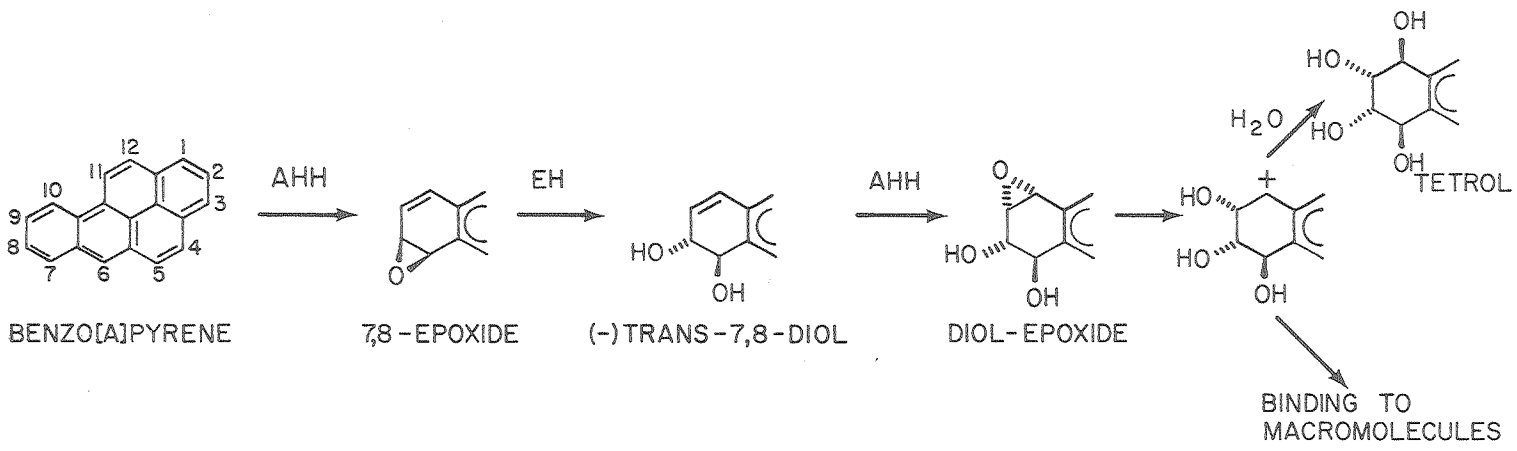

XBL 7712-6653

reach target macromolecules (49,50). The reported alkylation of DNA by the putative metabolite 9-hydroxybenzo[a]pyrene 4,5-oxide does not appear to be linked with the mutagenic or carcinogenic activity of BaP (51).

Positive correlation of tumorogenicity with the mutagenicity of a compound (4,5) or with the ability of that compound to covalently bind to DNA (3) supports the somatic mutation theory of cancer and implicates DNA as the target macromolecule in chemical carcinogenesis. This type of correlative reasoning has focused attention on the covalent binding of chemical carcinogens to DNA. Characterization of the adducts formed by BaP diol epoxide with DNA has proved to be very difficult due to the microgram quantities of alkylation products available for structural determination. The resolution and identification of these adducts has recently become possible with the development of high pressure liquid chromatography and fluorescence spectrophotometry. Recently published studies (6-8) indicate that BaP diol epoxide preferentially alkylates the exocyclic amino groups of deoxyguanosine (92% of stable adducts), deoxyadenosine (5%), and probably deoxycytidine ($\leq$3%). In each case covalent linkage to the hydrocarbon was at the C-10 position. No reaction was observed with deoxythymidine. A minor adduct appears to be formed with the N-7 position of deoxyguanosine (16,17), and indirect evidence obtained with poly(G) suggests that BaP diol epoxide forms a labile phosphotriester with DNA phosphate (12).

These modifications reduce the template activity of DNA (52-56) and induce mutagenesis and possibly carcinogenesis. If the latter phenomena are to be fully understood at the molecular level, the microenvironment of DNA at the sites of alkylation must be elucidated. This thesis de-

scribes the physical structure of SV40 DNA and chromatin modified *in vitro* with the (±) *anti* isomer of BaP diol epoxide. SV40 is a small oncogenic eucaryotic virus (57). Its DNA or chromatin can be conveniently extracted from lytically infected monkey cells (58,59). The superhelical genome contains 5200 base pairs which have recently been sequenced (60,61). The unique topological constraints characteristic of a covalently closed circular DNA have been utilized to study DNA strand scission induced by one or more minor BaP diol epoxide adducts and DNA helix unwinding associated with the major deoxyguanosine adduct. The effect of nucleosomal structure on DNA alkylation and strand scission has been probed using the SV40 minichromosome, a chromatin-like structure in which the viral DNA is complexed with cellular histones (62). The results presented here provide a firm base on which to further study the functional properties of BaP diol epoxide modified SV40 DNA and chromatin.

Chapter 2: Materials and Methods

Cells and Virus Stocks. TC-7 line African green monkey kidney cells, obtained from J. Robb of the University of California at San Diego, were grown at 37^{o} in a CO_2 incubator on 100 X 20 mm tissue culture dishes (Falcon Plastics). The dishes contained Eagle's medium as modified by Dulbecco (Gibco) with 10% calf serum (Flow Laboratories). Wild type SV40 small plaque strain Rh911 was a generous gift from R. Su of the Harvard Medical School. Confluent TC-7 cells were infected with SV40 at 10-20 plaque forming units (PFU)/cell. Large scale infections were carried out in Corning 490 cm^2 tissue culture roller flasks. The DNA was labeled by adding 1 mC_i of [^{32}P]-orthophosphate (ICN, Irvine, CA.), 200 μC_i of [^{14}C]-thymidine (New England Nuclear), or 200 μC_i of [^{3}H]-thymidine (New England Nuclear) to 10^7 cells 18 hr after infection. At the peak of SV40 replication, 42 hr after infection, viral DNA or chromatin was extracted from 10^8 cells.

Isolation of SV40 DNA. SV40 DNA was isolated from infected cells by a modification of the Hirt extraction (58). Approximately 10^8 cells (10 roller flasks) were washed with cold Tris-diluent (TD; 0.137 M NaCl-5 mM KCl-5 mM Na_2HPO_4-25 mM Trizma base [Sigma], pH 7.5) 42 hr postinfection and then gently suspended in 40 ml of 25 mM Tris-HCl (pH 7.5)-10 mM EDTA-0.6% sodium dodecyl sulfate (SDS; Sigma). After incubating the lysate 20 min at 37^{o}, it was made 1M in NaCl and stored overnight at 4^{o}. Cellular DNA was pelleted by centrifugation (Beckman JA-20 rotor, 15,000 rpm, 30 min, 4^{o}), and the supernatant, which contained

viral DNA, was subjected to 2 counter current extractions with Tris-buffered (10 mM Tris-HCl, pH 7.9-1 mM EDTA) phenol (Bethesda Research) to remove protein. The pooled aqueous phases were mixed with 2 volumes of NaCl-saturated ethanol and stored overnight at -20°. Viral DNA was collected by centrifugation (Beckman JA-14 rotor, 10,000 rpm, 60 min, 4°). The DNA pellet was dissolved in 10 ml of 20 mM Tris-HCl (pH 8.0) buffer containing 0.5 mM EDTA, 1.56 g/ml CsCl (Calbiochem), and 200 µg/ml ethidium bromide (Calbiochem). That solution was centrifuged for 48 hr in a Beckman SW 50.1 rotor at 35,000 rpm and 4°. The gradients were illuminated with uv light to visualize the DNA bands. The lower form I band was collected from the bottom of the tubes, extracted 4 times with NaCl-saturated butanol to remove ethidium bromide, and dialyzed overnight against 20 mM Tris-HCl (pH 8.0)-0.5 mM EDTA. DNA concentrations were determined using a cuvette with a 1 cm path length and assuming 50 µg/ml per 1.0 optical density unit at 257 nm (63). The DNA stocks were kept up to 1 year during which time there was a gradual increase in the amount of contaminating form II DNA.

Isolation of SV40 Chromatin. The procedure used here is similar to published methods (59,64-67) and was developed in this laboratory by H. Yokota. Approximately 10^8 cells were rinsed with cold TD and then scraped into the same buffer 42 hr postinfection. A loose cellular pellet was obtained by centrifuging the cell suspension (JA-20 rotor, 2 min, 2,000 rpm, 4°). The pellet was resuspended in 5.0 ml of cold TD and gently mixed with 80 ml of cell lysis buffer (50 mM Tris-HCl, pH 7.5-5 mM $MgCl_2$-25 mM KCl-0.25 M sucrose [Schwarz/Mann; RNase free]-0.5% Nonidet P-40 detergent [Shell Oil Ltd., London]). No intact cells were detectable microscopically after several minutes at 4°. Nuclei were

pelleted by contrifugation (JA-20 rotor, 5 min, 2,000 rpm, 4^{o}). The pellet was suspended in 2.0 ml of nuclei lysis buffer (10 mM Tris-HCl, pH 8.1-10 mM EDTA-0.13 M NaCl-0.5 mM dithiothreitol [Bio-Rad]-1.0 mM phenylmethylsulfonyl fluoride [Sigma]-0.25% Triton X-100 [Rohm & Haas]) and gently shaken 1-3 hr at 4^{o} to maximize extraction of minichromosomes. Cellular chromatin was removed by centrifugation (JA-20 rotor, 5 min, 8,000 rpm, 4^{o}). The supernatant, which contained viral chromatin, was layered onto two 5-40% sucrose gradients in 10 mM Tris-HCl (pH 7.8)-1 mM EDTA-0.13 M NaCl and centrifuged in a Beckman SW 27 rotor for 5 hr at 25,000 rpm and 4^{o}. The gradients were collected from the tube bottom in 1.0 ml fractions. These were characterized as to absorption and radioactivity and analyzed by gel electrophoresis. DNA and protein concentrations were estimated from the optical density values at 260 nm and 280 nm using a nomograph (68). Fractions containing SV40 minichromosomes were pooled and used within 72 hr.

Benzo[a]pyrene Derivatives. Crystalline ($\pm$)-7β,8α-dihydroxy-9α, 10α-epoxy-7,8,9,10-tetrahydrobenzo[a]pyrene (BaP diol epoxide) was synthesized by K. Straub of this laboratory essentially using the method of McCaustland and Engel (69). [^{3}H]-BaP diol epoxide, 1.5 mg/ml in 19:1 tetrahydrofuran-triethylamine, was also synthesized by K. Straub according to published procedures (70). It had a specific activity of 1.23 C_i/mmole. [^{14}C]-BaP diol epoxide, 0.33 mg/ml in 19:1 tetrahydrofuran-triethylamine, was obtained from Midwest Research Institute under auspices of the National Cancer Institute and had a specific activity of 28.2 mC_i/mmole. The BaP diol epoxide stocks were stored at -70^{o} and dilutions were made with dimethyl sulfoxide (DMSO; Eastman Kodak). Hydrolysis of BaP diol epoxide to 7,8,9,10-tetrahydroxy-7,8,9,10-tetrahy-

drobenzo[a]pyrene (BaP tetraol) was effected by storing it overnight at 37^{o} in DMSO containing 10% 0.12 M HCl.

The concentration and specific activity of the labeled diol epoxides were determined as follows: Samples were hydrolyzed in 1:1 water-dioxane (Matheson Coleman & Bell; spectroquality) containing 0.12 M HCl. The absorption spectra of the tetraol solutions were obtained; the radioactivity of the solutions was determined by liquid-scintillation counting (Aquasol-2, New England Nuclear). BaP tetraol derived from crystalline BaP diol epoxide was used as a concentration standard. Standard curves of automatic external standardization values (AES) versus % efficiency were used to convert cpm to dpm.

Electron Microscopy. Viral DNA was spread using a modification (71) of the Kleinschmidt procedure (72). The DNA concentration of the hyperphase was 0.5-3.0 µg/ml in 50 µl of formamide (Matheson Coleman & Bell), 5 µl of 10X EM buffer (1 M Tris-HCl, pH 8.5-0.1 M EDTA; filtered through a 0.22 µ Millipore HAWP filter), 45 µl of 20 mM Tris-HCl (pH 8.0)-0.5 mM EDTA, and 5 µl of 1 mg/ml cytochrome C (Sigma; beef heart, type IV) in 1 mM ammonium acetate. The hyperphase (50 µl aliquot) was delivered down a Pt slide onto the hypophase (25 ml of formamide, 1.5 ml of 10X EM buffer, and 123.5 ml of double distilled H_2O) and allowed 2 min to form a monolayer. The DNA was adsorbed onto Pelco #3HGC300 or #3HGC400 copper grids covered with parlodion film (Mallinckrodt), stained 15 sec in 90% ethanol containing 0.05 mM uranyl acetate (Mallinckrodt) and 0.05 M HCl, rinsed 10 sec in 90% ethanol, and air dried. Grids were rotary shadowed with 80% Pt-20% Pd (Ted Pella Co., Tustin, CA., #24 wire) and microscopy was carried out on a Zeiss EM-952 electron microscope.

Gel Electrophoresis. Vertical slab gel electrophoresis was conducted in an apparatus constructed according to the design of Studier (73). Agarose, polyacrylamide, and composite agarose-polyacrylamide gels were utilized. The gel was formed directly in the apparatus between two glass plates separated on the sides by plexiglass spacers and sealed at the bottom with a 1.4% agarose plug. The sample wells were formed by inserting a plexiglass comb into the top of the gel solution prior to cooling or polymerization. Gel dimensions were 13.3 X 13.0 X 0.3-0.5 cm. Current was supplied by a Bio-Rad model 400 power supply operating in the constant voltage mode. The pH of the gel was kept constant by circulating buffer between the two electrode reservoirs with a peristaltic pump. This was particularly important when the running buffer had a low buffering capacity or when the time of electrophoresis was extended. Fan cooling was employed when necessary to maintain the gel at room temperature.

Each gel could accomodate up to 12 samples. Electrophoretic analysis typically required 0.1-2.5 μg of SV40 DNA, 1.5-3.0 μg of SV40 chromatin, 25-75 μg of DNA homopolymer (all 4 were obtained from Miles Laboratories), or 2.6 μg of TMV RNA (obtained from B. Singer of the University of California at Berkeley) in 10-120 μl. The samples were mixed with 10 μl of weighting solution (20 mM Tris-HCl, pH 8.0-0.5 mM EDTA-25% sucrose-5% SDS-0.025% bromphenol blue [Bio-Rad]) before loading onto the gel. Chromatin samples and certain DNA samples electrophoresed for a short time (where the SDS band might interfere with detection of the DNA) were mixed with weighting solution minus SDS. Poly(dA)·poly(dT) and poly(dG) were electrophoresed in formamide. Prior to gel loading these samples were lyophilized, dissolved in formamide-2% 1 M NaCl, and

mixed with 20 µl of formamide weighting solution (formamide-2% 1 M NaCl-20% sucrose-0.005% bromphenol blue).

Agarose gels were formed by refluxing agarose (Bio-Rad) in electrophoresis buffer with magnetic stirring on a hot plate. After clarification the solution was poured into an electrophoresis apparatus and allowed to cool. SV40 DNA forms I, II, and III were electrophoresed at 50 V for 12 hr on 1.4% agarose gels prepared and run in 40 mM Tris-HCl (pH 7.9)-5 mM sodium acetate-1 mM EDTA. Partially relaxed covalently closed SV40 DNA was run in the same system for 16 hr and Col E1 DNA (obtained from J. Hearst of the University of California at Berkeley) for 18 hr. SV40 minichromosomes aggregate in the above buffer and so were electrophoresed 6 hr at 50 V on 1% agarose gels prepared in 10 mM Tris-HCl (pH 7.8)-2 mM EDTA (66). Disc gel electrophoresis of SV40 DNA was performed in a Hoefer model EF301 apparatus. Samples were electrophoresed on 0.5 X 11.5 cm 1.4% agarose gels for 400 min at 75 V.

Several substrates were analyzed on 2% polyacrylamide-0.5% agarose gels. The gel solution was prepared by mixing 2.37 g of acrylamide (Bio-Rad), 125 mg of N,N'-methylene-bis-acrylamide (Bio-Rad), 17 µl of N,N,N',N'-tetramethylethylenediamine (TEMED; Bio-Rad), 81 ml of distilled H_2O, 12.5 ml of 10X electrophoresis buffer, and 31.2 ml of hot 2% agarose (in H_2O) in a 250 ml suction flask. The buffer for superhelical SV40 DNA was 36 mM Tris-30 mM NaH_2PO_4 (pH 7.7)-1 mM EDTA (74); 89 mM Tris-89 mM boric acid (pH 8.3)-2.8 mM EDTA was used for all other substrates (75). After 5 min of degassing, 0.42 ml of 16% ammonium persulfate (Bio-Rad) was added to initiate polymerization. The solution was immediately poured into an electrophoresis apparatus which was kept under nitrogen at 37^{o} for 30 min. The gel was allowed to cool to room

temperature and prerun at least 30 min prior to loading. Substrates electrophoresed in this gel system were the Hind III SV40 restriction fragments (3 hr at 100 V), TMV RNA (4 hr at 150 V), poly(dA) (1.5 hr at 150 V), poly(dT) (3 hr at 150 V), and poly(dC) (2.5 hr at 150 V). Form I SV40 DNA was resolved into component superhelical bands by electrophoresis on a 22 cm long slab gel for 72 hr at 100 V with air cooling.

Polyacrylamide gels were prepared in Tris-borate buffer at room temperature as basically outlined in the preceding paragraph. Staphylococcal nuclease DNA digests were electrophoresed 2 hr at 150 V on 6% polyacrylamide gels containing 5.85% acrylamide and 0.15% N,N'-methylene-bis-acrylamide. Denaturing polyacrylamide gels were prepared and run in formamide as described by Staynov et al. (76). For a 4% gel 2.05 g of acrylamide, 0.35 g of N,N'-methylene-bis-acrylamide, and 120 µl of TEMED were dissolved in 60 ml of formamide. After addition of 1.2 ml of 1 M NaCl-6% ammonium persulfate (no degassing was required) the solution was poured into a gel apparatus, allowed to set overnight, and prerun at least 30 min in formamide-2% 1 M NaCl. Poly(dA)·poly(dT) and poly(dG) were electrophoresed 5 hr at 150 V in denaturing 4% and 8% polyacrylamide gels, respectively.

Gels containing SV40 DNA or chromatin were stained for at least 1 hr at 4^{o} in electrophoresis buffer containing 0.5 µg/ml ethidium bromide. The fluorescent DNA bands were illuminated from below or from the side with short wavelength uv (Ultra Violet Products, Inc., San Gabriel, CA.) and photographed on Polaroid type 665 positive/negative film through a Corning 3-69 filter. Tracings were obtained with a Schoeffel model SD3000 spectrodensitometer. Gels were scanned directly in the reflectance mode exciting at 310 nm and monitoring emission at a

45^{o} angle through a Corning 3-69 filter. Negatives were scanned in the transmission mode at 590 or 660 nm. Peak areas were determined using a "ball and disc" integrator (Disc Instruments, Inc., Costa Mesa, CA.) or by the cutting and weighing method.

For determination of radioactivity DNA bands were excised under uv illumination, dried overnight at 37^{o} on adsorbent pads, and then combusted in a Packard automatic combustion apparatus. $^{3}H_2O$ was counted in 15 ml of Monophase-40 (Packard) and $^{14}CO_2$ was counted in 9 ml of Carbo-sorb (Packard) plus 12 ml of Permafluor V (Packard). ^{32}P-labeled bands were solubilized for counting. Agarose gel slices were dissolved in 1.0 ml of H_2O at 100^{o}. Gel slices containing polyacrylamide were degraded in 1.0 ml of 30% H_2O_2 (Mallinckrodt) at 55^{o}. Excess H_2O_2 was destroyed by adding 200 µl of 1 M NaOH and incubating an additional 2 hr at 55^{o}. Chemiluminescence was minimized by acidifying with 1 drop of concentrated HCl. Solubilized gel solutions were mixed with 4.0 ml of Aquasol-2 and counted. For autoradiography, gels containing ^{32}P-labeled DNA were dried on filter paper in a Hoefer model SE540 slab gel dryer and exposed for 60 hr to Kodak SB-5 X-ray film.

TMV RNA gels were stained for 15 min in running buffer containing 30 µg/ml acridine orange (Calbiochem) and then destained with running buffer in an enameled pan (77). (Enamel adsorbs acridine orange.) The fluorescent bands were illuminated from the side with long wavelength uv and photographed on Polaroid type 108 color film through a Corning 3-69 filter. The DNA homopolymer gels were stained 1 hr in a 1:1 solution of 0.4 M sodium acetate-0.4 M acetic acid (pH 4.7) containing 0.2% toluidine blue O (Matheson Coleman & Bell) and destained in 10% acetic acid. The gels were illuminated from below with white light and photo-

graphed on Polaroid type 665 positive/negative film through a yellow filter. The negatives were traced as previously described.

Ultracentrifugation. The centrifugations described in this section were carried out in a Beckman SW 50.1 rotor in 0.5" X 2" cellulose nitrate tubes. ^{14}C-labeled SV40 DNA was analyzed by alkaline sucrose density gradient centrifugation. Viral DNA (0.38 μg in 50 or 100 μl) was layered on 5.0 ml 5-20% sucrose gradients prepared in 0.7 M NaCl-0.3 M NaOH-2.5 mM EDTA and centrifuged for 90 min at 50,000 rpm and 20°. The gradients were immediately fractionated from the bottom by taking 7 drop aliquots into 1.0 ml of 0.12 M HCl. The aliquots were counted for 2 min each in 4.0 ml of Aquasol-2. Two peaks corresponding to form I DNA and forms II + III DNA were present in the radioactivity profiles. The % form I DNA was readily determined from the peak areas.

^{3}H-labeled SV40 chromatin was analyzed by neutral sucrose density gradient centrifugation. The viral chromatin (1-3 μg in 100 μl) was layered on 5.0 ml 5-30% sucrose gradients prepared in 20 mM Tris-HCl (pH 8.0)-0.5 mM EDTA-0.13 M NaCl and centrifuged for 90 min at 50,000 rpm and 4°. The gradients were fractionated and counted as described above. Acidification of the gradient aliquots to prevent chemiluminescence was unnecessary. The sedimentation coefficient of chromatin was determined relative to form I SV40 DNA run on a separate gradient. For determination of the minichromosomal sedimentation coefficient at low ionic strength, viral chromatin was centrifuged in a sucrose gradient without 0.13 M NaCl.

The buoyant density of ^{3}H-labeled SV40 chromatin was determined by equilibrium centrifugation in 20 mM Tris-HCl (pH 8.0)-0.5 mM EDTA-0.13

M NaCl containing 0.73 g/ml CsCl. The chromatin (ca. 4.5 µg in 2 ml of Tris-HCl buffer) was fixed at 4^{o} by adding 200 µl of 10% formaldehyde (Mallinckrodt) and, 15 min later, 200 µl of 8% glutaraldehyde (Polysciences, Inc., Warrington, PA.) (78). After 30 min fixation the minichromosomes were dialyzed overnight, mixed with CsCl, and centrifuged for 48 hr at 35,000 rpm and 4^{o}. The gradient was collected from the bottom in 8 drop fractions. The refractive index was determined on 20 µl aliquots, after which the fractions were counted in 1.0 ml of H_2O and 4.0 ml of Aquasol-2. Refractive index values were converted to buoyant densities using an experimentally determined standard curve. Gradients spanned 1.34-1.62 g/ml.

Nitrocellulose Filter Retention Assay. BaP diol epoxide modified [^{14}C]-SV40 form I DNA (0.4-0.8 µg in 100 µl) was diluted with 5.0 ml of 50 mM Tris-HCl (pH 8.2)-1 M NaCl and filtered through a Schleicher & Schuell type B-6 0.45 µ pore size filter at a flow rate of 2.5 ml/min. The filter was washed with 5.0 ml of 0.03 M sodium citrate-0.3 M NaCl, dried at least 5 min under a heat lamp, and counted in Permafluor I (Packard). DNA containing approximately 1 adduct/10^{2} base pairs was stably retained on the filter. Total DNA in a sample was determined as basically described by Kuhnlein et al. (79). Prior to filtration the sample was mixed with 200 µl of 0.3 M $K_2HPO_4 \cdot KOH$ (pH 13.2), incubated 7 min at 30^{o}, and neutralized with 100 µl of 1 M $KH_2PO_4 \cdot HCl$ (pH 4.0). The high pH irreversibly denatured both superhelical and nicked circular DNA, which were retained on the filter. When nicked circular DNA was selectively denatured by substituting 0.3 M $K_2HPO_4 \cdot KOH$ (pH 12.3) in the 7 min incubation, only a slight enhancement of DNA filter binding was observed for the alkylated samples.

The kinetics of strand scission at apurinic sites was monitored using the filter retention assay. Apurinic DNA was prepared by incubating [^{14}C]-SV40 form I DNA (8.4 μg in 50 μl) with 150 μl of 50 mM sodium citrate-20 mM Tris-HCl (pH 3.5)-0.5 mM EDTA at 50° for 12.5 min (80). The solution was diluted 10X with 20 mM Tris-HCl (pH 8.0)-0.5 mM EDTA and kept at 37°. To monitor strand scission, aliquots (100 μl) were taken with time, pretreated with 200 μl of 0.3 M $K_2HPO_4 \cdot KOH$ (pH 12.3) as described above, and filtered. Hydrolysis of apurinic sites during this pretreatment was negligible (81). The total number of apurinic sites was determined by incubating an aliquot in 200 μl of 0.3 M $K_2HPO_4 \cdot KOH$ (pH 12.3) for 120 min at 30° prior to filtration. Under these conditions apurinic sites were quantitatively cleaved (79).

BaP Diol Epoxide Alkylation. SV40 form I DNA (ca. 0.1-2.5 μg in 50-250 μl) was modified with BaP diol epoxide or BaP tetraol in 20 mM Tris-HCl (pH 8.0)-0.5 mM EDTA-5-10% DMSO unless otherwise specified. Reaction mixtures were incubated in the dark at 37° for 2-48 hr. Aliquots were analyzed for strand scission either directly after reaction or following ethyl acetate extraction by gel electrophoresis, electron microscopy or ultracentrifugation. Alkylation was quantitated by radioactivity counting using [^{14}C]-SV40 DNA and [^{3}H]-BaP diol epoxide. The modified DNA was diluted to 1.0 ml with 20 mM Tris-HCl (pH 8.0)-0.5 mM EDTA-0.5 M NaCl and extracted 3 times with 1.0 ml of ethyl acetate. After adding 30 μg of carrier calf thymus DNA (Sigma), the DNA was precipitated from the aqueous phase by addition of 2.0 ml of NaCl-saturated ethanol and by storage overnight at -20°. The DNA was pelleted (Beckman 0.5" X 2" polyallomer tubes in a SW 50.1 rotor, 10,000 rpm, 4°, 30 min), washed, and resuspended in 1.0 ml of NaCl-saturated 70% ethanol. It

was then collected on a Millipore 0.45 μ HAWP filter, combusted and counted. Standard curves of AES values versus % efficiency were used to convert cpm to dpm. Binding data was calculated assuming SV40 DNA contained 5200 base pairs (61) and had a MW of 3.6×10^6 daltons (57). The adduct profile was determined as described elsewhere (7). After extraction and ethanol precipitation, the modified DNA was enzymatically hydrolyzed with DNase II, spleen phosphodiesterase, and alkaline phosphatase (Sigma). The modified nucleosides were isolated by Sephadex LH-20 chromatography and further resolved by high pressure liquid chromatography (HPLC). Radioactive peaks were identified by coelution with standards.

SV40 chromatin (ca. 10-25 μg/ml) was reacted with BaP diol epoxide in the sucrose gradient isolation buffer (5-40% sucrose in 10 mM Tris-HCl, pH 7.8-1 mM EDTA-0.13 M NaCl) or after dialysis into 20 mM Tris-HCl (pH 8.0)-0.5 mM EDTA with or without 0.13 M NaCl. Reaction aliquots were analyzed directly as chromatin or were deproteinized and analyzed as DNA. The chromatin was deproteinized by incubation with 0.85 mg pronase (Calbiochem; B grade, nuclease free)/ml solution for 3 hr at 37° followed by 2 equal volume extractions with chloroform-phenol-isoamyl alcohol (24:25:1). The phases were clarified by centrifugation at 2,000 rpm for 5 min and the precipitated protein was discarded. Alkylation of ^{32}P or ^{14}C labeled minichromosomal DNA was determined after deproteinization, ethyl acetate extraction, and ethanol precipitation as described above. For quantification of binding the minichromosomes were incubated 30 min at 37° with 90 ng RNase (Calbiochem; A grade, 5X crystallized)/ml solution immediately after alkylation.

TMV RNA (2.6 µg in 50 µl) was reacted for 3-15 hr at 37° with BaP diol epoxide in 20 mM Tris-HCl (pH 8.0)-0.5 mM EDTA-10% DMSO. The RNA was electrophoresed immediately after reaction or following 2 extractions with 50 µl of ethyl acetate. The DNA homopolymers (25-75 µg in 100-200 µl) were reacted for 24 hr at 37° with BaP diol epoxide or BaP tetraol (molar reaction ratio = 4.0) in 20 mM Tris-HCl (pH 8.0)-10-20% DMSO. Prior to electrophoresis the reaction mixtures were extracted twice with ethyl acetate. Poly(dA)·poly(dT), which was similarly modified, was prepared from equal amounts of the two homopolymers mixed together at 60° and slowly cooled to room temperature.

Preparative reaction of 59.9 mg of [^{32}P]-dibutyl phosphate with 39.1 mg of BaP diol epoxide (molar reaction ratio = 0.46) was carried out in 40 ml of acetone-H_2O (1:1; pH 7.5) for 24 hr at 37°. The reaction products were rotary evaporated, taken up in a small volume of H_2O, and loaded onto a Sephadex LH-20 column. The column was washed with 0.03 M bicarbonate (pH 8.3) and eluted with a 0-50% ethanol log gradient in the same buffer. Fractions (15 ml) were analyzed for ^{32}P label and for absorption at 254 nm.

Small scale reaction of 275 µg of [^{32}P]-dibutyl phosphate with 2 mg of BaP diol epoxide or BaP tetraol (molar reaction = 5.0) was carried out in 20 mM Tris-HCl, pH 7.4-DMSO (1:1) for 24 hr at 37°. The reaction mixtures were analyzed by thin layer chromatography (TLC) before and after heating at 85° for 15 min. Reaction aliquots were diluted with cold carrier monobutyl phosphate and dibutyl phosphate and spotted on an Eastman Kodak #6065 TLC plate. The plate was developed 4 hr in isopropanol-NH_4OH-H_2O (7:2:1), dried, and sprayed with a phosphate visualizing reagent (0.10 M ammonium molybdate-concentrated HCl-

12 N $HClO_4$-acetone; 8:3:3:86) (82). The phosphate spots were excised, scrapped into scintillation vials, and counted in H_2O-Aquasol-2 (1:3). A [^{32}P]-dibutyl phosphate control was similarly incubated, chromatographed, and counted.

Enzymatic Reactions: Apurinic Endonuclease (purified from Hela cells by C. Falce of the University of California at Berkeley): SV40 DNA (0.57 µg in 50 µl) was incubated 10 min at 37^{o} with 45 µl of assay solution (44 mM Tris-HCl, pH 7.5-22 mM $MgCl_2$-0.011% Triton X-100) and 5 µl of apurinic endonuclease stock (1 E.U./ml). The reaction was terminated by cooling to 4^{o} and adding 10 µl of 0.2 M EDTA. Superhelical DNA Relaxing Enzyme (Bethesda Research): Partially relaxed SV40 DNA standards were prepared by incubating 1-2 µg of form I DNA with 5-20 E.U. relaxing enzyme in 20 mM Tris-HCl (pH 8.0)-0.5 mM EDTA-2.5 mM $MgCl_2$ for 5-20 min at 37^{o}. The DNA was stored at 4^{o} in the presence of 0.02 M EDTA. Preparative relaxation of 18.8 µg of SV40 form I DNA was conducted in 940 µl of the above buffer containing 140 E.U. relaxing enzyme for 15 min at 37^{o}. After stopping the reaction with 50 µl of 0.2 M EDTA, the DNA was ethanol precipitated and dissolved in 20 mM Tris-HCl (pH 8.0)-0.5 mM EDTA prior to reaction with BaP diol epoxide. Restriction Endonucleases (Miles Laboratories): SV40 DNA (2.5 µg in 100 µl) was digested to completion with 10 E.U. Hind III in 20 mM Tris-HCl (pH 7.9)-0.5 mM EDTA-7 mM $MgCl_2$-60 mM NaCl at 37^{o} for 10-12 hr. Similar reaction conditions were employed for Hind II digestion of ϕX174 RF DNA (Bethesda Research) and Eco RI digestion of SV40 DNA. Restriction was terminated by addition of the SDS-containing electrophoretic weighting solution. Staphylococcal Nuclease (Worthington Biochemical): SV40 chromatin or DNA was digested with 1-10 E.U. staphylococcal nu-

clease/μg viral DNA at 37^{o} in 10-20 mM Tris-HCl (pH 7.8-8.0)-0.5-1.0 mM EDTA-3.0 mM $CaCl_2$-3.0 mM $MgCl_2$. Most incubations also included 0.13 M NaCl and 20-30% sucrose. Nuclease activity was abolished by raising the EDTA concentration to 18 mM.

Chapter 3: DNA Strand Scission

Nicking of SV40 DNA by BaP Diol Epoxide. A question of initial interest to me was the effect of BaP diol epoxide on the integrity of the DNA phosphodiester backbone. Covalently closed superhelical DNA, such as the SV40 genome, is a sensitive probe for detecting single strand scissions and double strand breaks. Cleavage of any one of the 10,400 phosphodiester linkages in SV40 DNA converts the superhelical form I DNA to nicked circular form II DNA. Introduction of another nick within 15 base pairs of the first but on the opposite strand or introduction of a double strand break generates linear form III DNA (83). All three forms are conveniently resolved by agarose gel electrophoresis.

Superhelical SV40 DNA was allowed to react 24 hr with a concentration series of BaP diol epoxide. By doing the reactions in vitro cleavage of the modified DNA by nucleolytic enzymes was excluded. The reaction mixtures were analyzed for strand scission by agarose gel electrophoresis (Figure 3). Track a contained a partial Eco RI digest of SV40 DNA consisting of DNA forms I, II, and III. Track b contained unreacted form I DNA with a small amount of nicked circular DNA present as an impurity. Tracks c through n contained the same DNA reacted with BaP diol epoxide at increasing molar reaction ratios ranging from 5×10^{-4} to 5.0. Throughout this thesis the molar reaction ratio refers to the molar ratio of hydrocarbon (BaP diol epoxide or BaP tetraol) to DNA mononucleotide in a reaction mixture. The gel clearly demonstrates that at low molar reaction ratios BaP diol epoxide nicked the DNA while at high ratios it

Figure 3.

Agarose slab gel of superhelical SV40 DNA reacted with BaP diol epoxide. Form I SV40 DNA (1.9 μg in 50 μl of 20 mM Tris-HCl, pH 8.0-0.5 mM EDTA-5% DMSO) was incubated at 37^{o} with BaP diol epoxide at hydrocarbon to DNA mononucleotide ratios of (b) 0, (c) 0.097, (d) 0.130, (e) 0.162, (f) 0.194, (g) 0.227, (h) 0.259, (i) 0.292, (j) 0.324, (k) 0.388, (l) 0.647, (m) 1.30, and (n) 3.24. After 24 hr the reaction mixtures were extracted with ethyl acetate and electrophoresed at 50 V for 12 hr on a 1.4% agarose gel. The direction of electrophoresis was downward. A partial Eco RI digest of SV40 DNA was run in track a.

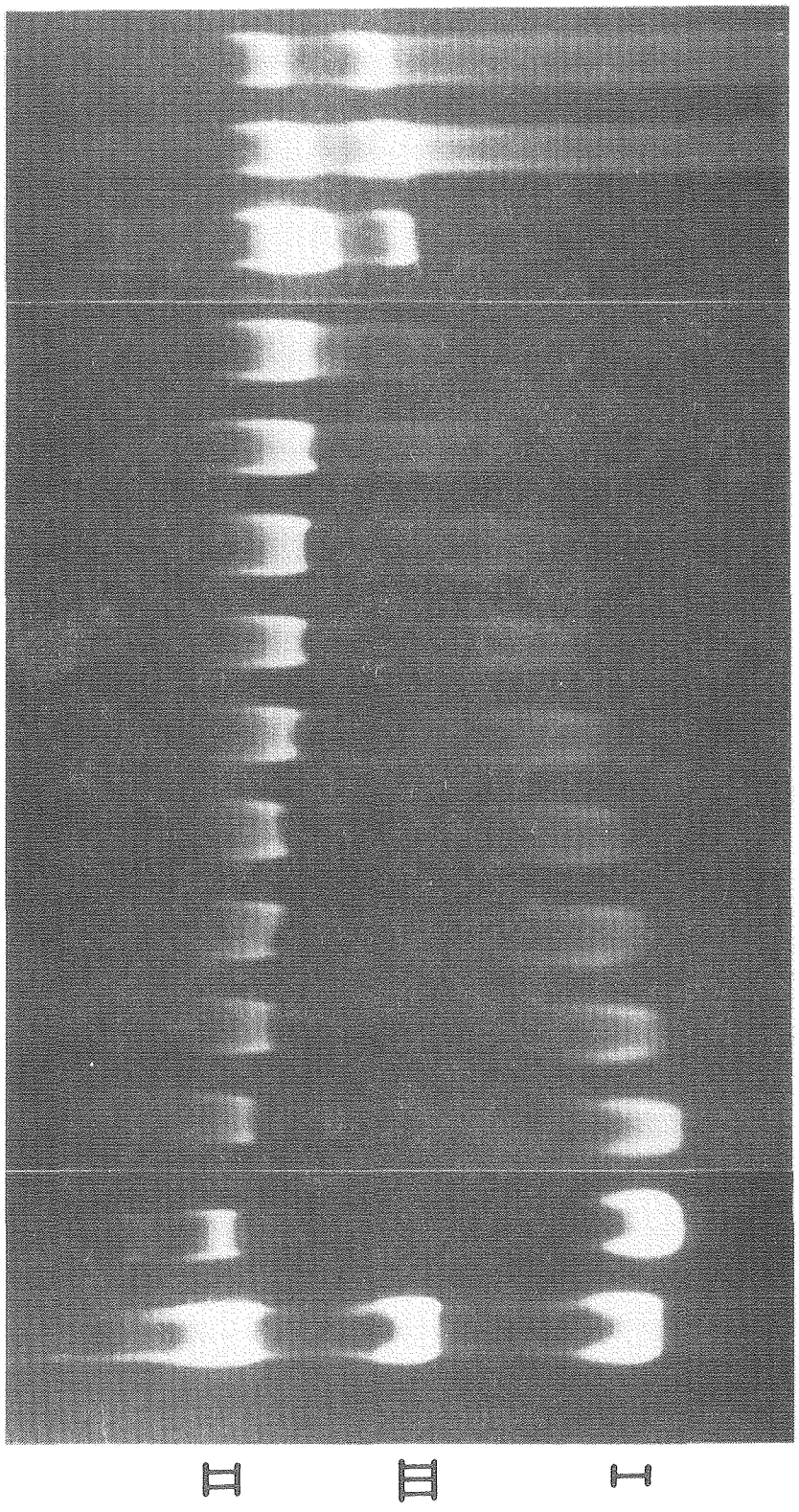

XBB 781-1009

broke the DNA generating linear form III as well as smaller fragments. The absence of form III DNA at lower molar reaction ratios implies that the fragmentation seen at high ratios resulted from two adjacent nicks on opposite strands as opposed to double strand breaks. Furthermore, the heterodisperse tail of low molecular weight fragments extending from the form III band in the last two tracks indicates that, at least at higher reaction ratios, nicking occurred randomly. Although this thesis is concerned with anti-BaP diol epoxide, I have previously shown that the geometric syn isomer has comparable nicking activity (49). The tetraol hydrolysis product of BaP diol epoxide had no effect on form I SV40 DNA (data not shown).

The remaining form I DNA band broadens and exhibits a decreased mobility with increasing modification (Figure 3). This results from local unwinding of the DNA helix brought about by covalently bound adducts. At the same time the form II DNA band exhibits an increased mobility. This reflects a reduction in the intrinsic viscosity of the DNA together with an overloading of the form II band. These phenomena will be discussed in detail in Chapter 4.

Analysis of representative reaction mixtures by electron microscopy substantiated the gel data. Electron micrographs of superhelical SV40 DNA reacted 24 hr with BaP diol epoxide at molar reaction ratios of (A) 0, (B) 0.65, and (C) 3.2 show superhelical, nicked circular, and fragmented linear DNA forms, respectively (Figure 4).

The significance of strand scission was ascertained by reacting ^{3}H-BaP diol epoxide with ^{14}C-SV40 form I DNA and quantifying the frequency of adducts and nicks per genome as a function of the molar reaction ratio. Covalent binding was determined after removal of BaP

Figure 4.

Electron micrographs of SV40 DNA reacted with BaP diol epoxide at hydrocarbon to DNA mononucleotide ratios of (A) 0, (B) 0.647, and (C) 3.24. After 24 hr of reaction and ethyl acetate extraction, the DNA samples were spread in the presence of denatured cytochrome C, picked up on parlodion coated grids, stained with uranyl acetate, and shadowed with Pt/Pd. The bar equals 0.5 microns.

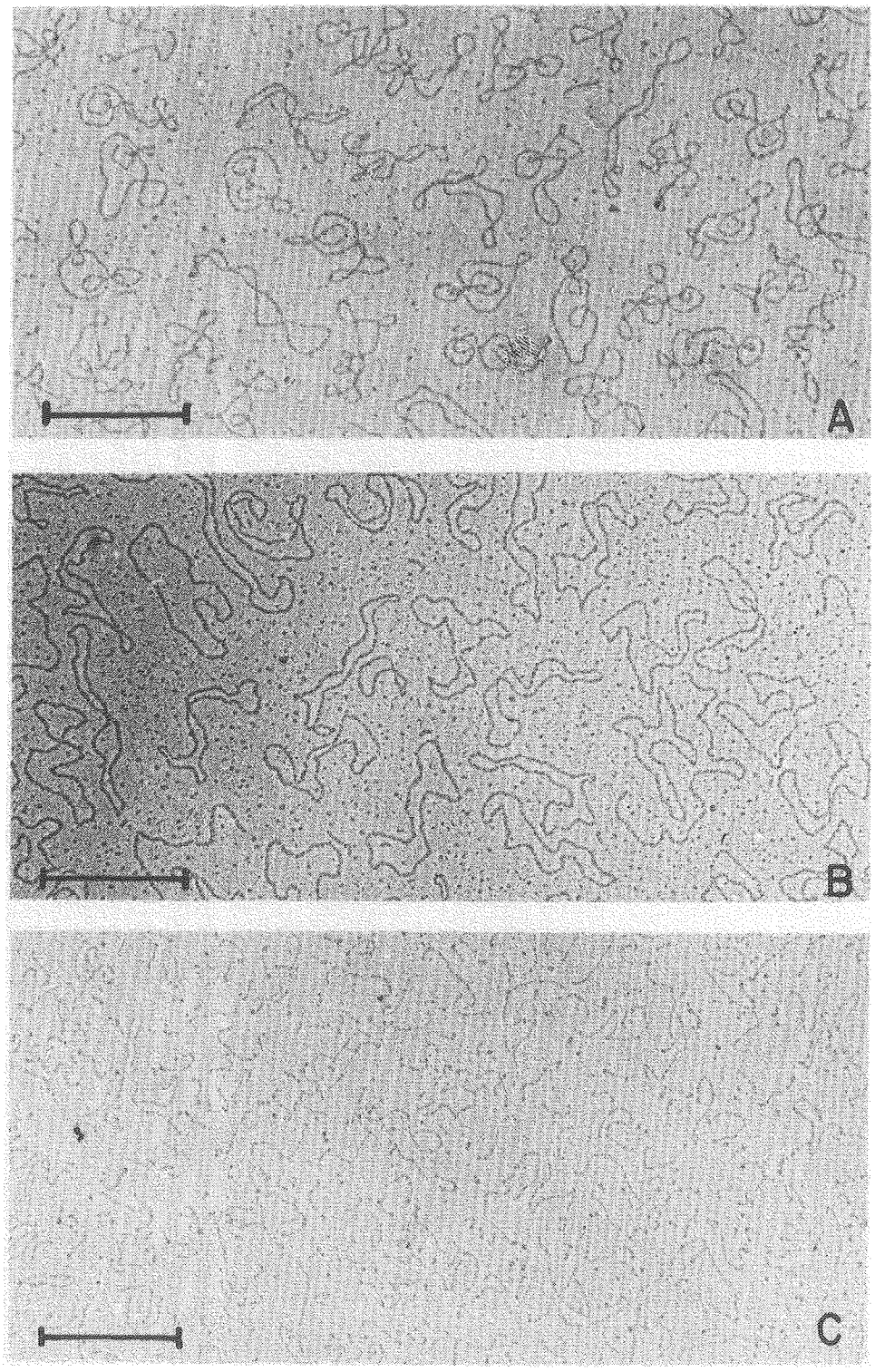

XBB 781-1011

tetraol from the DNA by ethyl acetate extraction and ethanol precipitation. The average number of nicks per DNA molecule (μ) was calculated from the equation (79) $U = e^{-\mu}$ following electrophoretic determination of the fraction of form I DNA (U) remaining in the reaction mixture after 24 hr incubation. Figure 5a shows that only 3% of the epoxide alkylated the DNA and that strand scission occurred to an extent less than 1% of the alkylation events. The proportion of nicking to covalent binding increased with the molar reaction ratio (Figure 5b) indicating a decreased binding efficiency and a constant or increased nicking efficiency for BaP diol epoxide (see Figure 14). Enhanced nicking may be brought about by an acceleration of the rate of strand scission or by an increase in the proportion of adducts which lead to strand scission.

Over 97% of the labeled hydrocarbon which coprecipitates with DNA in ethanol has been identified as comprising guanine and adenine adducts modified at the N^2 and N^6 positions, respectively (6-8). For SV40 DNA modified at a molar reaction ratio of 0.04 in Tris buffer, pH 8.0, 86% of the binding was to guanine and 14% to adenine (see Chapter 4). These purine adducts should not give rise to strand scission under physiological conditions. This implies that DNA nicking is due to one or more minor alkylation sites representing less that 1% of the ethanol precipitable adducts or to labile adducts which are lost in the ethanol supernatant.

In general the nicking values presented in this chapter are consistent with one another. Where differences exist they are attributed to variation in the actual molar reaction ratios which inevitably arises when different DNA preparations and BaP diol epoxide dilution series are used. Of course, within a given experiment absolute data comparison may

Figure 5.

Comparison of SV40 DNA alkylation and strand scission by BaP diol epoxide. [^{14}C]-SV40 form I DNA (1.87 µg in 150 µl of 20 mM Tris-HCl, pH 8.0-0.5 mM EDTA-10% DMSO) was reacted at 37^{o} with a concentration series of [^{3}H]-BaP diol epoxide. After 2 hr incubation 100 µl aliquots were extracted with ethyl acetate, ethanol precipitated, combusted, and counted for adduct determination. After an additional 22 hr incubation the remaining reaction mixtures were electrophoresed and the DNA bands excised, combusted, and counted for estimation of strand scission. Details of the methodology are presented in Chapter 2.

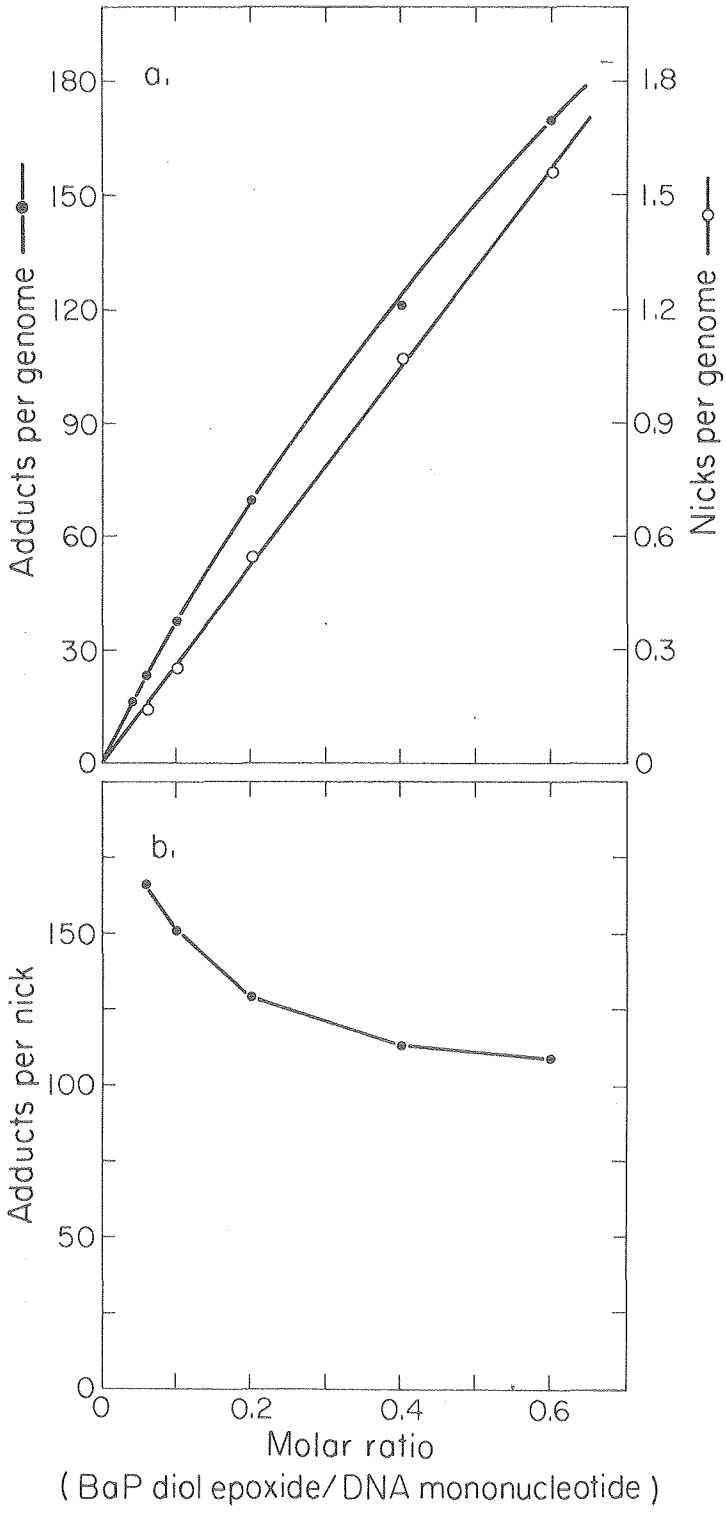
a.
b.
Adducts per genome
Nicks per genome
Adducts per nick
180
150
120
90
60
30
0
1.8
1.5
1.2
0.9
0.6
0.3
0
150
100
50
0
0
0.2
0.4
0.6
Molar ratio
(BaP diol epoxide/ DNA mononucleotide)

XBL796-4814

be made.

The experiments which follow were designed to elucidate the mechanism of strand scission by BaP diol epoxide. Highly alkylated DNA substrates were employed due to the infrequency of strand scission. In vivo modification of DNA by metabolically activated BaP rarely introduces more than 1 adduct per 10^4 nucleotide residues (84). This is far below even the lowest level of modification reported in this chapter. Although the data obtained from molar reaction ratios below 0.10 are probably biologically significant, caution should be exercised in extrapolating the results to biological systems.

Strand Scission Mechanisms. BaP diol epoxide induced DNA strand scission is likely to proceed through one or more of the commonly accepted pathways for nucleic acid degradation by exogenous agents: i.e. photochemical, free radical, depurination/depyrimidination strand scission, and phosphotriester hydrolysis.

The first two mechanisms are unlikely to apply to BaP diol epoxide. Its reactions with nucleophiles are mediated by a highly stabilized benzylic carbonium ion and exhibit considerable S_N1 character. Furthermore, the modification of SV40 DNA reported here was carried out under subdued lighting and neither covalent binding or nicking were affected by 0.5 M isopropyl alcohol, a free radical scavenger.

DNA fragmentation by alkylating agents is most commonly attributed to depurination and depyrimidination strand scission (85-87). Electrophilic attack at guanine N-7, adenine N-3, or pyrimidine O^2 introduces a formal positive charge into the π-system of the base. This labilizes the glycosidic linkage and leads to loss of the modified base. The rate of loss is dependent upon the base as well as the alkylating agent

but is several orders of magnitude greater than spontaneous depurination. Surprisingly, these same modified bases in RNA are quite stable under physiological conditions (86). Strand scission through rearrangement of the deoxyribose sugar at an apurinic or apyrimidinic site is multistep (88) and involves ring opening, tautomerization, and β-elimination to give a nick in the phosphodiester backbone (Figure 6). The resultant nick has a free sugar at the 3' terminus and a phosphate at the 5' terminus. Scission by 3',4' cyclic phosphate formation or by 4',5' cyclization are minor pathways. The entire reaction sequence occurs slowly under physiological conditions but is catalyzed by amines, aldehydes, and alkali (88).

Recently, Osborne et al. (16) and King et al. (17) characterized a BaP diol epoxide N-7 guanine adduct. The modified base readily depurinated and had a half-life of 3 hr. At pH 7.0 it accounted for 20% of the total alkylation. However, these studies were conducted in 40% methanol with a BaP diol epoxide to DNA mass ratio of 3.0 thus bringing into question their biological significance. At much lower reaction levels, K. Straub and I have been unable to detect an N-7 guanine adduct in either the ethanol supernatant or the DNA pellet. If small amounts of this adduct were indeed formed (ca. 1%), it could account for the observed strand scission and yet be undetectable by adduct analysis.

The final mechanism by which alkylating agents can induce strand scission is through the formation and subsequent hydrolysis of phosphotriesters. In RNA (89), triester hydrolysis is catalyzed by the 2'-hydroxyl group of ribose, which can displace either the alkyl group or the adjacent 5' sugar from the phosphate through a cyclic triester intermediate. If the sugar is displaced a nick is generated which

Figure 6.

Mechanism of depurination/depyrimidination DNA strand scission.

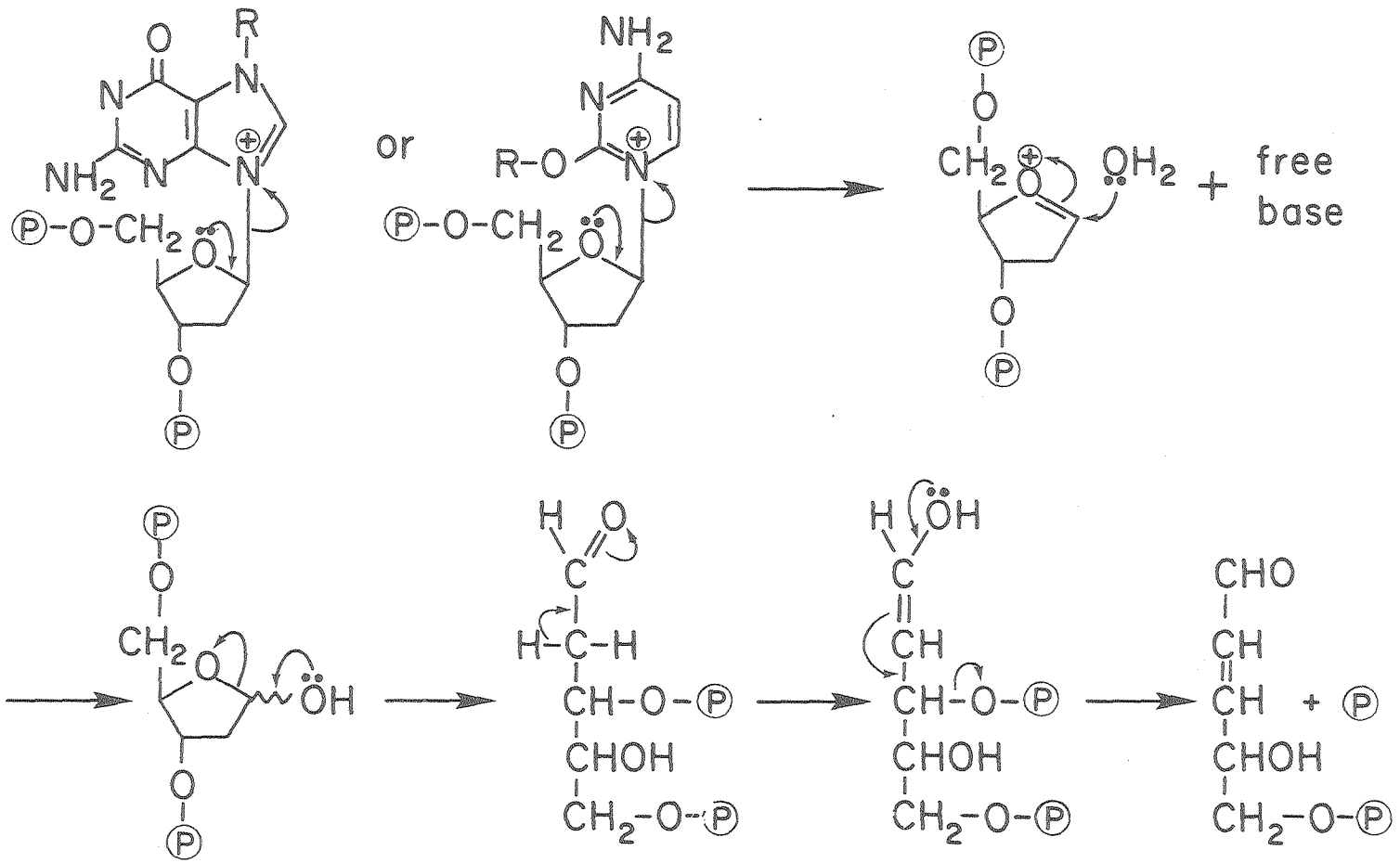

XBL798-4976

contains a 2' or 3'-phosphate and a 5'-hydroxyl. Simple alkyl ribophosphotriesters hydrolyze rapidly at pH 7.0 with a half-life of less than 8 hr (89). In DNA (90), which lacks 2'-hydroxyl groups, phosphotriesters are stable. Hydrolysis of deoxyribophosphotriesters requires prolonged incubation at high pH (91,92).

In 1976 Koreeda et al. (12) showed that BaP diol epoxide reacts with inorganic phosphate to form a heat labile product which released BaP tetraol upon brief incubation at 85°. When alkylated poly(G) was similarly heated 15% of the hydrocarbon incorporated solvent water and was released as BaP tetraol. This was taken as evidence for the formation of ribophosphotriesters. The lability of the triesters was presumably due to unimolecular breakage of the oxygen-hydrocarbon linkage to give a C-10 carbonium ion which then reacted with water to form BaP tetraol. Possible strand scission of the alkylated poly(G), expected from the presence of 2'-hydroxyl groups, was not investigated.

It is plausible that BaP diol epoxide could form phosphotriesters in DNA as well as in poly(G). A unique feature of these triesters would be the presence of a β-hydroxyl group on the hydrocarbon. Acting much like the 2'-hydroxyl in RNA, this group could catalyze triester hydrolysis with concomitant strand scission (93). A mechanism for such a hydrolysis is presented in Figure 7. Since DNA phosphate does not readily displace electrophiles, ester formation at the C-10 position of the hydrocarbon would likely proceed through an S_N1 mechanism (94,95). The C-9 hydroxyl group could then displace one of the sugars, thereby breaking the DNA backbone and forming a cyclic triester. Tertiary cyclic phosphates, like the one proposed, hydrolyze rapidly to relieve ring strain (96). Upon hydrolysis the hydrocarbon would remain attached to

Figure 7.

Postulated BaP diol epoxide initiated DNA phosphotriester strand scission mechanism (49).

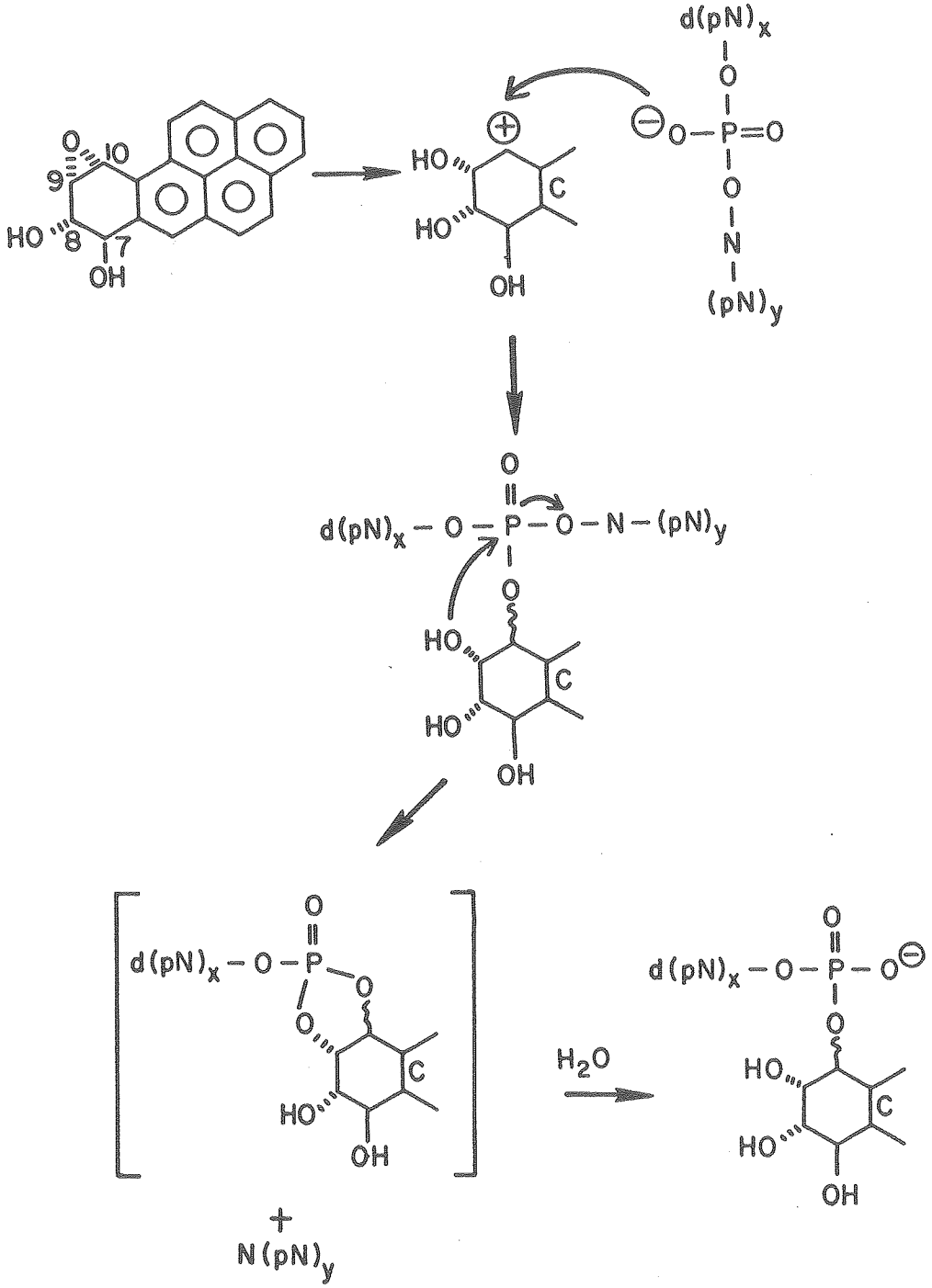

XBL771-4115A

the phosphate, although it would eventually be lost through the unimolecular reaction described in the preceding paragraph. Since the β-hydroxyl group is on the hydrocarbon and not the sugar, each triester hydrolysis would give a nick. Depending upon which ester linkage is cleaved, the phosphate could be on either side of the nick. It must be emphasized that this proposed mechanism requires actual reaction of BaP diol epoxide with DNA phosphate and proper orientation of the C-9 hydroxyl to permit catalysis.

In the following sections I describe a detailed study of BaP diol epoxide induced DNA strand scission which indicates that depurination followed by β-elimination is the actual mechanism responsible for nicking. Although phosophotriesters may be formed in DNA, no evidence was found for their hydrolysis by the proposed mechanism shown in Figure 7. Additional evidence is presented for the formation of an alkali labile rearrangement product which might arise from the major N^2 guanine adduct.

Kinetics of Covalent Binding and Nicking. BaP diol epoxide is an extremely reactive electrophile and is rapidly hydrolyzed in aqueous solutions to BaP tetraol. In my standard pH 8.0 reaction buffer (20 mM Tris-HCl, 0.5 mM EDTA, 5% DMSO) at 37^{o} the epoxide had a half-life of 21 min. The kinetics of hydrolysis was determined indirectly by taking aliquots of an aqueous BaP diol epoxide solution for reaction with superhelical DNA and plotting (on a semi-logarithmic scale) the nicked circular DNA produced as a function of hydrolysis time (Figure 8). The value obtained is comparable to the 38 min half-life reported by Drinkwater et al. (50) for BaP diol epoxide (10 mM Tris-HCl, pH 7.4, 1 mM EDTA, 20% DMSO, 37^{o}).

Figure 8.

Hydrolysis of BaP diol epoxide. An aqueous solution of BaP diol epoxide (10 µg/ml in 20 mM Tris-HCl, pH 8.0-10% DMSO) was incubated in the dark at 37°. Aliquots of 27.5 µl were withdrawn as a function of time into 30.2 µl of a superhelical Col E1 DNA solution (18 µg/ml in 20 mM Tris-HCl, pH 8.0) and kept for 24 hr at 37°. The % form II DNA was determined by agarose gel electrophoresis.

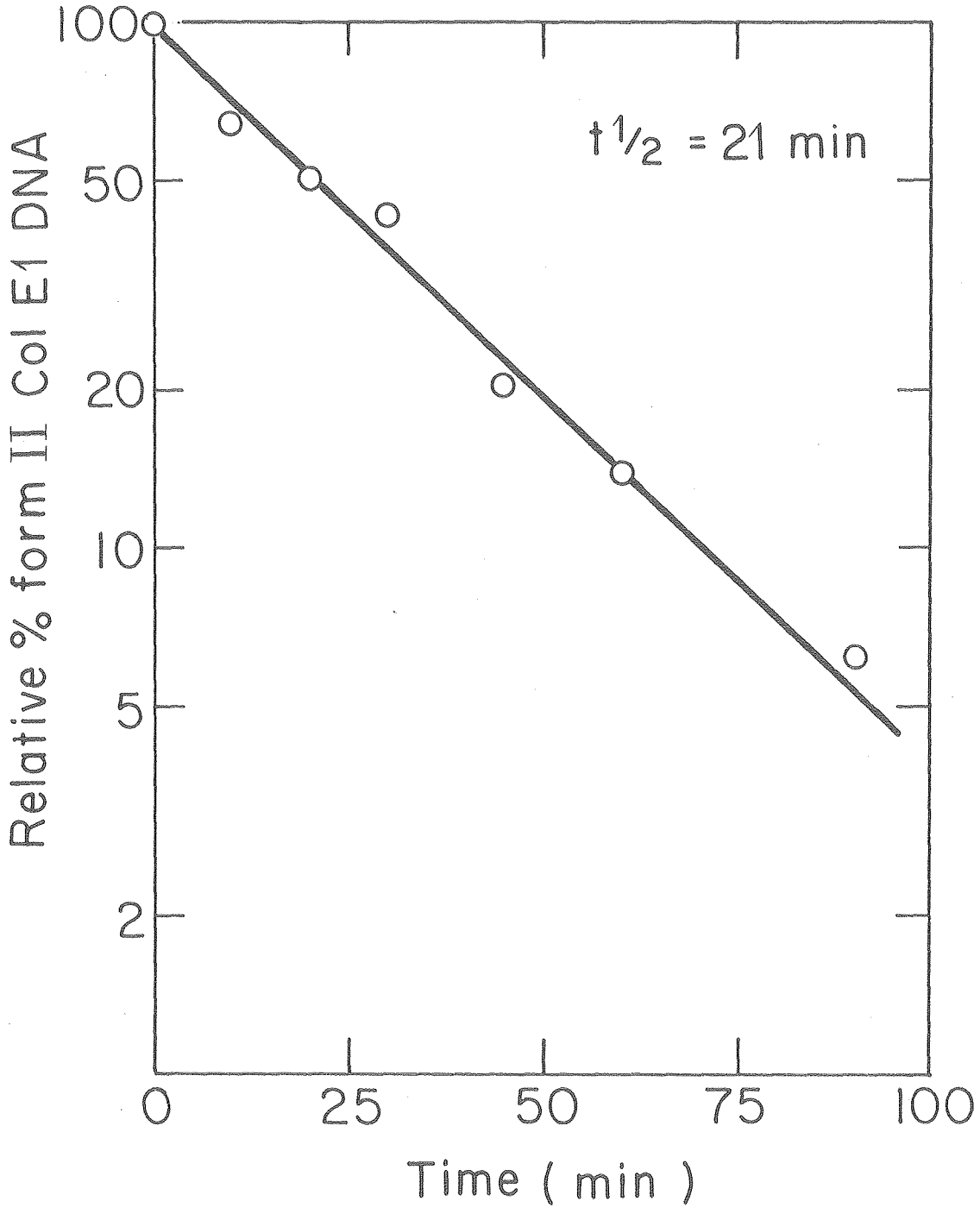
100
50
20
10
5
2
Relative % form II Col E1 DNA
t 1/2 = 21 min
0
25
50
75
100
Time (min)

XBL 798-4970

I have found that 2-mercaptoethanol reacts instantaneously with BaP diol epoxide and is quite effective in stopping its reaction with DNA. This has allowed me to follow the covalent binding of BaP diol epoxide to SV40 DNA. After reaction mixture aliquots were quenched by the sulfhydryl reagent, the modified DNA was analyzed by gel electrophoresis or nitrocellulose filtration. Sufficiently modified form I SV40 DNA binds to nitrocellulose filters. The binding is probably mediated by externally bound hydrocarbon adducts or by localized single stranded regions induced by alkylation (see Chapter 4). At a molar reaction ratio of 0.15 approximately 60% of the modified DNA was retained by nitrocellulose. When the reaction time course was monitored at this molar ratio (Figure 9), it was apparent that covalent binding of the hydrocarbon to DNA was complete within 20 min. The initial lag in filter binding is not reflective of reaction kinetics and presumably arises from the requirement for multiple alkylation sites on the DNA if stable filter binding is to occur. The rapidity of DNA modification, which has also been reported by others (97,98), suggests that hydrolysis of BaP diol epoxide is in some way catalyzed by DNA.

Covalent binding of BaP diol epoxide to SV40 DNA was also monitored by gel electrophoresis (Figure 10). At a molar reaction ratio of 0.60 the reaction was nearly complete in 10 min. During this period there was a rapid decrease in mobility and a broadening of the form I DNA band. These changes are attributed to local unwinding of the helix by BaP diol epoxide adducts and to strand scission during the electrophoretic analysis. The latter process was predominant over a longer time period since nearly all of the DNA migrated as nicked circles after a 25 hr incubation. The negligible increase in form II DNA after the first 30 min of

Figure 9.

BaP diol epoxide alkylation of SV40 DNA monitored by nitrocellulose filtration. [^{14}C]-SV40 form I DNA (4.2 µg/ml in 20 mM Tris-HCl, pH 8.0-0.5 mM EDTA-10% DMSO) was reacted at 37^{o} with BaP diol epoxide at a molar reaction ratio of 0.15. Aliquots of 100 µl were taken as a function of time into 10 µl of 2.5 M 2-mercaptoethanol. The alkylated DNA was filtered through nitrocellulose and counted as described in Chapter 2.

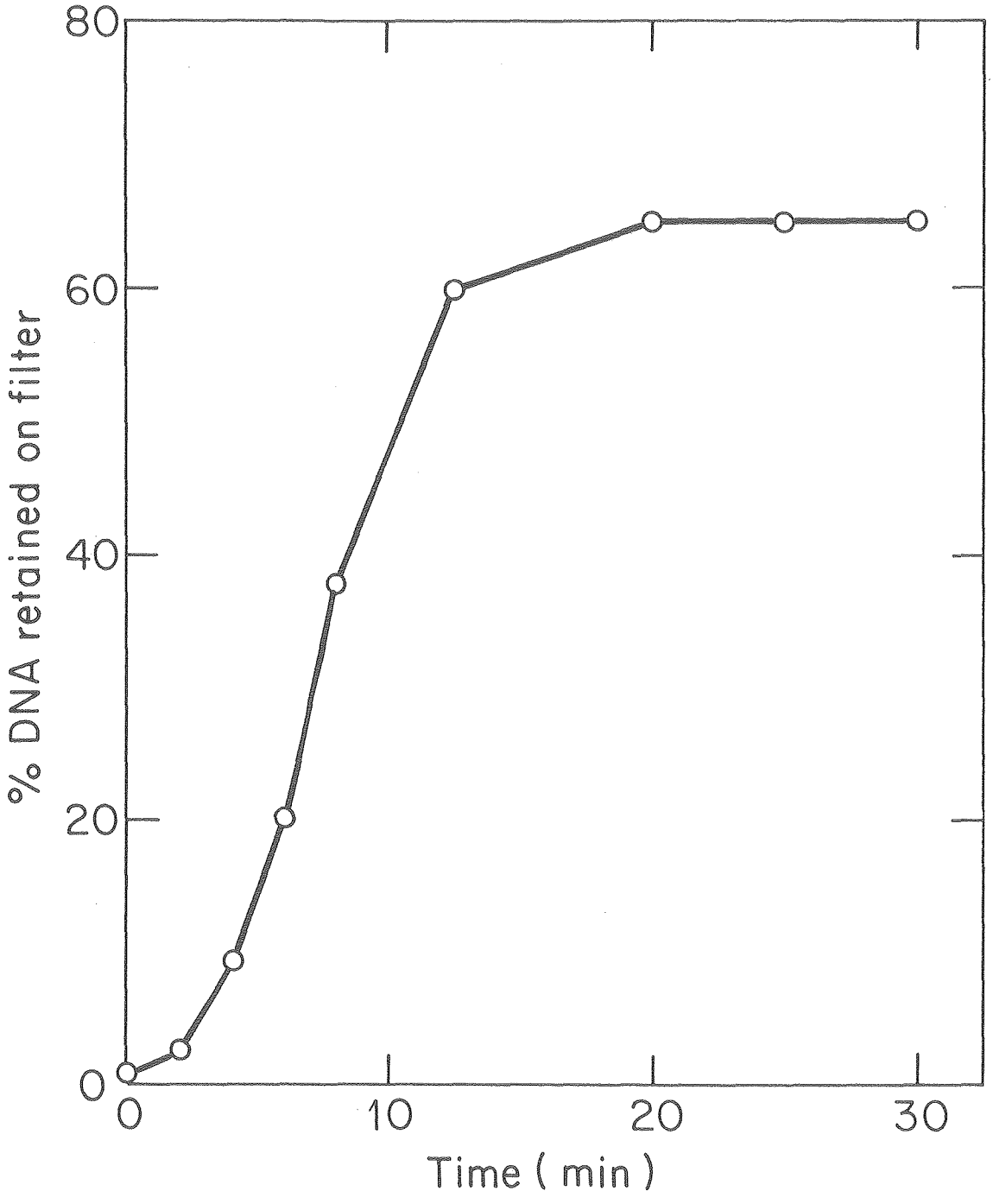

XBL 798-4972

Figure 10.

BaP diol epoxide alkylation of SV40 DNA monitored by agarose gel electrophoresis. [^{14}C]-SV40 form I DNA (8.4 µg/ml in 20 mM Tris-HCl, pH 8.0-0.5 mM EDTA-10% DMSO) was reacted at 37^{o} with BaP diol epoxide at a molar reaction ratio of 0.60. Aliquots of 50 µl were taken at the indicated times into 10 µl of 2.5 M 2-mercaptoethanol. The alkylated DNA was electrophoresed downward at 50 V for 12 hr on a 1.4% agarose slab gel.

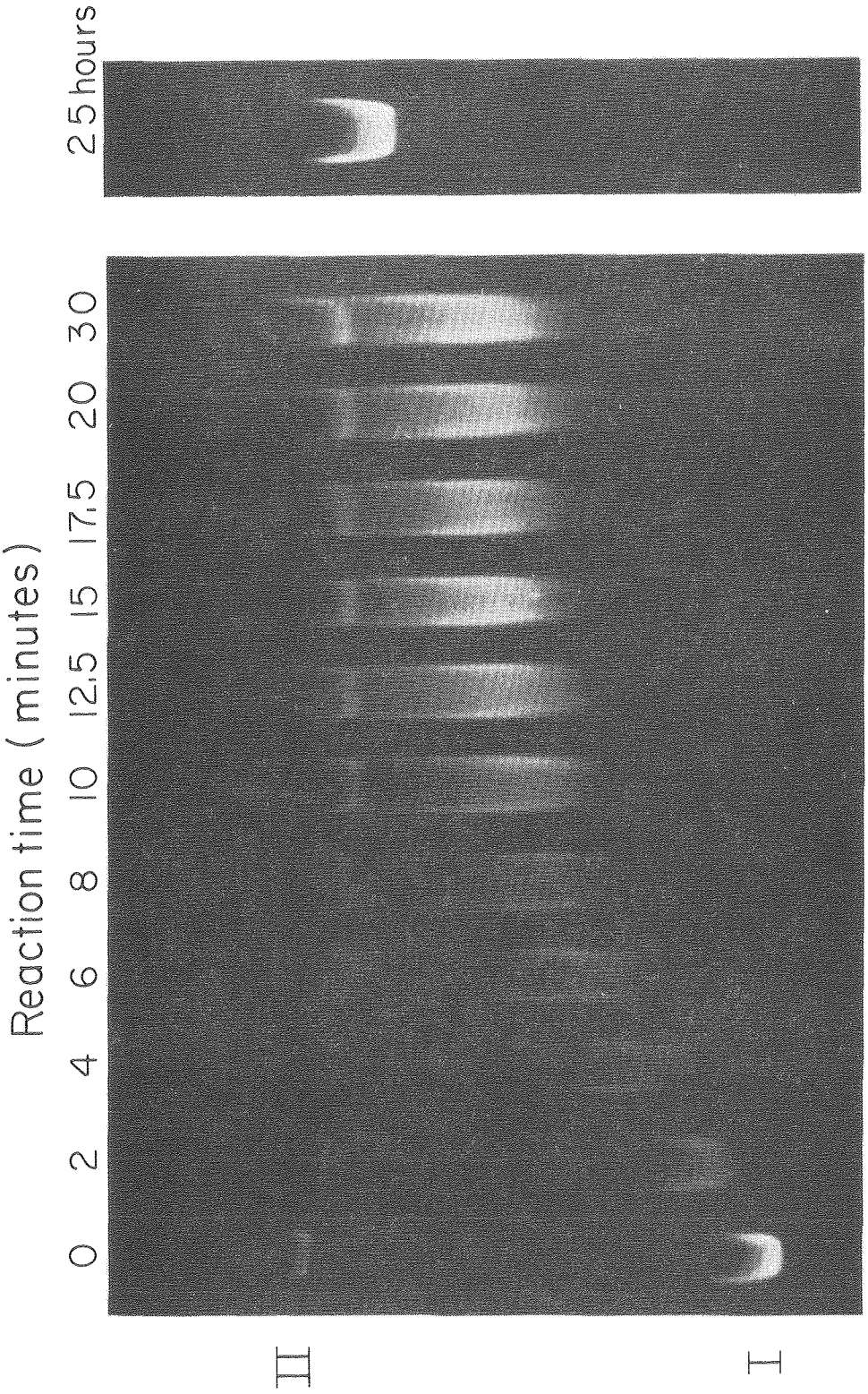

XBB 796-7856

incubation implies that strand scission is a secondary event which results from the rearrangement of one or more primary adducts.

The kinetics of strand scission was determined by disc gel electrophoresis of alkylated SV40 DNA at 30 min intervals. Figure 11 shows the time course of nicking and the gel pattern from which it was derived for SV40 DNA modified at a molar reaction ratio of 0.60. In contrast to the rapid covalent modification of DNA, BaP diol epoxide induced strand scission proceeded slowly with time throughout the 25 hr experiment. This is consistent with nicking occurring through rearrangement of one or more BaP diol epoxide adducts. Furthermore, the increase in slope of the nicking curve in Figure 11 with time is indicative of a multistep rearrangement which terminates in strand scission. Depurination/depyrimidination strand scission is such a mechanism, although phosphotriester hydrolysis could account for some of the initial nicking.

Lindahl and Andersson (88) have calculated that in Mg^{2+} containing buffer (pH 7.4, 37^{o}) the average lifetime of the DNA chain at an apurinic site is 190 hr. If this half-life holds for my standard reaction buffer (20 mM Tris-HCl, pH 8.0, 0.5 mM EDTA, 5-10% DMSO) then production of a very high number of apurinic sites would be required to account for the amount of strand scission reported in Figure 5. Production of so many sites is questionable given the inability to detect any labile base adducts released from DNA modified at lower molar reaction ratios. An alternative possibility is that apurinic sites rearrange more rapidly in my standard reaction buffer; then fewer such sites would be required to account for the extent of strand scission seen in Figure 5. To resolve this question the stability of apurinic sites in SV40 DNA was determined in my standard reaction buffer by the method of Kuhnlein et al.

Figure 11.

Kinetics of BaP diol epoxide induced DNA strand scission. [^{14}C]-SV40 form I DNA (8.4 μg/ml in 20 mM Tris-HCl, pH 8.0-0.5 mM EDTA-10% DMSO) was reacted at 37^{o} with BaP diol epoxide at a molar reaction ratio of 0.60. Aliquots of 30 μl were taken into 10 μl of SDS weighting solution (see Chapter 2) and 10 μl of 2.5 M 2-mercaptoethanol and electrophoresed downward at 75 V for 400 min on 1.4% agarose disc gels. The DNA bands were excised, combusted, and counted as described in Chapter 2. Strand scission was quantified using the equation (79) $U = e^{-\mu}$. The 25 hr time point was obtained from the gel in Figure 10.

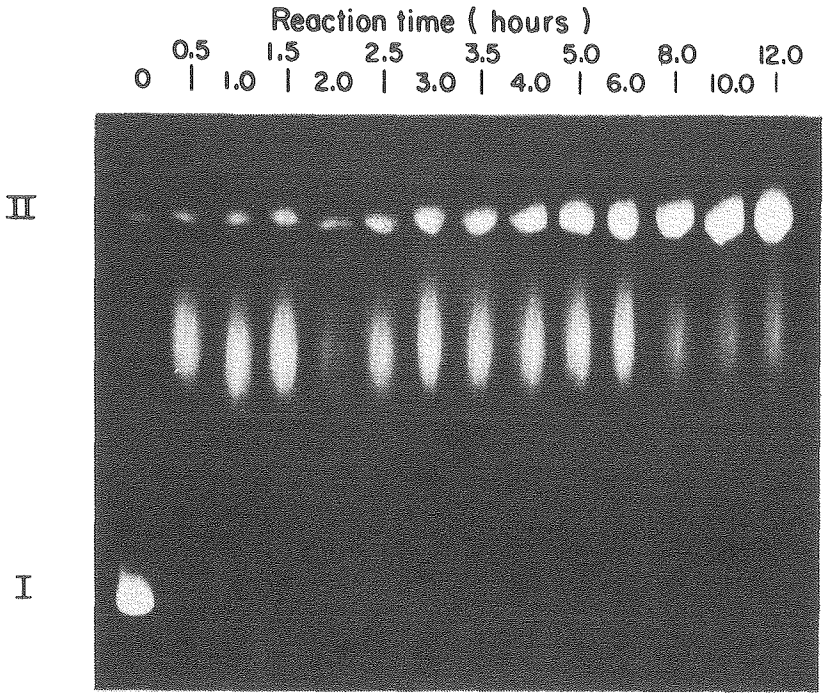

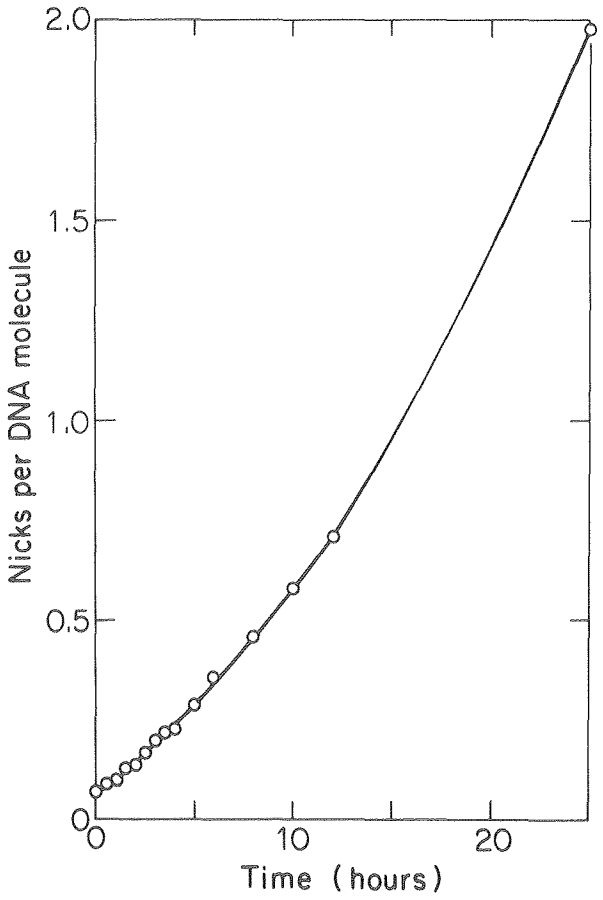

XBB 796-7855A

(79). Extrapolation of the data in Figure 12 gives a half-life of only 16 hr for these sites, significantly less than that found by Lindahl and Andersson (88). I propose that the relative instability of apurinic sites in my buffer is accounted for by the slightly higher pH and the previously reported catalytic effect of Tris itself (88). As expected, BaP tetraol did not influence the conversion of apurinic sites to nicks (data not shown).

Effect of Alkali and Na/Mg Counterions on Strand Scission. The electrophoretic patterns of SV40 DNA alkylated with a concentration series of BaP diol epoxide and held at 37^{o} for 24 hr or 48 hr were similar (Figure 13). The only appreciable difference was that at higher molar reaction ratios extended incubation led to a slight decrease in form I and increase in form III DNA. When the average number of nicks per genome was calculated and plotted (Figure 14), it was apparent that the rate of strand scission was dependent upon the extent of modification. At molar reaction ratios below 0.20, DNA nicking appeared to terminate within 24 hr. At higher molar reaction ratios, DNA nicking continued past this time, perhaps reflecting the slow rearrangement of an adduct which was only present in highly modified DNA.

Alkaline sucrose density gradient profiles of representative SV40 DNA samples incubated 1 hr with varying amounts of BaP diol epoxide are presented in Figure 15. Denatured form I DNA has a sedimentation coefficient of 53S while denatured form II DNA sediments as a 18S single-stranded circle and a 16S single-stranded linear (57). The extent of strand scission was identical to that observed after 24 hr incubation at neutrality (Figure 15). Thus BaP diol epoxide induced nicking is catalyzed by brief exposure to high pH. Alkaline catalysis has been

Figure 12.

Kinetics of strand scission at apurinic sites. An average of 1.67 apurinic sites were introduced into [^{14}C]-SV40 form I DNA by incubating it at 50^{o} and pH 3.65 for 12.5 min. The depurinated DNA was diluted 10X with 20 mM Tris-HCl (pH 8.0)-0.5 mM EDTA and kept at 37^{o}. Triplicate aliquots (100 µl containing 0.42 µg DNA) were withdrawn as a function of time for determination of strand scission. These samples were briefly treated with pH 12.3 buffer to irreversibly denature form II DNA, passed through single-strand adsorbing nitrocellulose filters, and counted. Strand scission was equated with hydrolysis of apurinic sites. This study is described in Chapter 2.

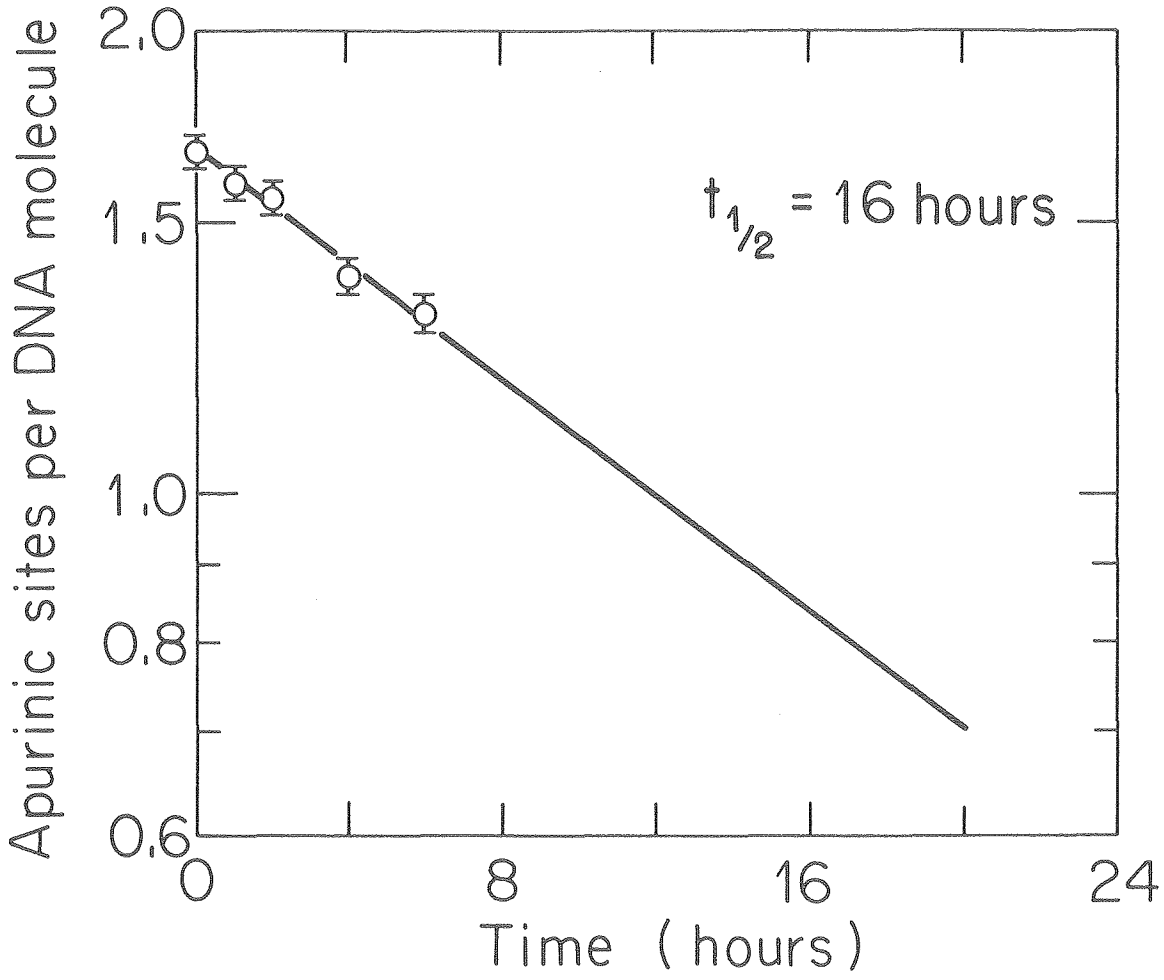
Apurinic sites per DNA molecule
2.0
1.5
1.0
0.8
0.6
0
8
16
24
Time (hours)
$t_{1/2}$ = 16 hours

XBL 792-4647

Figure 13.

Electrophoretic analysis of BaP diol epoxide modified SV40 DNA after (A) 24 hr and (B) 48 hr of reaction. [^{14}C]-SV40 form I DNA (0.84 µg in 100 µl of 20 mM Tris-HCl, pH 8.0-0.5 mM EDTA-10% DMSO) was reacted at 37^{o} with BaP diol epoxide at molar reaction ratios of (a) 0, (b) 0.02, (c) 0.04, (d) 0.06, (e) 0.08, (f) 0.10, (g) 0.20, (h) 0.30, (i) 0.40, (j) 0.60, (k) 0.80, and (l) 1.0. After (A) 24 hr or (B) 48 hr 50 µl aliquots were electrophoresed downward on a 1.4% agarose slab gel. The DNA bands were excised, combusted, and counted for determination of % form I DNA.

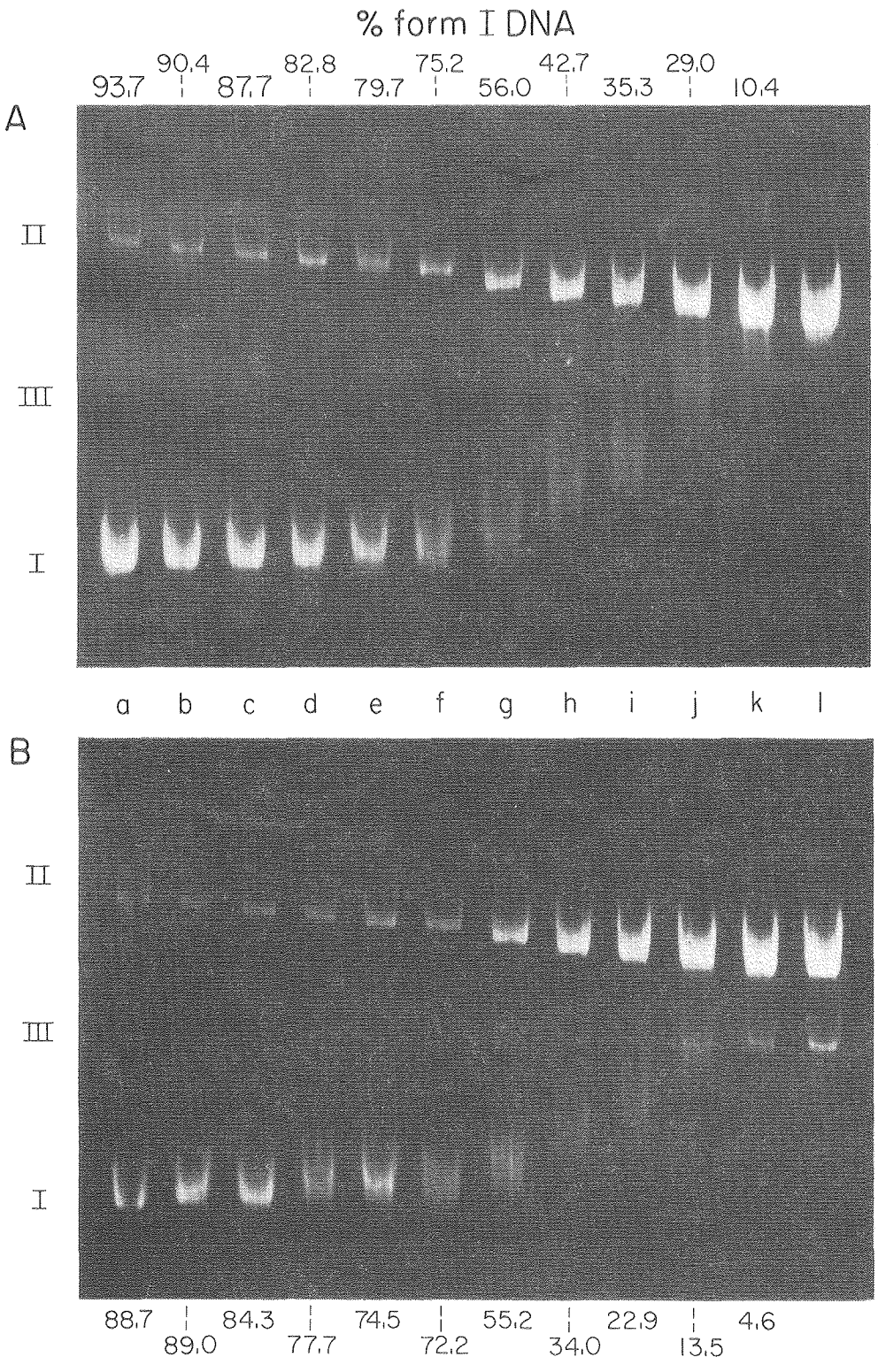
% form I DNA
93.7
90.4
87.7
82.8
79.7
75.2
56.0
42.7
35.3
29.0
10.4
A
II
III
I
a b c d e f g h i j k l
B
II
III
I
88.7
89.0
84.3
77.7
74.5
72.2
55.2
34.0
22.9
13.5
4.6

XBB 796-7858

Figure 14.

Strand scission of BaP diol epoxide modified SV40 DNA determined by agarose gel electrophoresis and alkaline sucrose gradient centrifugation. [^{14}C]-SV40 form I DNA was reacted at 37^{o} in 20 mM Tris-HCl (pH 8.0)-0.5 mM EDTA-10% DMSO with BaP diol epoxide at the indicated molar reaction ratios. Strand scission was quantified by agarose gel electrophoresis or alkaline sucrose gradient centrifugation as described in Figures 13 and 15. (●), electrophoretic analysis after 24 hr incubation; (o), electrophoretic analysis after 48 hr incubation; (□), alkaline gradient analysis after 1 hr incubation; (▲), alkaline gradient analysis after 24 hr incubation; (Δ), alkaline gradient analysis after 24 hr incubation followed by 4 hr incubation at room temperature with an equal volume of 2 M glycine-NaOH (pH 13.1).

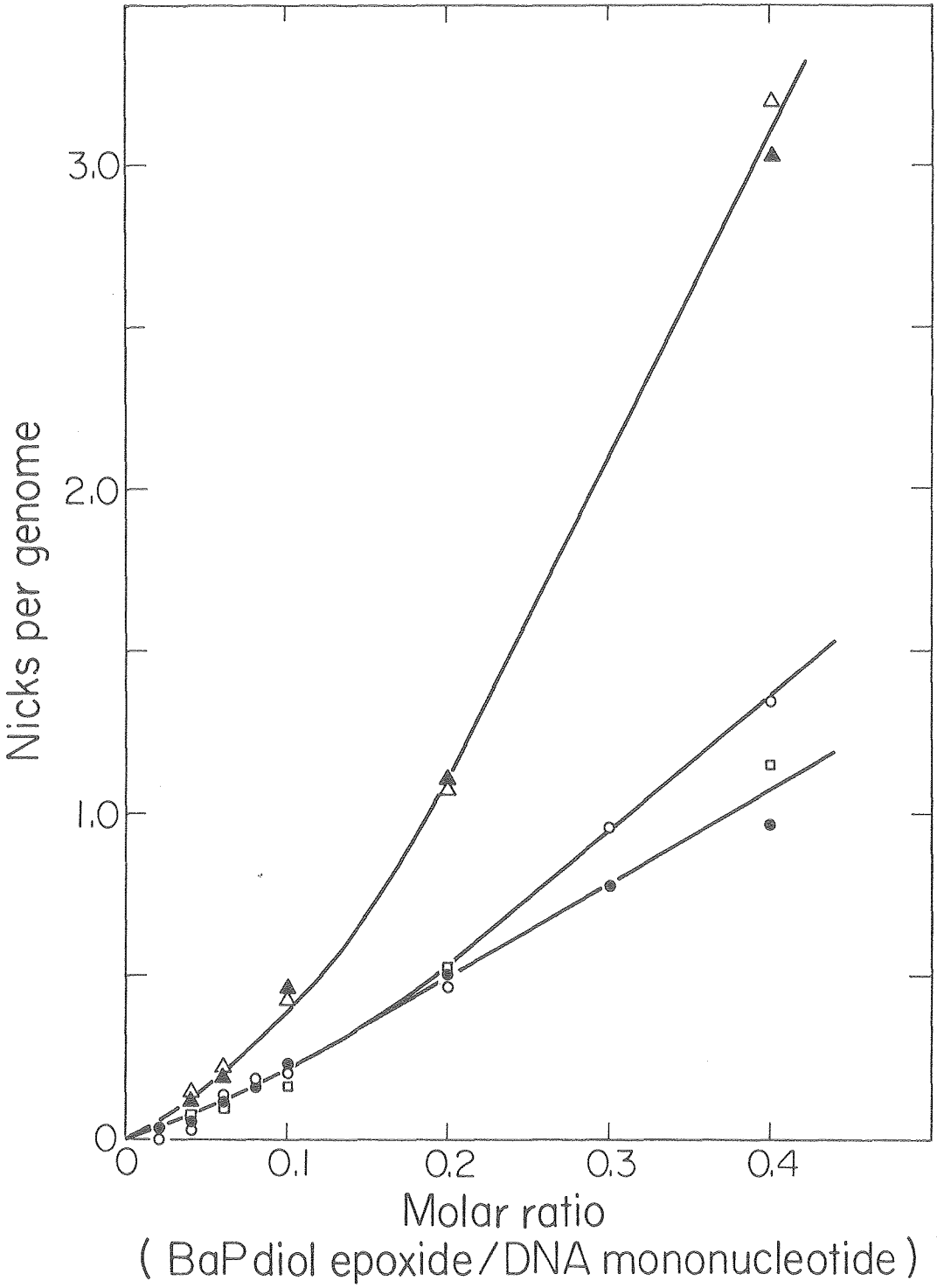
Nicks per genome
3.0
2.0
1.0
0
0
0.1
0.2
0.3
0.4
Molar ratio
(BaP diol epoxide / DNA mononucleotide)

XBL 796-4818

Figure 15.

Alkaline sucrose gradient analysis of BaP diol epoxide modified SV40 DNA after 1 hr of reaction. [^{14}C]-SV40 form I DNA (0.42 µg in 50 µl of 20 mM Tris-HCl, pH 8.0-0.5 mM EDTA-10% DMSO) was reacted for 1 hr at 37^{o} with BaP diol epoxide at molar reaction ratios of (a) 0, (b) 0.04, (c) 0.06, (d) 0.10, (e) 0.20, and (f) 0.40. The reaction mixtures were layered onto 5.0 ml alkaline sucrose gradients and centrifuged for 90 min at 50,000 rpm in an SW 50.1 rotor. The gradients were fractionated from the bottom and counted. The % form I DNA was determined from the areas under the 53S and 16S peaks.

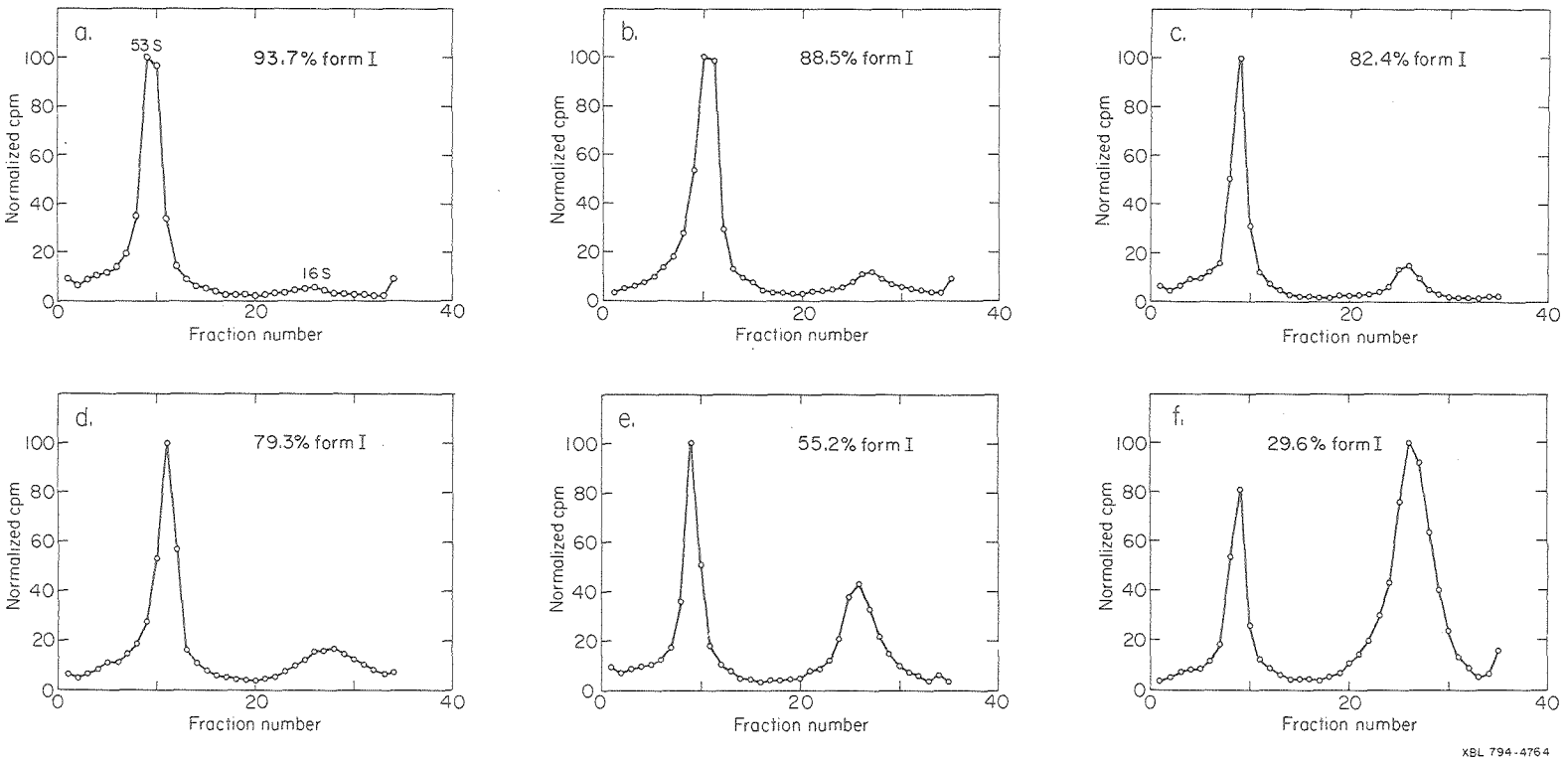
a.
53 S
16 S
93.7% form I
b.
88.5% form I
c.
82.4% form I
d.
79.3% form I
e.
55.2% form I
f.
29.6% form I
Normalized cpm
Fraction number
0
20
40
60
80
100
XBL 794-4764

demonstrated for both deoxyribophosphotriester hydrolysis and β-elimination at apurinic sites (92) and hence the data is consistent with either mechanism. It should be noted that BaP tetraol treated DNA controls retained their superhelicity in alkaline sucrose gradients (data not shown).

A significant increase in the frequency of alkali labile sites was observed for BaP diol epoxide modified SV40 DNA incubated 24 hr prior to centrifugation (Figure 14). At higher molar reaction ratios these sites actually outnumbered DNA nicks. The sites were rapidly cleaved at high pH, and no additional sites were exposed by a 4 hr pretreatment with pH 13.1 buffer. Although extremely labile in alkali, at neutral pH these sites are relatively stable. Thus despite the appreciable number of such sites in alkylated DNA after 24 hr incubation, only minor strand scission at high molar reaction ratios was observed in the subsequent 24 hr period. The time dependent accumulation of these sites indicates that most if not all are secondary rearrangement products. Their identity remains to be determined. Although phosphotriesters and apurinic sites rapidly hydrolyze with strand scission in alkali, neither is a likely candidate. The concentration of triesters would obviously decrease with time and could only account for a small proportion of the sites present after 24 hr incubation. On the other hand, the half-life of apurinic/apyrimidinic sites is too low to account for the stability of these alkali labile products at pH 8.0. As will be shown, the DNA backbone at most of these sites is resistant to apurinic endonuclease. One possibility that must be considered is that these sites represent an alkali labile rearrangement product of the major N^2 guanine adduct.

As part of a study of the BaP diol epoxide SV40 DNA reaction complex, the effect of Na^+ and Mg^{2+} on covalent binding and nicking was determined. Figure 16 shows that both processes were inhibited by the counterions. It is well known that Na^+ and Mg^{2+} bind electrostatically to DNA phosphate, the latter 50 fold more effectively (99). The mirroring of this difference in the binding and nicking curves indicates that the interaction of these ions with DNA is responsible for the inhibition. Bound counterions inhibit alkylation of DNA phosphate and nearby sites such as N-7 guanine by electrostatic masking (100,101). Of course, these are the groups which are likely to rearrange with strand scission when modified with BaP diol epoxide. The reduction of covalent binding to N^2 guanine is believed to occur through a different mechanism. By shielding the DNA phosphates, counterions increase the stability of the double helix, bring the base pairs together, and reduce the probability of intercalation (102). In Chapter 4 it is postulated that intercalation of BaP diol epoxide precedes its reaction with the exocyclic amino group of guanine.

Attempts to Detect Phosphotriester Hydrolysis. Ever since Koreeda et al. (12) reported the reaction of BaP diol epoxide with RNA phosphate, it has been recognized that certain unidentified reaction products with DNA could represent hydrocarbon phosphate adducts (13,34,103). The difficulty of isolating such adducts intact from a DNA reaction mixture prompted an investigation, in collaboration with K. Straub, of BaP diol epoxide binding to the model phosphodiester [^{32}P]-dibutyl phosphate. Reaction was allowed to proceed in 50% aqueous acetone, pH 7.5. After 24 hr the products were analyzed by Sephadex LH-20 chromatography. Less than 0.1% of the label was retained by the column and it eluted as a

Figure 16.

Inhibition of Bap diol epoxide alkylation and strand scission of SV40 DNA by NaCl and $MgCl_2$. [^{14}C]-SV40 form I DNA (1.5 µg in 145 µl of 20 mM Tris-HCl, pH 8.0-10% DMSO) was reacted with [^{3}H]-BaP diol epoxide at a molar reaction ratio of 0.60 in the presence of the indicated concentrations of NaCl or $MgCl_2$. After 3 hr at 37^{o} 100 µl aliquots were withdrawn, extracted with ethyl acetate, ethanol precipitated, combusted, and counted to estimate covalent binding. The remaining reaction mixtures were incubated an additional 21 hr at 37^{o} and electrophoresed on an agarose slab gel. The DNA bands were excised, combusted, and counted to estimate strand scission. The DNA control contained 197 adducts/genome and 2.45 nicks/genome. (●—●), covalent binding in the presence of NaCl; (●---●), strand scission in the presence of NaCl; (o—o), covalent binding in the presence of $MgCl_2$; (o---o), strand scission in the presence of $MgCl_2$.

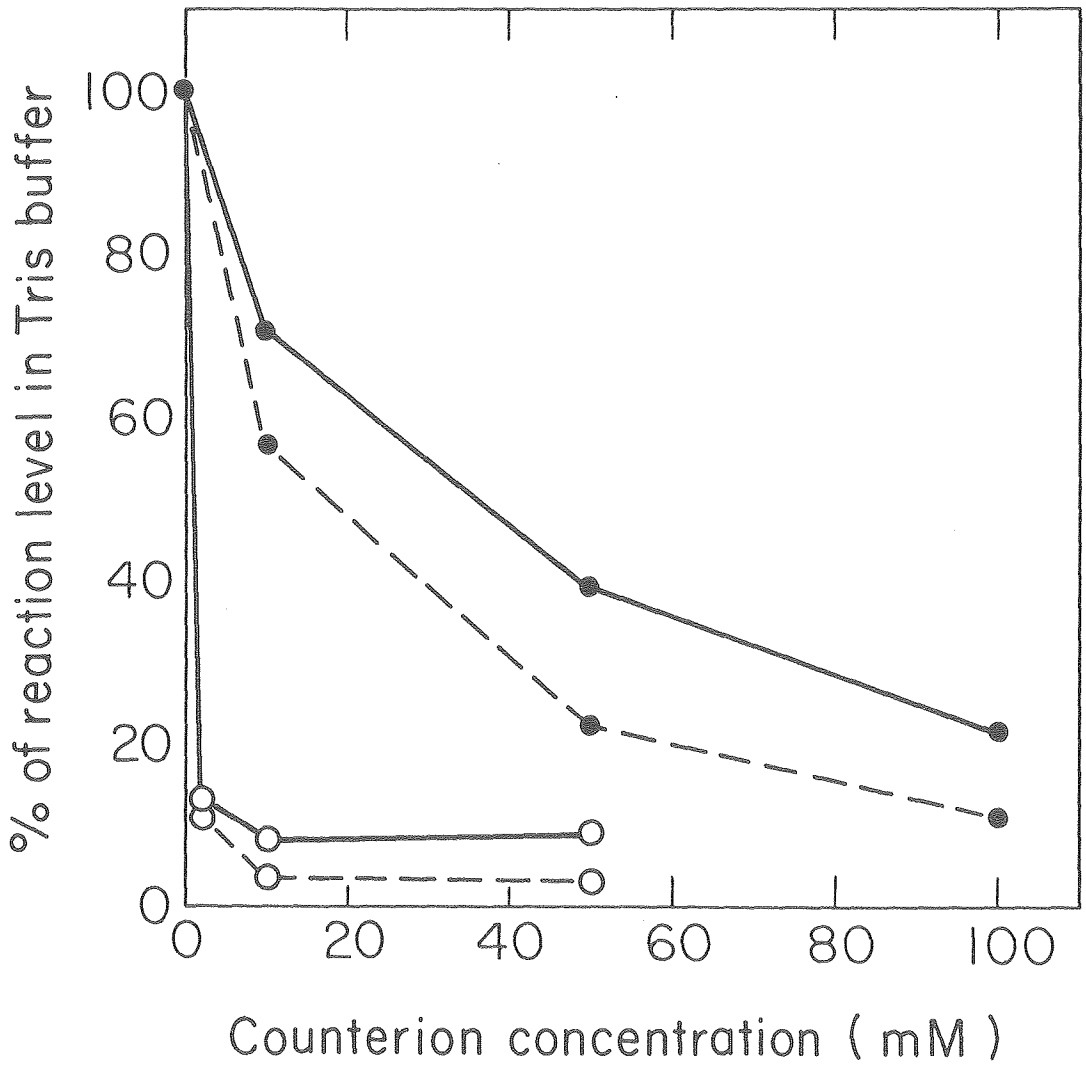
% of reaction level in Tris buffer
100
80
60
40
20
0
0
20
40
60
80
100
Counterion concentration (mM)

XBL 795-4812

shoulder on a BaP tetraol peak. The low recovery and the contamination with BaP tetraol precluded characterization of the hydrocarbon phosphate adduct as either a phosphotriester or a phosphodiester. Although a phosphodiester would be expected from rearrangement of the triester, it could also arise from reaction of the diol epoxide with contaminating [^{32}P]-monobutyl phosphate. Given this ambiguity, the small amount of adduct found does not conclusively demonstrate triester formation.

In an attempt to indirectly detect phosphotriester formation and subsequent rearrangement by the mechanism outlined in Figure 7, the monobutyl phosphate content of BaP diol epoxide and BaP tetraol reaction mixtures with dibutyl phosphate was determined by thin layer chromatography either immediately after reaction or following heating at 85^{o} for 15 min. If BaP diol epoxide formed phosphotriesters, they would be expected to rearrange to phosphodiesters with release of n-butyl alcohol. Upon exposure to brief heating or to the high pH of the chromatography solvent, the diesters should rapidly convert through an S_N1 mechanism to monobutyl phosphate and BaP tetraol. Thus an increase in monobutyl phosphate content would be indicative of phosphotriester formation with subsequent hydrolysis through a cyclic intermediate. No significant increase in monoester content was found even after heat treatment (Table 1). A maximal increase of 0.12% would have been expected from the frequency of DNA strand scission, assuming it was mediated by phosphotriester hydrolysis.

A second approach undertaken to detect phosphotriester induced nicking involved reacting each of the four homopolydeoxyribonucleotides with BaP diol epoxide and analyzing for degradation by gel electrophoresis. If nicking occurred through a triester mechanism then each of the

Table 1.

Percent Monobutyl Phosphate Present in Dibutyl Phosphate*

Sample	% ± standard deviation	
	After 24 hr at 37°	After additional 15 min at 85°
Control	0.56 ± 0.09	---
BaP tetraol treated	0.56 ± 0.04	0.51 ± 0.05
BaP diol epoxide treated	0.53 ± 0.02	0.59 ± 0.01

* [^{32}P]-dibutyl phosphate was reacted with BaP tetraol or BaP diol epoxide (molar reaction ratio = 5.0) at 37° for 24 hr. The % monobutyl phosphate was determined by TLC. Each % is an average from at least 4 determinations. The reaction protocol and TLC analysis are described in Chapter 2.

polymers should have been degraded. The experiment with poly(dT) could be particularly revealing since the diol epoxide does not react with thymidine (6). After reaction, ethyl acetate extraction, and gel electrophoresis, the tracings in Figures 17 and 18 were obtained. Electrophoresis was from left to right with the modified polymer in the lower track and the control above it. At a molar reaction ratio of 4.0, poly(dA), poly(dG), and poly(dC) were degraded while poly(dT) was unaffected. No degradation was observed with BaP tetraol controls.

The selectivity of strand scission is consistent with nicking originating from a base modification as opposed to a phosphate or deoxyribose modification. The extensive degradation of poly(dA) may reflect reaction of BaP diol epoxide with the N-3 position while the lesser degradation of poly(dG) and poly(dC) may reflect reaction at the N-7 and O^2 positions, respectively. It is interesting to note that the three degraded polymers, unlike poly(dT), possess secondary structure. Poly(dA) and poly(dC) are single-stranded helices with base stacking (104-106) and poly(dG) is a four-stranded helix with base stacking and hydrogen bonding (107). In contrast, poly(dT) is a random coil with little or no base stacking (104). Hybridization of poly(dT) to poly(dA) imparts secondary structure to the former polymer but does not facilitate its degradation by BaP diol epoxide (Figure 17). This counters the possible argument that phosphotriesters are formed on each polymer but are able to rearrange with strand scission only when the bound hydrocarbon is properly oriented by a helix.

Conclusive evidence against phosphotriester induced strand scission is provided by the molecular weight integrity of BaP diol epoxide modified RNA. Strand scission of alkylated RNA is considered diagnostic for

Figure 17.

Electrophoretic pattern of poly(dT), poly(dA), and poly(dA)·poly-(dT) after prior reaction with BaP diol epoxide or BaP tetraol. The DNA homopolymers (25-75 μg) were reacted in 100-200 μl of 20 mM Tris-HCl (pH 8.0)-10-20% DMSO with BaP diol epoxide or BaP tetraol at a molar reaction ratio of 4.0. After 24 hr at 37^{o} the homopolymers were extracted with ethyl acetate to remove unreacted hydrocarbon and electrophoresed as described in Chapter 2. Poly(dA)·poly(dT) and poly(dG) were electrophoresed in formamide to minimize secondary structure. The gels were stained with toluidine blue O, photographed, and scanned. The upper track (—) contained homopolymer reacted with BaP tetraol and the lower track (---) contained the same homopolymer reacted with BaP diol epoxide. Electrophoresis was from left to right.

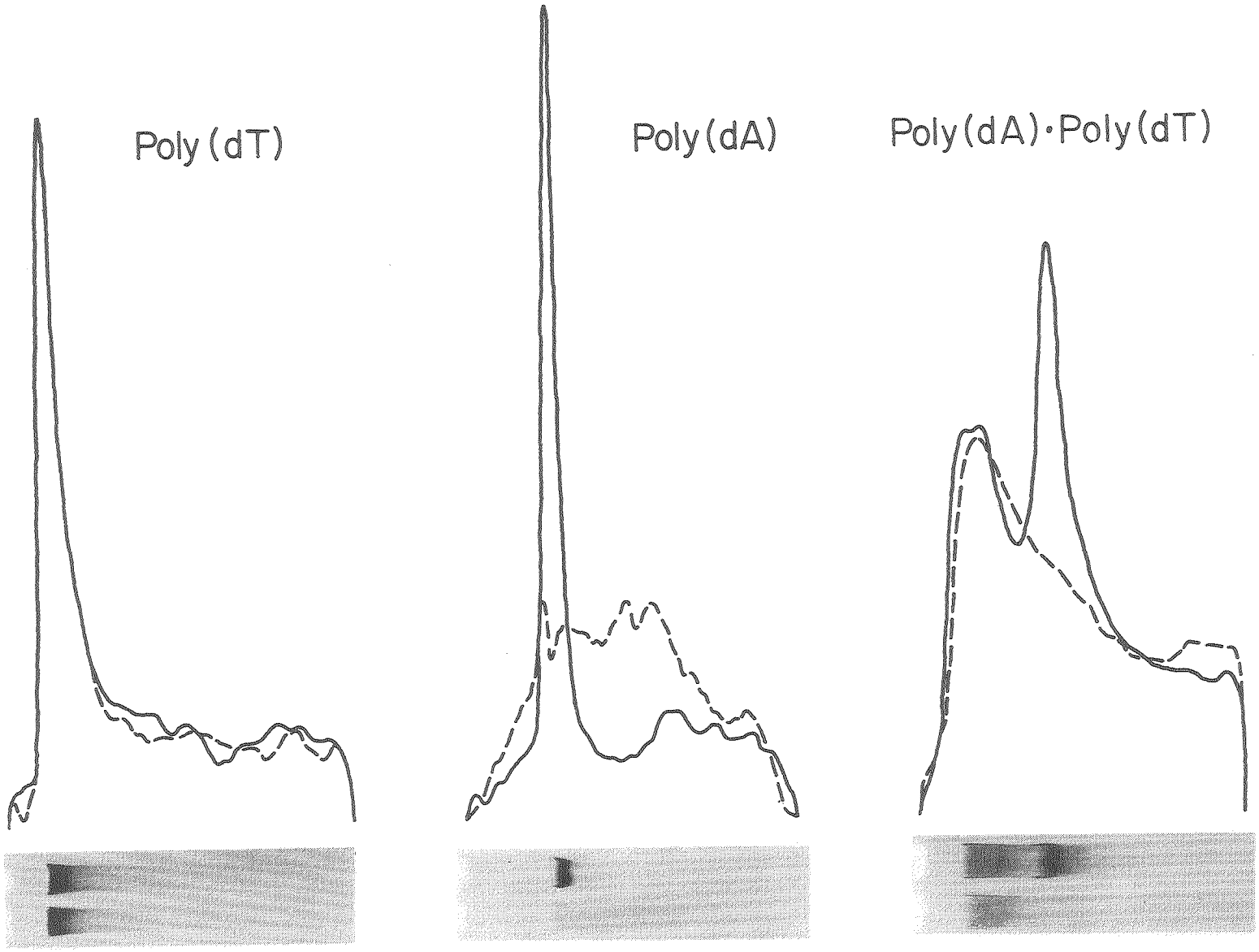

XBB 781-1008

Figure 18.

Electrophoretic pattern of poly(dC) and poly(dG) after prior reaction with BaP diol epoxide or BaP tetraol. See legend to Figure 17.

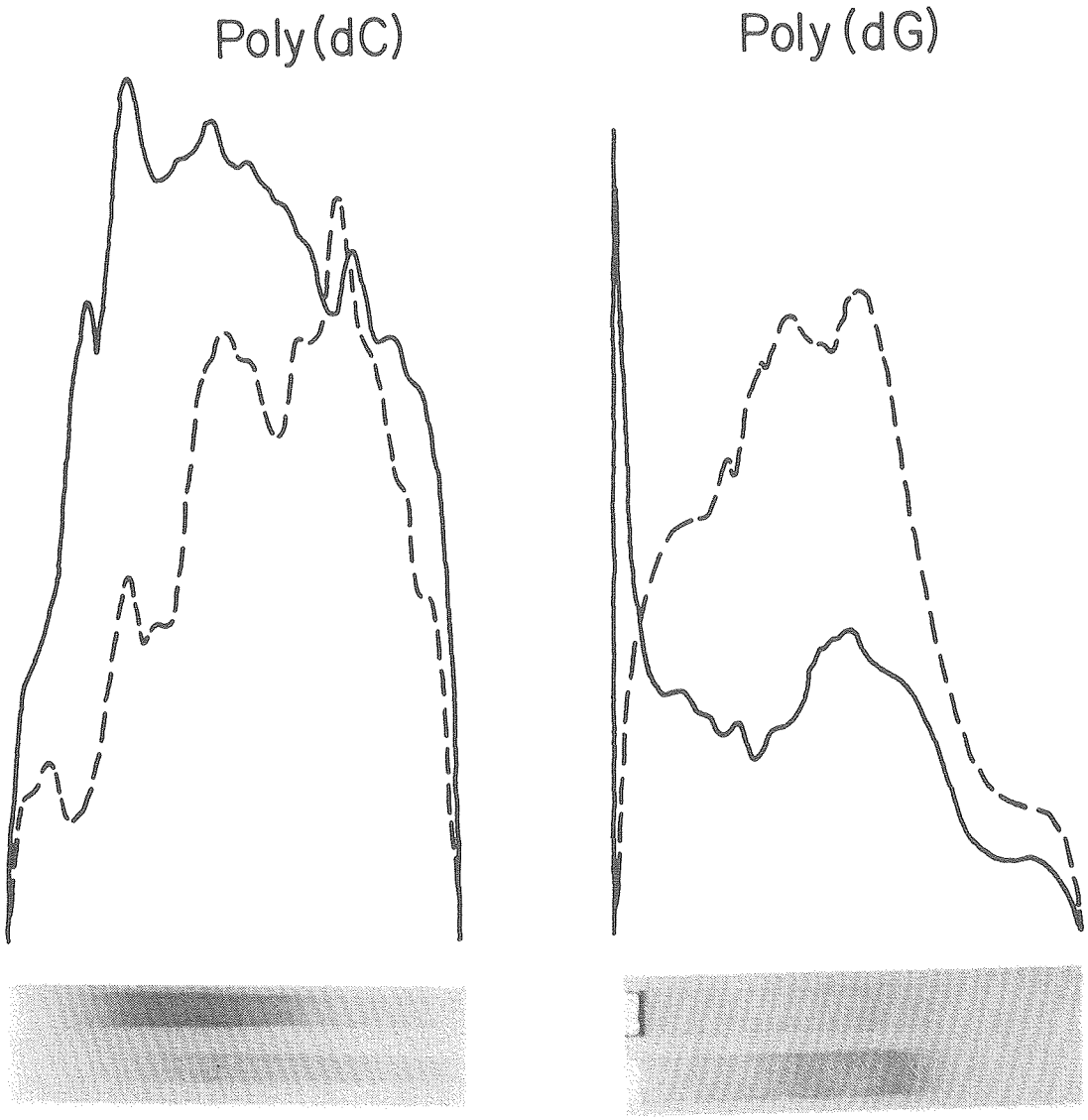

XBB 781-1005

phosphotriester hydrolysis (89), and I previously reported that MS2 RNA was so degraded by BaP diol epoxide (49). However, a more careful study with TMV RNA failed to demonstrate nicking even after several hours incubation at high molar reaction ratios (Figure 19). Alkylation of the viral RNA disrupted secondary structure (see Chapter 4) but did not induce strand scission. A similar conclusion regarding strand scission was reached by Shooter et al. (97) with bacteriophage R17 RNA.

If phosphotriesters are formed in DNA and RNA, they rearrange to diesters with exclusive loss of the hydrocarbon. In DNA the loss is mediated by an S_N1 mechanism, while in RNA it could proceed through a cyclic triester intermediate as well. The half-life of the putative phosphotriesters is unknown. It is possible that they are extremely short-lived, in which case a mechanism is provided for the catalytic hydrolysis of BaP diol epoxide in the presence of nucleic acid. If this is so, the hydrocarbon phosphate adducts detected by Koreeda et al. (12) could represent terminal phosphodiesters.

Susceptibility of BaP Diol Epoxide Modified DNA to Apurinic Endonuclease. With phosphotriester induced nicking unlikely, DNA strand scission by BaP diol epoxide is probably attributable to the loss of alkylated bases followed by rearrangement of apurinic/apyrimidinic sites. The existence of such sites in alkylated SV40 DNA was probed with apurinic endonuclease. This enzyme, which nicks the helix adjacent to free sugars, was purified to homogeneity by C. Falce. Viral DNA, modified with a concentration series of BaP diol epoxide, was incubated with a saturating amount of apurinic endonuclease 2 hr and 24 hr after addition of the hydrocarbon and analyzed for nicking by gel electrophoresis. For comparison, parallel DNA samples were assayed at the same time for

Figure 19.

Polyacrylamide-agarose slab gel of TMV RNA reacted with BaP diol epoxide. TMV RNA (2.6 μg in 55 μl of 20 mM Tris-HCl, pH 8.0-0.5 mM EDTA-10% DMSO) was incubated at 37^{o} with BaP diol epoxide at hydrocarbon to RNA mononucleotide ratios of (a) 0, (b) 0.05, (c) 0.10, (d) 0.20, (e) 0.30, (f) 0.40, (g) 0.60, (h) 0.80, (i) 1.0, (j) 1.5, (k) 2.0, and (l) 3.0. After 6 hr the reaction mixtures were extracted with ethyl acetate and electrophoresed downward for 4 hr at 150 V on a 2% polyacrylamide-0.5% agarose slab gel. The gel was stained with acridine orange.

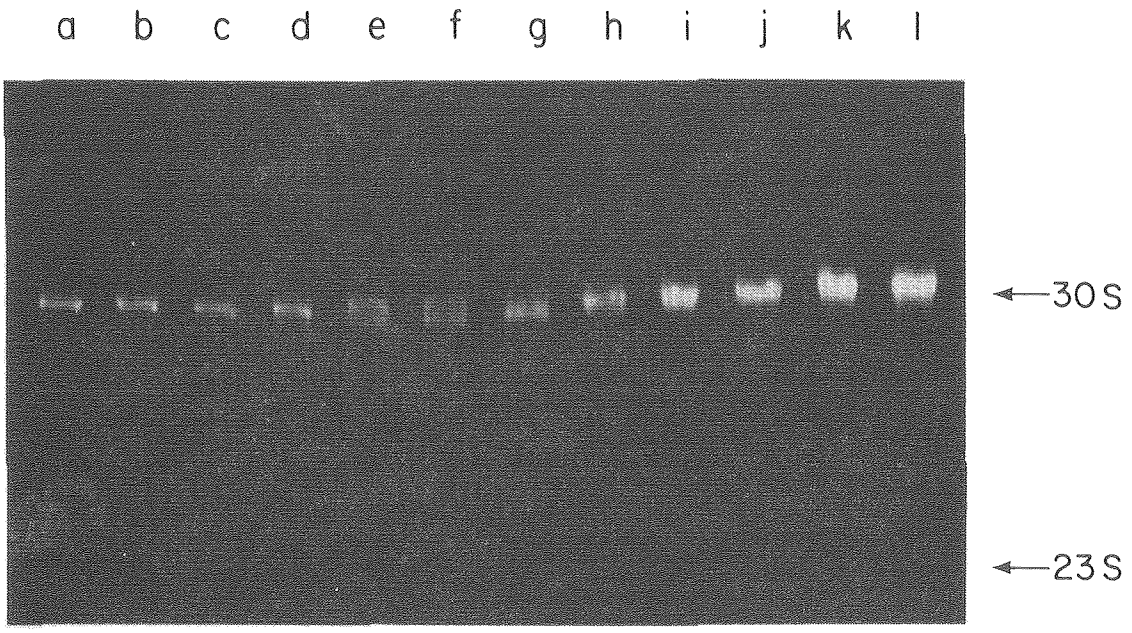

CBB 780-13406

spontaneous and alkali catalyzed strand scission. The results are presented in Figure 20.

The plots demonstrate that BaP diol epoxide modified DNA is a substrate for apurinic endonuclease. The apurinic/apyrimidinic sites appeared rapidly and were readily detectable after 2 hr incubation. These sites probably arise from depurination of the N-7 guanine adduct characterized by Osborne et al. (16), although release of labile adenine and cytosine derivatives, implicated by the homopolymer studies, may occur to a slight extent. Given the respective half-lives of 3 hr and 16 hr for depurination and β-elimination, the level of apurinic sites at 2 hr incubation is entirely consistent with spontaneous nicking occurring at such sites, especially at lower molar reaction ratios.

At both reaction times, treatment of modified SV40 DNA with alkali generated far more strand scission than did reaction with apurinic endonuclease. Therefore apurinic/apyrimidinic sites represent only a fraction of the total alkali labile sites present in modified DNA. The remaining sites, which account for up to 4% of the modification, have not been characterized. Recently, Mizusawa and Kakefuda (56) reported that heat-alkali treatment of BaP diol epoxide modified Col E1 DNA led to strand scission at the sites of alkylation. Their results, however, were not clearcut since Col E1 DNA, which contains RNA segments, exhibited appreciable strand scission in the absence of BaP diol epoxide modification. Nonetheless, this observation suggests that the major N^2 guanine adduct slowly rearranges to an alkali labile product under physiological conditions. Such a product could account for the alkali catalyzed nicking I have observed. In light of this possibility, I intend to verify the putative rearrangement by determining if strand

Figure 20.

Comparison of strand scission elicited by apurinic endonuclease and alkali treatment of BaP diol epoxide modified SV40 DNA. [^{14}C]-SV40 form I DNA (12.5 μg/ml in 20 mM Tris-HCl, pH 8.0-0.5 mM EDTA-10% DMSO) was reacted with BaP diol epoxide at the indicated molar reaction ratios. After (a) 2 hr and (b) 24 hr incubation at 37^{o} three sets of 50 μl aliquots were withdrawn. One set was layered onto 5.0 ml alkaline sucrose gradients and centrifuged. The other two sets were electrophoresed on a 1.4% agarose slab gel after incubation for 10 min at 37^{o} with either 0 E.U. or 0.005 E.U. of apurinic endonuclease. The enzyme reaction and the analytical separation of superhelical and nicked circular DNA are described in Chapter 2. (●), gel electrophoresis after apurinic endonuclease treatment; (o), gel electrophoresis after mock apurinic endonuclease treatment; (□), alkaline sucrose gradient centrifugation.

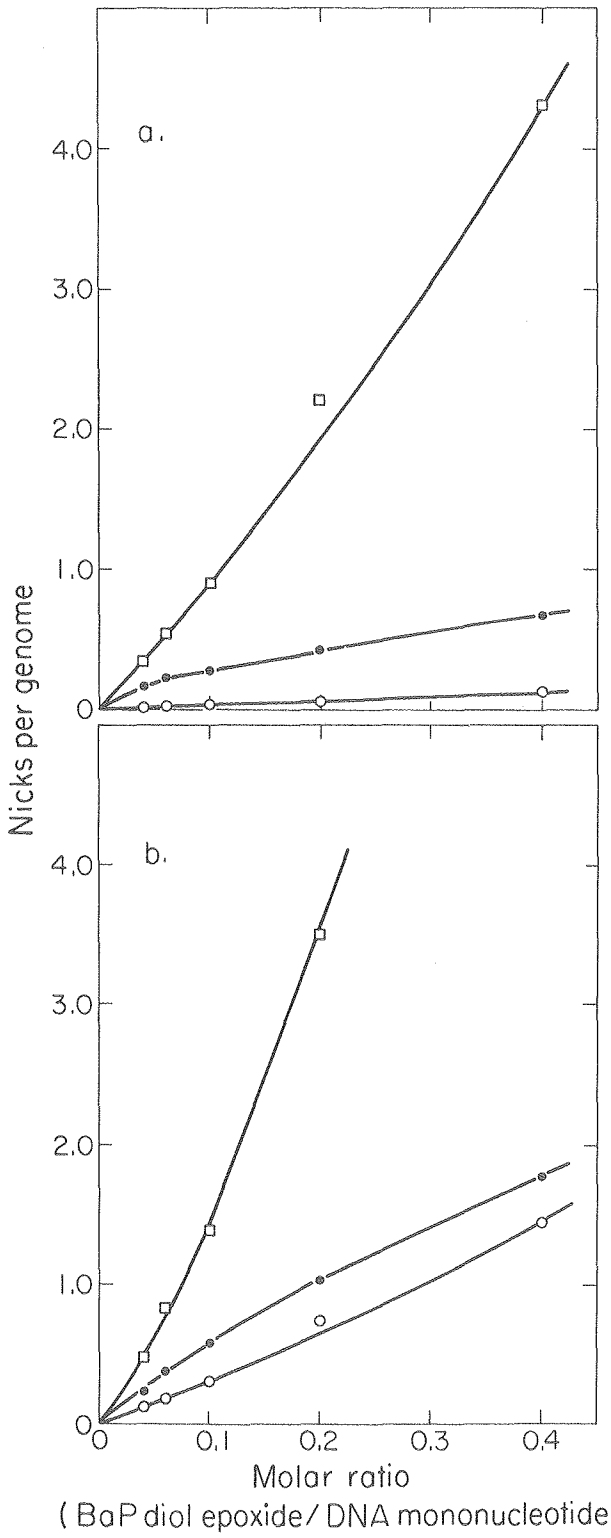
a.
b.
4.0
3.0
2.0
1.0
0
0
0.1
0.2
0.3
0.4
Nicks per genome
Molar ratio
(BaP diol epoxide/ DNA mononucleotide)

XBL796-4815

scission is equivalent to BaP diol epoxide binding after heat-alkali treatment of modified SV40 DNA.

Summary. Approximately 1% of BaP diol epoxide DNA alkylation sites rearrange with strand scission at neutrality. Two mechanisms, phosphotriester hydrolysis and depurination/depyrimidination strand scission, have been proposed to account for this phenomenon (49,97). Both explain the catalysis of nicking by alkali and the inhibition of nicking by counterions. The kinetics of nicking, however, are characteristic of a multistep rearrangement such as depurination/depyrimidination strand scission. Characterization of a BaP diol epoxide N-7 guanine adduct which rapidly depurinates (16,17) and detection of apurinic sites in BaP diol epoxide alkylated DNA also support this mechanism. The number of such sites, especially at lower molar reaction ratios, is probably sufficient to account for strand scission. There is no direct evidence for nicking occurring through phosphotriester hydrolysis. Studies with model substrates, including dibutyl phosphate, DNA homopolymers, and TMV RNA, indicate that if BaP diol epoxide does form phosphotriesters in DNA, they do not rearrange by the mechanism in Figure 7.

Besides apurinic/apyrimidinic sites, a second alkali labile rearrangement product is present in BaP diol epoxide modified DNA. These latter sites accumulate with time and after 24 hr represent as much as 4% of the initial alkylation events. Although relatively stable at neutrality, they spontaneously nick the DNA backbone at high pH. It is possible that these sites arise from a rearrangement of the major N^2 guanine adduct.

Chapter 4: DNA Unwinding

Introduction. Several groups have independently characterized the primary adduct between BaP diol epoxide and DNA as a trans addition product between the N^2 amino group of guanine and the C-10 position of the hydrocarbon (7,11,14,15). To better understand the biological consequences of this adduct it is important to know its physical structure and microenvironment. In this chapter I will discuss how BaP diol epoxide binding to DNA is modulated by ionic strength and superhelicity and also how the resultant adducts decrease the helical density of both superhelical and covalently closed partially relaxed SV40 DNA. The results lead to definite conclusions about the microenvironment of physically and covalently bound BaP diol epoxide in DNA.

The unique topology of covalently closed DNA, either superhelical or relaxed, makes it an ideal system in which to study how the structure of the DNA helix is affected by the addition of large polycyclic adducts, such as BaP diol epoxide. These topological relationships are set forth by the equation (108,109)

$$\alpha = \tau + \beta \qquad (1)$$

where α is the topological winding number, τ is the number of superhelical turns, and β is the number of helical turns in the molecule. For a covalently closed circular DNA α is necessarily integral and invariant. In naturally occurring DNAs β and τ have opposite polarities. Thus an unwinding of the helix is balanced by a decrease in superhelicity, while a winding of the helix leads to an increase in superhelicity.

For superhelical SV40 DNA in 0.2 M NaCl at 37^{o} β = ca. 520 and τ = 24-26 (110-112). It is apparent that a small percentage change in β leads to a large percentage change in τ. Under appropriate electrophoretic conditions the mobility of covalently closed circular DNA is a sensitive function of its superhelicity (74,111,112). As the superhelicity of the molecule is reduced its mobility decreases and eventually coincides with that of nicked circular DNA. Further unwinding of the helix introduces superturns of opposite polarity and is accompanied by an increase in electrophoretic mobility. The detection of very small changes in helical density through concomitant large changes in superhelicity imparts extreme sensitivity to the technique.

In the investigation of BaP diol epoxide induced strand scission it was observed that increasing modification of form I SV40 DNA led not only to strand scission but also to decreased electrophoretic mobility and broadening of the remaining form I band in agarose gel electrophoregrams (Figures 3 and 13). At the highest reaction level still containing covalently closed DNA, the form I band had almost merged with the form II band. The form I band pattern was unaffected by longer reaction periods prior to gel analysis. This eliminates strand scission of the superhelical DNA during electrophoresis as the cause of the observed pattern, leaving as the most likely explanation BaP diol epoxide induced unwinding of the DNA helix.

Three mechanisms exist by which exogenous molecules unwind the DNA helix: intercalation, denaturation, and external binding. Calculation of the Bap diol epoxide unwinding angle (degree of helix unwinding per bound hydrocarbon residue) should help characterize the unwinding mode and therefore the physical structure of the adduct.

The concept of intercalation was proposed 18 years ago by Lerman et al. (113) and has since been demonstrated for the physical binding to DNA of a wide variety of compounds including ethidium bromide (114,115), proflavine (116), 9-aminoacridine (117), actinomycin (118), and benzo[a]-pyrene (119). All of these compounds possess a planar aromatic nucleus which is able to insert itself between and parallel to two adjacent base pairs. The stacking complex is stabilized by several interactions including π-π electron overlap, hydrophobic bonding, and van der Waals forces. These interactions actually increase the T_m of DNA. Recently, intercalative binding has also been demonstrated for covalently bound psoralen derivatives (102,120).

Intercalation requires that the two adjacent base pairs separate from one another sufficiently to accomodate the bound drug; this local lengthening of the helix causes unwinding. The unwinding angle for intercalative drugs varies from 12^{o} for daunomycin (121) and bleomycin (122) to $26\text{-}28^{o}$ for ethidium bromide (111,112,120,123,124). The local lengthening of the helix varies from 2.0-3.7 $\mathring{A}$ (125). Intercalative unwinding of form I DNA leads to the removal and reversal of supercoiling (126) which can be monitored as an initial fall and later rise in sedimentation coefficient or electrophoretic mobility. Intercalative drugs increase the intrinsic viscosity of DNA by increasing both the persistence length (a measure of rigidity) and the molecular length (127). This leads to a decrease in both the sedimentation coefficient and the electrophoretic mobility of nicked circular DNA. As will be discussed later, the level of intercalative binding is positively modulated by superhelicity and negatively modulated by ionic strength.

Recently, two modifications of the classical intercalation model have been proposed. Each explains the existence of excluded sites and is based on a postulated structure for B-form DNA. Sobell et al. (127) proposed a model based on the X-ray crystallographic structure of ethidium-dinucleoside monophosphate complexes. They postulated that intercalating drugs insert into DNA at naturally occurring bends or kinks. In the resultant complex the adjacent base pairs are twisted and tilted and the helical screw axis is dislocated. In contrast, the linear dichroism study by Hogan et al. (125) indicated that intercalation occurs with no net bending or kinking of the helix axis. Their data, however, suggested that intercalating drugs are not oriented 90^{o} to the helix axis as generally thought but are tilted from perpendicularity by 21 ± 7^{o}. This tilt is consistent with the propeller-twister DNA model proposed by Levitt (128) in which the bases are not coplanar but rather propeller twisted with respect to each other by 35^{o}. Intercalation of a rigidly planar heterocycle flattens the two adjacent base pairs. In so doing the entire complex must be tilted to be accomodated in the DNA. Obviously, the acceptance of either intercalation model must await further characterization of the dynamic structure of DNA in aqueous solution.

Base pair denaturation is the second mode by which the double helix can be unwound. Formaldehyde (129), carbodiimide (130), and dichlorodiammineplatinum (131) covalently bind to and denature DNA. The former two compounds react with single-stranded regions normally present in duplex DNA because of the dynamic breathing of the helix or the existence of hairpins. The reaction site of dichlorodiammineplatinum is unknown. At low levels of modification these reagents increase the sedimentation coefficient and electrophoretic mobility of superhelical

Figure 21A.

Polyacrylamide slab gel of superhelical SV40 DNA reacted with BaP diol epoxide. [^{14}C]-SV40 form I DNA ($\bar{\tau}$ = -21.0; 2.12 µg in 250 µl of 20 mM Tris-HCl, pH 8.0-0.5 mM EDTA-10% DMSO) was reacted for 90 min at 37^{o} with [^{3}H]-BaP diol epoxide at molar reaction ratios of (a) 0.002, (b) 0, (c) 0.005, (d) 0.01, (f) 0.02, (g) 0.04, (i) 0.06, (j) 0.10, and (l) 0.15. Aliquots (200 µl) were extracted with ethyl acetate, precipitated with ethanol, combusted, and counted to determine the level of alkylation. The remaining reaction mixtures were electrophoresed downward for 72 hr at 100 V on a 22 cm long 2% polyacrylamide-0.5% agarose slab gel (74). Tracks e, h, and k contained 0.43 µg of partially relaxed form I SV40 DNA prepared as described in Chapter 2.

Figure 21B.

Agarose slab gel of partially relaxed SV40 DNA reacted with BaP diol epoxide. Partially relaxed [^{14}C]-SV40 form I DNA ($\bar{\tau}$ = -6.56) was prepared by incubating 18.8 µg of form I DNA with 140 E.U. of relaxing enzyme for 15 min at 37^{o} as described in Chapter 2. The partially relaxed DNA was precipitated with ethanol and reacted in 20 mM Tris-HCl (pH 8.0)-0.5 mM EDTA-10% DMSO with [^{3}H]-BaP diol epoxide at molar reaction ratios of (c) 0, (d) 0.02, (f) 0.04, (g) 0.06, (i) 0.10 and (j) 0.15. Reaction mixtures contained 2.42 µg of DNA in 230 µl. After 3 hr at 37^{o} 175 µl aliquots were removed for determination of covalent binding as described above. The remaining mixtures were electrophoresed downward for 16 hr at 50 V on a 1.4% agarose slab gel. Tracks b,

e, h, and k contained 0.56 μg of a mixture of SV40 DNA incubated for 15 min and for 20 min with DNA relaxing enzyme. Track a contained 0.50 μg of superhelical form I SV40 DNA.

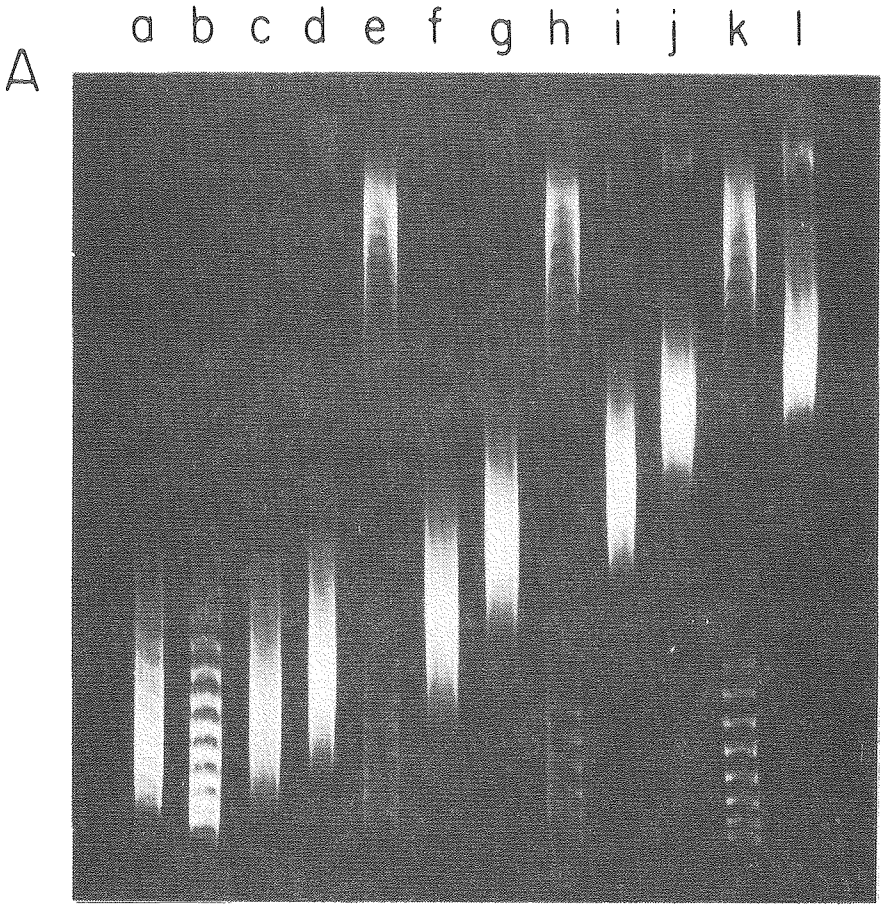

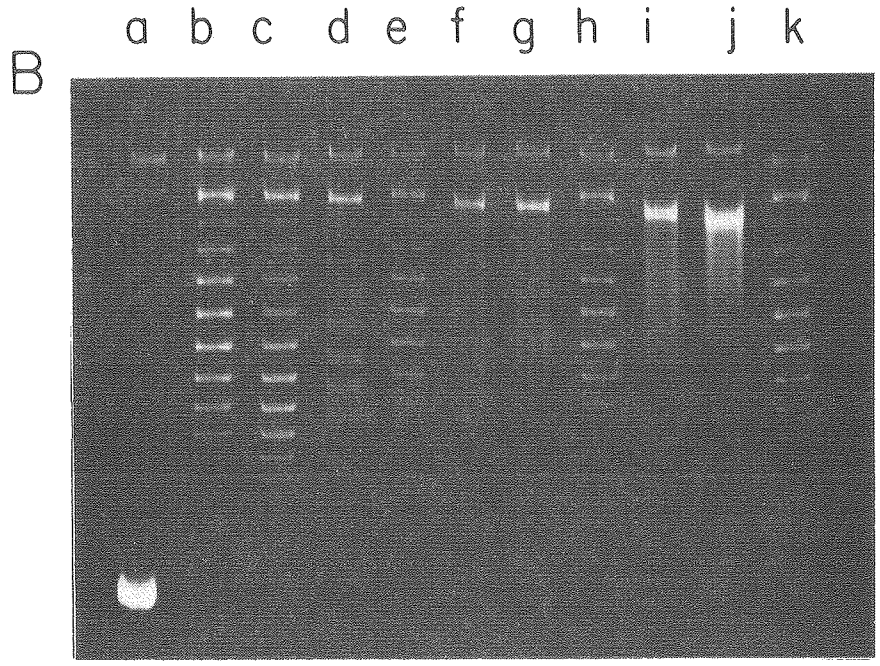

XBB 795-6963

cular DNAs with low superhelical densities (120). The slow moving band present in every track of the agarose gel is unresolved low molecular weight cellular DNA.

BaP diol epoxide alkylation of both DNA substrates (1.5-44 adducts/genome) led to a loss of fine structure and a reduction in electrophoretic mobility. The decrease in mobility is interpreted as a loss of superturns directly resulting from local unwinding of the DNA helix by hydrocarbon adducts. The loss of fine structure reflects the inability of either gel system to resolve the component DNA bands which result from the presence of a Gaussian distribution of adducts on each parental DNA band. Thus each band in the unreacted DNA is converted into a set of bands too closely spaced to be resolved. These bands differ in superhelicity by the BaP diol epoxide unwinding angle. Both effects are due to covalently bound BaP diol epoxide, since the electrophoretic pattern of DNA treated under identical conditions with BaP tetraol was unchanged (data not shown).

The magnitude of both effects was greater for superhelical than partially relaxed DNA. This was apparent when the mean number of superhelical turns was plotted as a function of the number of adducts per genome for the two DNA substrates (Figure 22). The decrease in slope of the curve for superhelical DNA indicates that hydrocarbon induced unwinding is a function of superhelical density at high $\bar{\tau}$. The nearly linear curve obtained for partially relaxed DNA indicates that unwinding is almost independent of superhelicity at low $\bar{\tau}$.

Table 2 summarizes the data from the unwinding experiments and lists the incremental unwinding angles and open base plates per adduct for superhelical and partially relaxed DNA. The extremely large unwind-

Figure 22.

Removal of superhelical turns by BaP diol epoxide adducts in (a) superhelical and (b) partially relaxed SV40 DNA. Negatives of the gels in Figure 21 were scanned. An average gel position for each of the alkylated DNA samples was determined from the respective tracings and a mean superhelicity ($\bar{\tau}$) was assigned by locating these positions on the trace of a partially relaxed DNA standard run on the same gel. The level of alkylation was determined with separate reaction mixture aliquots as described in Chapter 2.

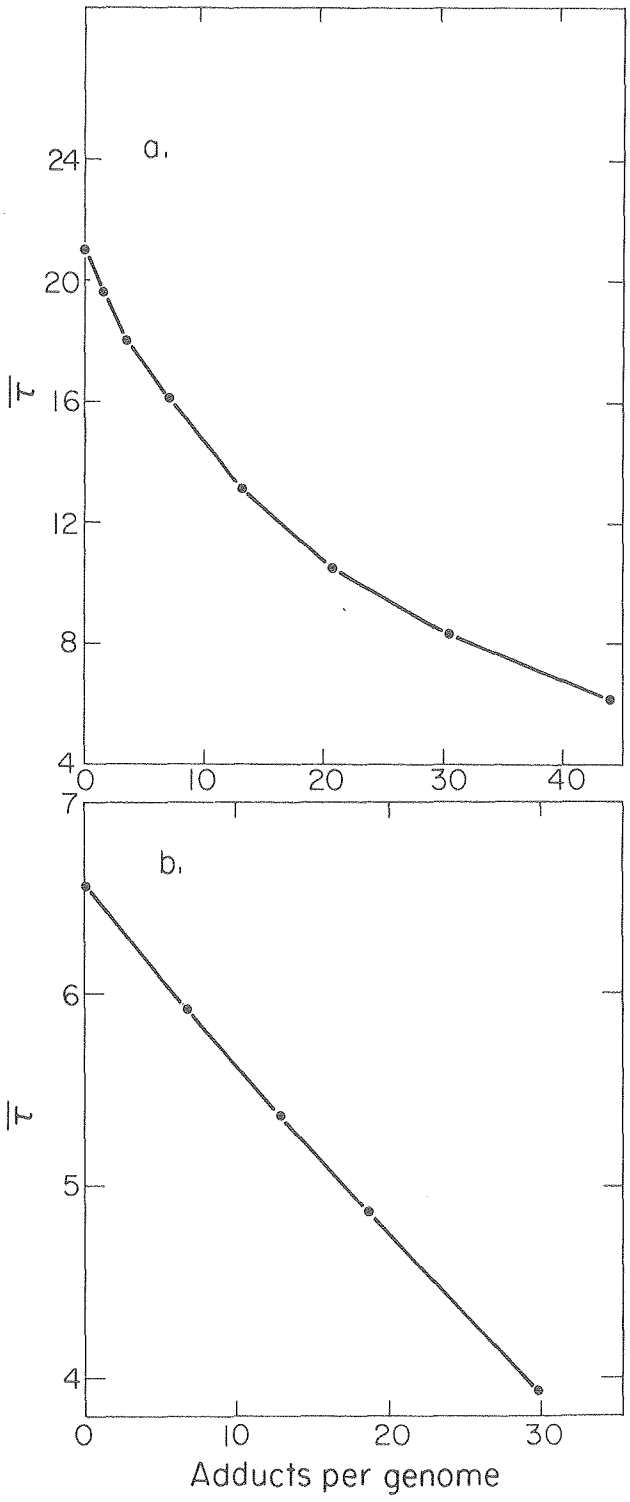
a.
24
20
16
12
8
4
$\bar{\tau}$
0
10
20
30
40
b.
7
6
5
4
$\bar{\tau}$
0
10
20
30
Adducts per genome

XBL796-4817

Table 2.

Unwinding of Superhelical and Partially Relaxed SV40 DNA by BaP Diol Epoxide*

Molar Ratio	Adducts per Genome	Decrease in $\bar{\tau}$	Incremental Relaxation per Adduct: Open base plates	Incremental Relaxation per Adduct: Unwinding angle
Superhelical DNA ($\bar{\tau}$ = 21.0)				
0.005	1.54	1.4	9.1	328°
0.01	3.53	3.0	8.0	290
0.02	7.10	4.9	5.3	192
0.04	13.2	7.9	4.9	177
0.06	20.7	10.5	3.5	125
0.10	30.5	12.7	2.2	81
0.15	43.9	14.9	1.6	59
Relaxed DNA ($\bar{\tau}$ = 6.56)				
0.02	6.62	0.64	0.97	35.1°
0.04	12.9	1.20	0.88	31.8
0.06	18.6	1.70	0.87	31.4
0.10	29.7	2.63	0.84	30.3

* Data obtained from Figures 21 and 22.

ing angles obtained with superhelical DNA reflect localized denaturation at the site of alkylation. The degree of denaturation is primarily determined by the superhelicity of the molecule and is probably enhanced by the low ionic strength of the electrophoresis buffer. Reaction of BaP diol epoxide with the exocyclic amino group of guanine impairs hydrogen bonding of the modified base to cytosine (134,135). These destabilized sites can then relieve torsional strain through the occurence of additional denaturation. The release of torsional strain on a per adduct basis decreased with superhelicity and ranged from 4.5-2.2%. The single-stranded regions adjacent to the hydrocarbon adducts are unlikely to be stabilized by intrastrand hairpins, since BaP diol epoxide modification of the SV40 genome is a random event, even at low reaction levels (136).

In the absence of significant torsional strain, the unwinding angle plateaued at about 31^{o} suggesting a distinct structure for the hydrocarbon DNA complex. The most likely physical structure involves destabilization or disruption of the modified G-C base pair and localization of the hydrocarbon in either the minor or major groove. Consistent with this model is the increased electrophoretic mobility of BaP diol epoxide modified form II DNA in agarose gels. In Figure 10, where the quantity of DNA in the form II band remained constant, this effect is seen without the added complication of band overloading. By acting as flexible "hinges", the alkylation sites decrease the intrinsic viscosity of the nicked circular DNA and increase its mobility. Similar changes are induced by dichlorodiammineplatinum (131). Intercalating agents act in the opposite fashion (132). They stabilize base pairs, lengthen and stiffen the helix, and increase the intrinsic viscosity of DNA.

In Chapter 3 it was shown that BaP diol epoxide both depurinates and nicks DNA. It is important when determining the unwinding angle of BaP diol epoxide modified guanine that the electrophoretic pattern observed actually represent the unwinding of the helix by this adduct and not strand scission or depurination. At a molar reaction ratio of 0.10, the highest level employed with partially relaxed DNA, approximately 1 alkylation event out of 150 will give rise to strand scission over a 24 hr period. The frequency of depurination is about the same. This is equivalent to 0.20 nicks or apurinic sites in a SV40 DNA molecule containing 30 adducts. The local unwinding associated with depurination is insignificant given the infrequency of the event. The effect of strand scission, however, is far more dramatic since it leads to an entire loss of superhelical turns. Prior to electrophoretic analysis, strand scission removes DNA molecules from the unwinding angle determination. Preferential removal of DNA molecules with higher than mean values of superhelicity or alkylation may occur. As discussed by Wiesehahn and Hearst (120), these phenomena exert slight opposing effects on the calculated unwinding angle which can probably be neglected.

Strand scission during the time span of electrophoresis could lead to a significant overestimation of the unwinding angle by decreasing the mobility of the DNA. The frequency of strand scission increases with the number of adducts. In Figure 21 the tailing of the covalently closed DNA bands at higher molar reaction ratios is probably due to nicking during electrophoresis. The effect of nicking on the unwinding angle calculations was minimized for partially relaxed DNA by measuring the mobility in terms of the most intense band, which was resolvable up to a molar reaction ratio of 0.10. The same approach was precluded for superhelical

DNA by the loss of band structure at very low levels of modification, and the unwinding angles calculated from this substrate are therefore overestimated at higher molar reaction ratios. The magnitude of this error is indicated by a comparison of the incremental unwinding angles from superhelical and partially relaxed SV40 DNA samples with similar torsional strain, i.e. 59^{o} and 35^{o}, respectively, at $\bar{\tau} = -6$.

The lower intrinsic viscosity of modified DNA and the single-stranded character of the alkylation sites in superhelical DNA will partially offset the effect of nicking by enhancing the electrophoretic mobility of covalently closed DNA. In both cases, however, the enhancement is minor. The 10% greater mobility of alkylated form II DNA relative to control is attributed to an increased flexibility. Given the more compact structure of superhelical and partially relaxed DNA, the increased flexibility will exert a proportionately smaller effect on the mobility of these molecules. In addition, the single-stranded alkylation sites in superhelical DNA will likely collapse in the low ionic strength electrophoresis buffer, thus shortening the molecules and increasing their mobility. Here, again, the effect is minor since even at a molar reaction ratio of 0.15 only 3% of the base pairs are denatured.

Another possible objection to my unwinding data is that the decreased electrophoretic mobility of BaP diol epoxide modified covalently closed DNA might be due to a structural effect other than local unwinding of the helix at the site of alkylation. For example, Hsieh and Wang (137) have found the sedimentation coefficient of superhelical DNA containing bound ethidium to be different from that of free DNA with the same superhelical density. In response, it can be stated that at the

low levels of modification employed in these studies other structural alterations in the DNA are unlikely. In the absence of a reasonable alternative, the decreased electrophoretic mobility is taken to reflect local unwinding.

My interpretation of the unwinding angle data has implicitly assumed that alkylation of SV40 DNA results in almost exclusive formation of N^2 guanine adducts. This assumption was tested in collaboration with K. Straub by determining the adduct distribution in SV40 DNA modified with BaP diol epoxide at a molar reaction ratio of 0.04. After modification, the viral DNA was freed of BaP tetraol and enzymatically degraded to mononucleosides. The hydrocarbon modified nucleosides were isolated by LH-20 Sephadex chromatography and analyzed by HPLC. The HPLC profile for superhelical DNA is shown in Figure 23. The fluorescent peaks, derived from hydrocarbon modified calf thymus DNA carrier, permitted identification of the radioactive adducts from SV40 DNA. Noting that BaP diol epoxide is an enantiomeric mixture and that each enantiomer can potentially react by cis or trans addition at the C-10 position, peaks 3, 5, and 6 are deoxyguanosine adducts, peaks 7, 8, and 9 are deoxyadenosine adducts, and peaks 2 and 4 are deoxycytidine adducts (6-8). All of these nucleosides are probably alkylated at the exocyclic amino position (N^2 of guanine, N^6 of adenine, and N^4 of cytosine). Peak 1 and part of peak 4 represent BaP tetraol. The two early eluting radioactive peaks probably represent BaP diol epoxide solvent addition products. The four modified nucleoside peaks obtained from alkylated form I SV40 DNA represent trans addition of the (+) and (-) BaP diol epoxide enantiomers to the N^2 and N^6 positions of guanine and adenine. Quantification of the peaks showed that 86% of the reaction

Figure 23.

High pressure liquid chromatography profile of co-injection of [^{3}H]-BaP diol epoxide SV40 DNA adducts plus unlabeled BaP diol epoxide calf thymus DNA adducts. SV40 form I DNA (5 µg in 440 µl of 20 mM Tris-HCl, pH 8.0-0.5 mM EDTA-10% DMSO) was reacted with [^{3}H]-BaP diol epoxide at a molar reaction ratio of 0.04. After 3 hr at 37^o the DNA was extracted with ethyl acetate, ethanol precipitated, and enzymatically digested to mononucleosides. The modified nucleosides were isolated by Sephadex LH-20 chromatography and analyzed by HPLC. The fluorescence profile represents unlabeled BaP diol epoxide adducts derived from alkylated calf thymus carrier DNA.

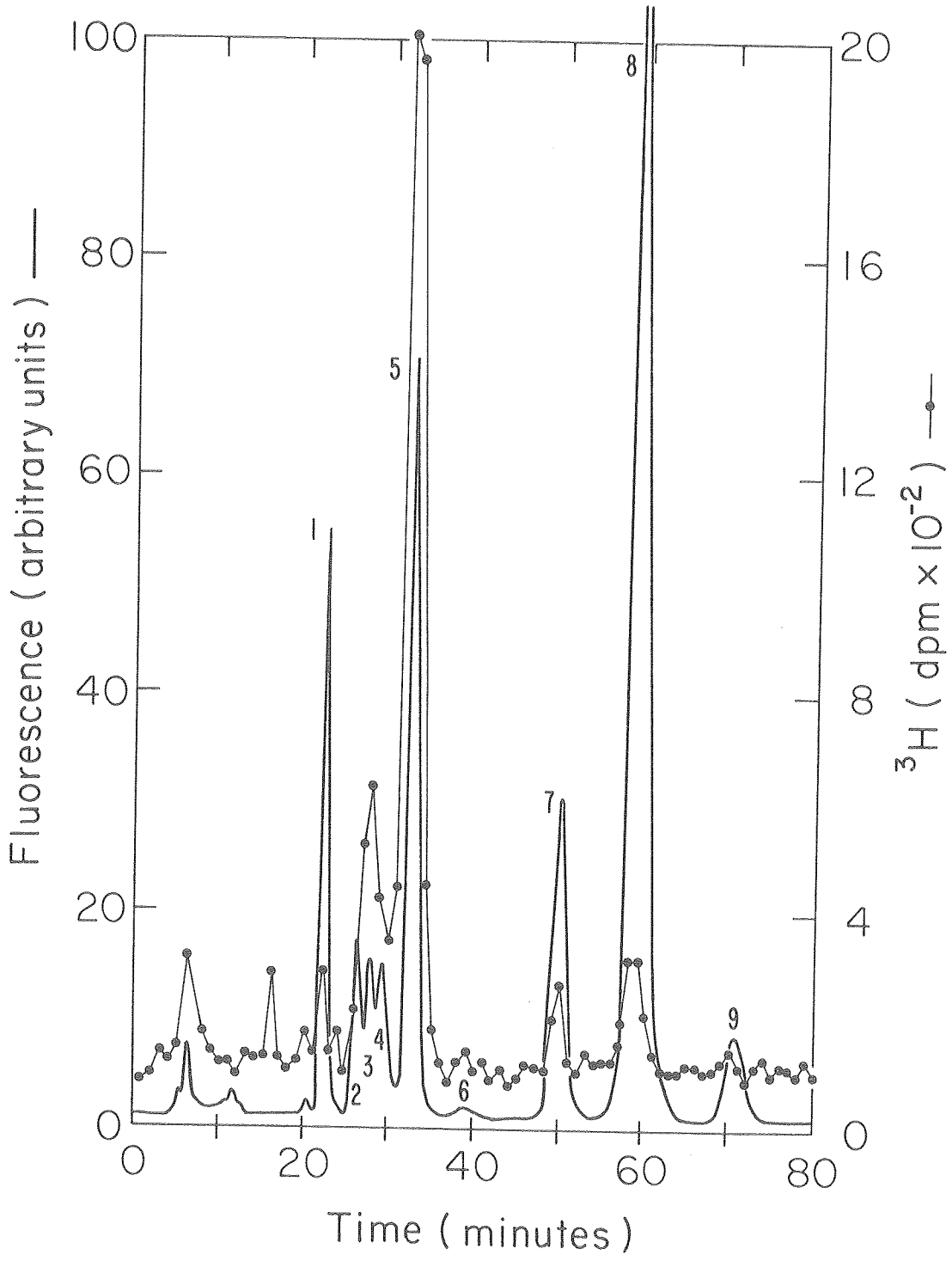
Fluorescence (arbitrary units)
^{3}H (dpm x 10^{-2})
Time (minutes)
0
20
40
60
80
100
4
8
12
16
1
2
3
4
5
6
7
8
9

XBL796-4816

was with guanine and 14% with adenine. There was no detectable reaction with cytosine. A similar reaction pattern was obtained for partially relaxed SV40 DNA (see Table 4).

The reaction with adenine complicates analysis of the unwinding angle data. If the unwinding angle of the adenine adduct is significantly different from that of the guanine adduct, then an average value will be obtained and interpretation could be misleading. Fortunately, there is no reason to expect a large difference. Since the N^6 position of adenine is involved in base pairing, binding of BaP diol epoxide to that site will probably disrupt the A-T base pair. In superhelical DNA, where torsional strain amplifies the unwinding angle, both adducts should have identical unwinding angles. In partially relaxed DNA, the two unwinding angles may be slightly different but both should reflect local denaturation.

Physical Structure of BaP Diol Epoxide Adducts. Superhelical SV40 DNA reacted with BaP diol epoxide and filtered through nitrocellulose exhibited an alkylation dependent adsorption (Figure 24). Identical samples incubated with BaP tetraol were not retained. The relatively high molar reaction ratios required to obtain substantial filter binding indicated that a large number of modified sites (~30-60 adducts per genome) were required for stable binding. Nitrocellulose filters selectively bind single-stranded DNA; however, polycyclic aromatic hydrocarbons such as BaP tetraol are also bound. Therefore adsorption of modified superhelical DNA is due to the presence of single-stranded regions and/or externally bound hydrocarbon adducts. Since the DNA retained on the filter was strongly adsorbed and could not be readily washed off, changes in superhelical density per se did not contribute to the reten-

Figure 24.

Adsorption of BaP diol epoxide modified SV40 DNA to nitrocellulose filters. [^{14}C]-SV40 form I DNA was reacted with BaP diol epoxide for 1 hr at 37^{o} in 110 µl of 20 mM Tris-HCl (pH 8.0)-0.5 mM EDTA-10% DMSO. The modified DNA (0.84 µg) was diluted with 5.0 ml of 50 mM Tris-HCl (pH 8.2)-1 M NaCl and filtered through a Schleicher & Schuell type B-6 0.45 µ pore size filter. The filters were washed with 5.0 ml of 0.03 M sodium citrate-0.3 M NaCl, dried, and counted in Permafluor I.

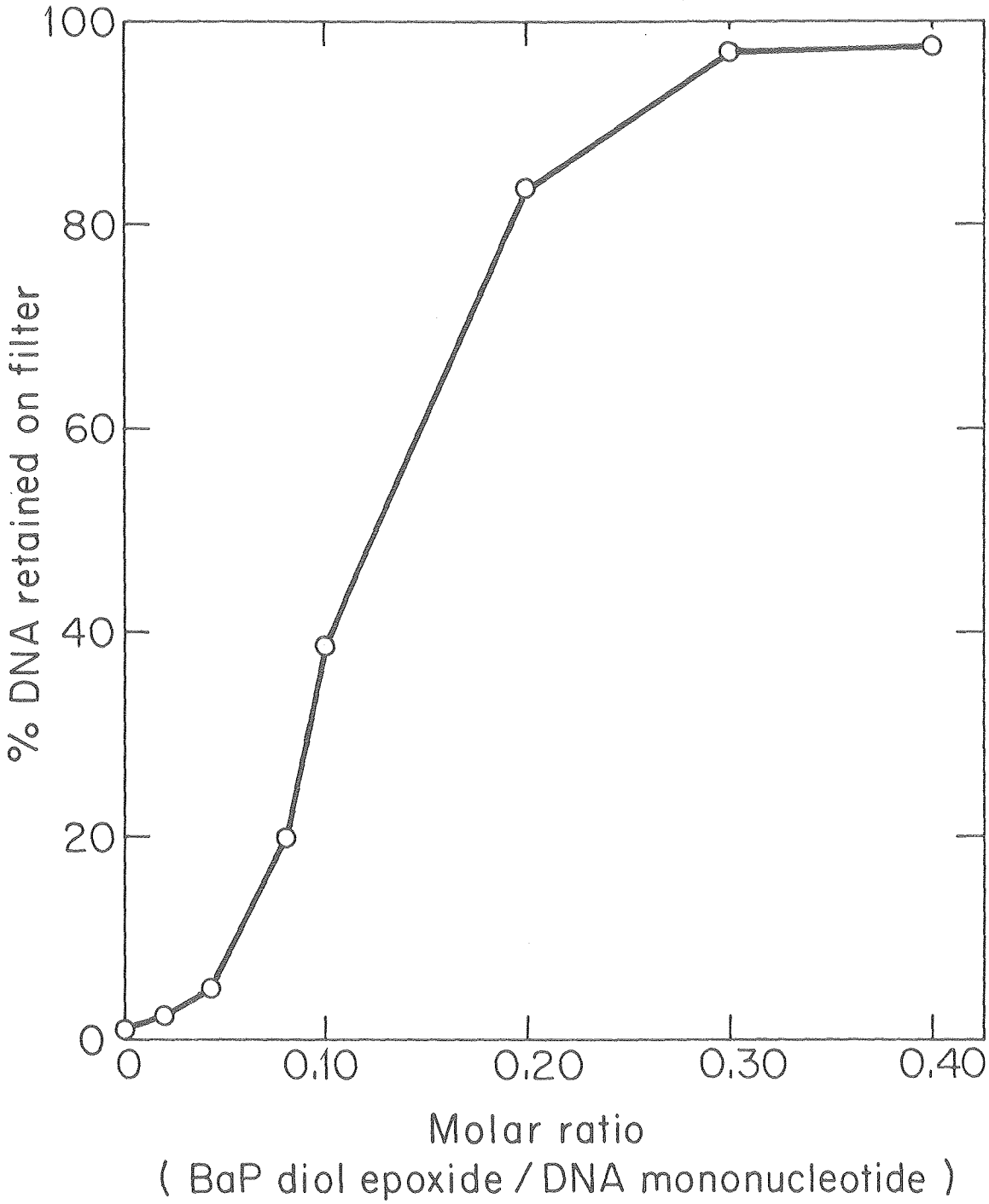
100
80
60
40
20
0
% DNA retained on filter
0
0.10
0.20
0.30
0.40
Molar ratio
(BaP diol epoxide / DNA mononucleotide)

XBL798-4971

tion (138).

When BaP diol epoxide modified form I DNA was briefly exposed to pH 12.3 buffer as described by Kuhnlein et al. (79) there was only a slight shifting of the adsorption curve to lower reaction ratios. Since this pH denatures form II DNA but does not affect form I, the slight percentage increase in adsorption is due to denaturation of nicked circular DNA originally present in the DNA preparation or generated by BaP diol epoxide reaction and subsequent alkali catalyzed strand scission. These results indicate that hydrocarbon modified form I DNA is resistant to irreversible denaturation at pH 12.3. The binding of modified form II SV40 DNA to nitrocellulose filters was not further investigated.

A more direct visualization of the helix destabilization was provided by electron micrographs of SV40 DNA containing 1 BaP diol epoxide adduct per 5 base pairs (Figure 25). This highly fragmented DNA contains the forks and bubbles characteristic of partial denaturation.

Further evidence for BaP diol epoxide induced helix destabilization was fortuitously provided by the single-stranded RNA of tobacco mosaic virus. In a study of the backbone stability of this RNA towards BaP diol epoxide, I found that the RNA underwent a conformational change (Figure 19). After reaction with a concentration series of BaP diol epoxide, the modified TMV RNA was electrophoresed and the gel was stained with the metachromatic dye acridine orange (77). Acridine orange intercalates into double-stranded nucleic acid and this type of nucleic acid-dye interaction results in green fluorescence at 530 nm upon excitation with blue (488 nm) light. In contrast, acridine orange stacks on single-stranded nucleic acids and the dye-dye interactions

Figure 25.

Electron micrographs of SV40 DNA extensively alkylated with BaP diol epoxide. SV40 form I DNA was reacted in 20 mM Tris-HCl (pH 8.0)-0.5 mM EDTA-10% DMSO for 24 hr at 37^{o} with BaP diol epoxide (molar reaction ratio = 3.24) and prepared for electron microscopy as described in Chapter 2. The DNA in micrograph A is highly fragmented and some of the fragments appear to be partially denatured. Selected fragments with this morphology are enlarged in micrographs B and C. The bar equals 0.5 μ in A and 0.2 μ in B and C.

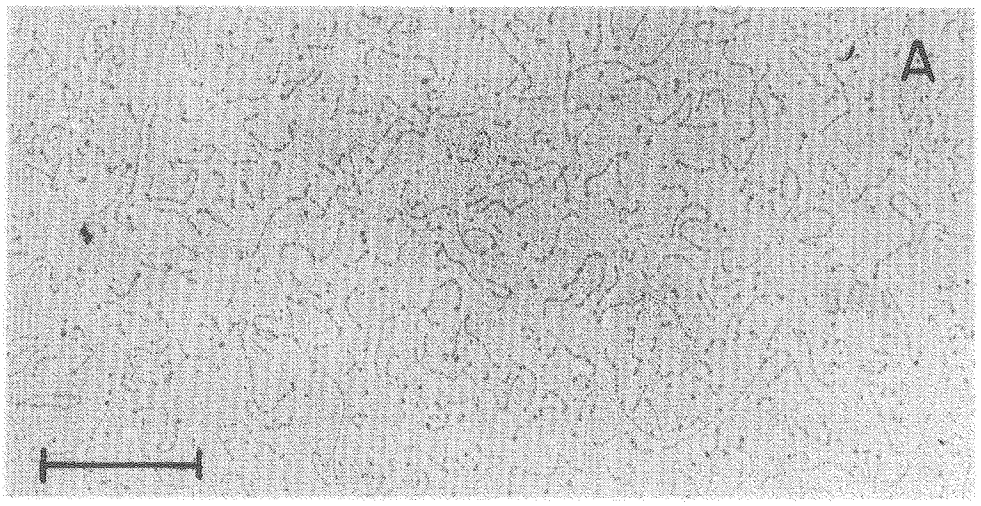

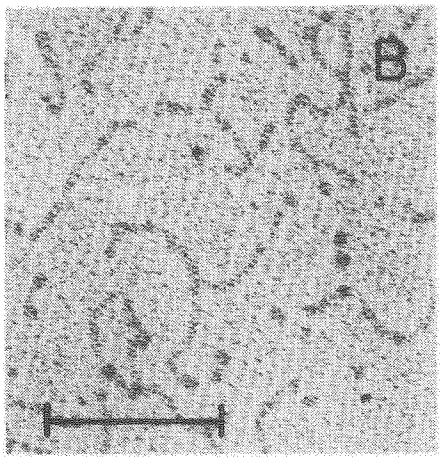

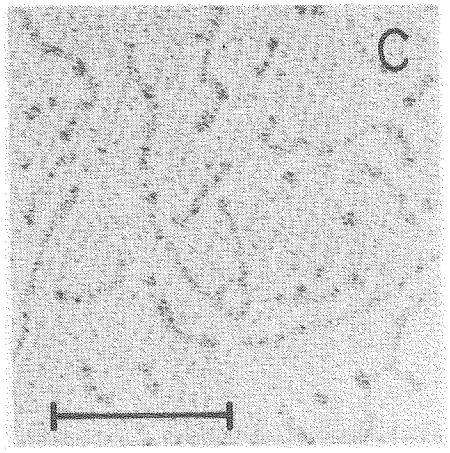

XBB 798-11012

due to dye stacking are manifested in red metachromasia (640 nm). The green fluorescence of native TMV RNA indicates the presence of considerable secondary structure in the molecule despite the low ionic strength of the electrophoresis buffer, a phenomenon studied in detail by Boedtker (139). At a molar reaction ratio of 0.20-0.40 there was a distinct conformational change in the RNA induced by BaP diol epoxide. The abrupt mobility increase appeared to correlate with the appearance of red fluorescence and the loss of secondary structure. Assuming binding efficiencies comparable to SV40 DNA, the loss of secondary structure was brought about by the presence of ~10 adducts per 10^3 nucleotides. As is the case with DNA, reaction with RNA occurs primarily at the N^2 position of guanine (9,12). The sensitivity of TMV RNA secondary structure to BaP diol epoxide modification is indicative of the decreased stability of base pairs in RNA relative to DNA (140). The decrease in electrophoretic mobility of TMV RNA at higher levels of modification probably reflects a molecular weight increase due to alkylation, while the increased staining intensity of the modified RNA may be due to interaction of acridine orange with bound BaP diol epoxide.

Date from the literature also supports the idea of localized denaturation at BaP diol epoxide alkylation sites. Several groups have reported that the diol epoxide sensitizes DNA to S_1 endonuclease (141-144). Although Kakefuda and Yamamoto (143) found preferential release of deoxyadenosine adducts, Yamasaki et al. (144) found that S_1 solubized deoxyguanosine adducts as well. In a detailed study of the conformation of calf thymus DNA modified by BaP diol epoxide, Pulkrabek et al. (141) found that the DNA exhibited a slightly decreased T_m and a slightly increased susceptibility to formaldehyde. The kinetics of for-

maldehyde reaction provided evidence for locally destabilized regions ranging from 1 to 7 base plates, depending on the extent of modification.

During the period of my unwinding experiments Drinkwater et al. (50) published a study on the removal and reversal of superturns in SV40 DNA by BaP diol epoxide and N-acetoxy-2-acetylaminofluorene (AAAF). By employing short reaction times and rapid electrophoretic analysis, strand scission was minimized and recoiling of the covalently closed DNA was observed at high adduct levels. The level of covalent binding required to cause comigration of superhelical DNA with nicked circular DNA was 0.049 and 0.050 adducts/nucleotide for BaP diol epoxide and AAAF, respectively. From the corresponding value for physically intercalated ethidium bromide (0.042) and its published unwinding angle (26^{o}), an average unwinding angle of 22^{o} was calculated for the two carcinogens. By analogy with the known conformation of the major AAAF adduct in DNA, Drinkwater et al. (50) proposed a "covalent intercalative" mode of binding for BaP diol epoxide. After covalent linkage to the N^{2} position of guanine the pyrene nucleus of the hydrocarbon was postulated to insert into the helix coplanar to the base pairs with simultaneous rotation of the modified guanine about its glycosidic linkage to a position outside the helix. Such a conformation is consistent with the circular dichroism of BaP diol epoxide modified GpU (145). This model has been documented for AAAF and is referred to as "base displacement" (132) or "insertion-denaturation" (146-149).

Unlike classical intercalation, binding of AAAF to the C-8 position of guanine destabilizes the helix by disrupting a G-C base pair. A comparison of the destabilization of calf thymus DNA by AAAF and BaP

diol epoxide (Table 3) shows that while both decrease the T_m of modified DNA and increase its sensitivity to S_1 nuclease and formaldehyde, AAAF has a greater effect (150). This suggests that the modes of binding may not be identical and that the similarity in unwinding angles may be fortuitous.

It is difficult to reconcile the unwinding angle obtained by Drinkwater et al. (50) with the values presented here. Instead of monitoring incremental relaxation, they measured total relaxation of the superhelix and obtained an average value of 22^{o}. This is below the range of unwinding angles reported here and may be due to the extensive alkylation required for comigration of DNA forms I and II (~500 adducts per genome). At high modification the alkylation sites may interact and so possess an altered conformation with a reduced unwinding angle. Extensive alkylation may also change the spectrum of adducts as well as alter the electrophoretic mobility of the DNA through phenomena other than unwinding. These factors could reduce apparent relaxation.

Is covalent intercalation as proposed by Drinkwater et al. (50) a valid model for BaP diol epoxide adducts at low molar reaction ratios? Obviously not for superhelical DNA, where substantial denaturation accompanies covalent binding. For DNA nearly free of torsional strain, where unwinding angles of $30\text{-}35^{o}$ reflect an ordered physical structure, the model is possible. Other models, however, in which the hydrocarbon remains externally bound are equally plausible.

In several recent papers, Geacintov has investigated the orientation of physically bound BaP (119,151) and covalently bound BaP diol epoxide (151,152) in DNA. By studying the fluorescence quenching and linear dichroism of the bound hydrocarbons, he conclusively showed that

Table 3.

Comparative Effects of Modification of the Bases in DNA with AAAF or BaP Diol Epoxide*

	AAAF	BaP diol epoxide
Decrease in T_m	1.1^o	0.75^o
Formaldehyde unwinding: Relative fraction open base plates	0.172	0.023
Average number open base plates per modified base	12-13	0-1
S_1 nuclease digestion	15%	0%

* From data of Fuchs and Daune (147) and Weinstein et al. (150). Extrapolated to a 1% modification of the total bases.

BaP was intercalated while BaP diol epoxide adducts were externally bound. Thus, physically bound BaP was oriented almost 90^{o} to the DNA axis and was susceptible to "internal" fluorescence quenchers while covalently bound BaP diol epoxide was oriented 35^{o} to the DNA axis and was susceptible to "external" fluorescence quenchers. Although Yang et al. (153) have argued that the fluorescence quenching of DNA bound BaP diol epoxide is indicative of covalent intercalation, Geacintov has clearly showed that this phenomenon can be attributed to concentration dependent intermolecular DNA-DNA interactions and is consistent with external binding of the hydrocarbon.

The fluorescence quenching and linear dichroism studies cannot differentiate between localization of BaP diol epoxide adducts in the minor or major grooves or in locally denatured regions of DNA. Taking into account my unwinding data, it is apparent that while the covalent binding sites are denatured under conditions of strain (i.e. superhelicity, extremes of pH, high temperature, etc.), these sites possess an ordered structure under physiological conditions. In vivo, BaP diol epoxide modification of DNA probably unwinds the helix by $30\text{-}35^{o}$. The major perturbation induced by covalent binding and the probable cause of unwinding is destabilization if not complete disruption of the modified G-C base pair (134,135). The hydrocarbon could reside in the minor groove since the exocyclic amino group of guanine is found there. Computer modeling indicates that only minor perturbation of the helix is caused by this orientation of the adduct (154). Alternatively, the hydrocarbon could reside in the more exposed major groove; that would require a 180^{o} rotation of the modified guanine about its glycosidic linkage.

Physical Structure of the BaP Diol Epoxide DNA Reaction Complex. While a large amount of effort has been expended in characterizing the microenvironment of the BaP diol epoxide adduct, little is known about the corresponding reaction complex. Evidence to be presented in this section favors intercalation of BaP diol epoxide prior to its reaction with deoxyguanosine as originally proposed by Meehan and Straub (8). Intercalation orients the hydrocarbon within the helix and so explains the stereoselective reaction of enantiomeric BaP diol epoxide with DNA. BaP readily intercalates into DNA and it is expected that BaP diol epoxide, which retains the flat aromatic pyrene nucleus, should do so as well. Model building studies indicate that intercalated BaP diol epoxide can react with the exocyclic amino group of guanine.

The extent of reaction of double stranded DNA with BaP diol epoxide is modulated by the conformation of the double helix. When the helix is stabilized by addition of counterions to the solvent, there is a significant inhibition of BaP diol epoxide alkylation. The inhibition of binding by Na^+ and Mg^{2+} ions is shown in Figure 16 and is comparable to similar data for the photobinding of psoralen derivatives, agents known to intercalate and crosslink DNA (102). Both ions bind electrostatically to the negatively charged phosphates of DNA. By shielding the phosphates these ions wind the helix and decrease base pair separation thereby increasing the free energy barrier to intercalation (155). At the highest concentrations tested, both ions inhibited BaP diol epoxide modification of DNA by about 90%. Hydrocarbon binding was far more sensitive to Mg^{2+} than Na^+, reflecting the greater stabilization of the double helix by Mg^{2+} relative to Na^+ (99). The differential inhibition by the two ions argues that they reduce binding by changing the confor-

mation of DNA rather than by interacting with BaP diol epoxide.

A similar phenomenon may be responsible for the preferential alkylation of internucleosomal DNA in chromatin. Although SV40 minichromosomal DNA is uniformally alkylated (see Chapter 5), internucleosomal DNA of cellular chromatin is 2-4 times more susceptible to BaP diol epoxide alkylation than nucleosomal DNA (98,144,156). The intercalative photobinding of psoralen derivatives to chromatin exhibits an even greater selectivity for internucleosomal DNA (157,158). In both cases the positively charged histone cores probably act like counterions tightening the helix and reducing intercalation within the nucleosome.

BaP diol epoxide binding to SV40 DNA is also modulated by torsional strain. At identical molar reaction ratios the modification of superhelical SV40 DNA was consistently greater than partially relaxed DNA (Table 2). Torsional strain present in superhelical DNA facilitates any binding mode which unwinds the helix. The reduction of superhelical turns adds an extra favorable free energy term to the binding and enhances affinity relative to relaxed DNA. In the following analysis the partially relaxed covalently closed DNA in Table 2 is assumed equivalent to nicked circular DNA. For BaP diol epoxide, binding was approximately 6% greater with superhelical relative to relaxed DNA. This compares favorably with the 10% enhancement of reactivity seen with the intercalating agents psoralen (102) and bleomycin (122). These studies employed superhelical and nicked circular Col E1 DNA in low ionic strength Tris-HCl buffers and monitored covalent binding or strand scission, respectively.

The relative affinity of a molecule for superhelical and relaxed forms of a DNA is a function of its unwinding angle and is given by the

relationship (159)

$$\nu_s/\nu_r = e^{-A\phi/kT} \quad (2)$$

where ϕ is the unwinding angle, A is the torsional free energy change per degree of unwinding, and ν_s/ν_r is the partition of the molecule between superhelical and relaxed forms of DNA. For SV40 DNA in Tris-HCl buffer the quantity A is unknown, but it can be estimated from the partition ratios (~1.10) and unwinding angles (28^o and 12^o, respectively) of psoralen (102) and bleomycin (122). If BaP diol epoxide denatures superhelical DNA upon physical binding, just as it does when covalently bound, a high partition ratio would be expected. From equation (2), if $\phi = 280^o$ then ν_s/ν_r = 3-10. This is a minimum estimate since the unwinding angle is not constant and is much smaller with relaxed DNA. The minimum estimate is far greater than the value of 1.06 actually obtained (Table 2) and clearly indicates that BaP diol epoxide disrupts base pairing only after covalent linkage to the guanine exocyclic amino group. The experimental partition ratio is consistent with a small unwinding angle accompanying the physical binding of BaP diol epoxide to both superhelical and relaxed DNA.

Although intercalation prior to reaction is consistent with modulation of BaP diol epoxide binding by positively charged ions and torsional strain, an alternative binding mode is possible but unlikely. BaP diol epoxide might preferentially react with transiently denatured single-stranded regions in duplex DNA. Such a mechanism has been proposed for the carcinogen AAAF (132,147). Hydrogen exchange (160) and formaldehyde titration (161) studies have documented that the duplex structure of DNA at any time contains a small number of denatured base pairs. These transiently denatured regions represent dynamic "breath-

ing" of the duplex. By increasing the ionic strength the base paired duplex is stabilized and breathing is reduced. In superhelical DNA torsional strain destabilizes the helix and is expected to increase breathing. The binding of single strand specific reagents is thus modulated in a fashion similar to intercalating agents. The stereoselectivity exhibited by enantiomeric BaP diol epoxide in binding to deoxyguanosine and deoxyadenosine in both superhelical and relaxed SV40 DNA (Table 4) is indicative of an ordered DNA structure at the site of reaction and does not support preferential reaction of the hydrocarbon with single-stranded DNA. Such a reaction does not exhibit stereoselectivity and leads to increased deoxyadenosine modification (8). The decreases in deoxyguanosine binding and overall stereoselectivity obtained with superhelical relative to relaxed DNA might be significant and could result from a slight reaction of BaP diol epoxide with naturally occurring or hydrocarbon stabilized single-stranded regions in the superhelical DNA. The even greater differences between SV40 and calf thymus DNA probably arise from the 20 fold greater level of modification employed in this study as well as the greater A-T content of SV40 DNA (59.5% versus 56.0%). In any case the adduct profile for SV40 DNA is characteristic of double and not single-stranded DNA.

In order to definitively rule out preferential reaction of BaP diol epoxide with single-stranded regions in SV40 DNA a sequence specificity study was undertaken. In superhelical SV40 DNA there appears to be two broad site specific regions with interrupted secondary structure (162). These locally unwound regions may contain sufficient intrastrand complementarity to permit the formation of hairpin structures which stabilize the transiently separated strands. The two sites are sensitive to S_1

Table 4.

Stereoselectivity in the Reaction of (±) anti-BaP Diol Epoxide with DNA*

Sample	% guanine	Isomer ratio	% adenine	Isomer ratio
Superhelical SV40 DNA	86.0	1:3.03	14.0	1:0.44
Partially relaxed SV40 DNA	86.9	1:3.38	13.1	1:0.38
Calf thymus DNA	90.0	1:21.5	10.0	1:1

* The adduct profile of BaP diol epoxide alkylated SV40 DNA was determined as described in Figure 23. The isomer ratio refers to the ratio of (-) anti to (+) anti-BaP diol epoxide alkylation products. The data for calf thymus DNA was extracted from reference 8.

endonuclease and are modified by carbodiimide, a reagent which covalently reacts with the imino sites of unpaired thymine and guanine bases. Chen et al. (163) have shown that carbodiimide only binds to those Hind II + III restriction fragments containing the S_1 sensitive sites. I have carried out an analogous study with BaP diol epoxide (136). After introducing 2.3 adducts per genome, the superhelical SV40 DNA was digested to completion with Hind III restriction endonuclease and the six fragments generated were isolated by gel electrophoresis and analyzed for the presence of adducts.

The low level of modification employed in the site specificity analysis is comparable to that seen in vivo (84) and had no effect on Hind III digestion. Hydrocarbon induced strand scission was negligible at these levels. Figure 26a shows the distribution of adducts among the six Hind III fragments. The extent of adduct formation was not strictly dependent upon DNA length, and this appeared to reflect variability in the G-C content of the fragments. Those fragments with high G-C content lay above the line, while those with low G-C content lay below. By normalizing the fragment length to 10^3 base pairs, the effect of G-C content on BaP diol epoxide binding was examined (Figure 26b). Within the limited range covered, binding was clearly dependent upon G-C content. A least squares fit of the average values in Figure 26b to linear and exponential curves gave correlation coefficients of 0.93 and 0.94, respectively. Extrapolation of these curves to the homopolymer limits suggested that 95% of the alkylation was restricted to G-C base pairs, in good agreement with the 86% value obtained experimentally.

Figure 26a.

Distribution of BaP diol epoxide adducts among SV40 Hind III restriction fragments. [^{14}C]-SV40 form I DNA was incubated for 24 hr at 37^{o} in 20 mM Tris-HCl (pH 8.0)-0.5 mM EDTA-5% DMSO with [^{3}H]-BaP diol epoxide at a molar reaction ratio of 0.007. The alkylated DNA (2.5 µg in 100 µl) was extracted with ethyl acetate and digested to completion with 10 E.U. of Hind III restriction endonuclease. The 6 fragments were isolated by 2% polyacrylamide-0.5% agarose slab gel electrophoresis, combusted, and counted. The fragments are labeled A through F on the basis of decreasing size. Each point is an average value from at least 5 independent experiments.

Figure 26b.

Linear correlation of BaP diol epoxide binding with % G-C content for SV40 Hind III restriction fragments.

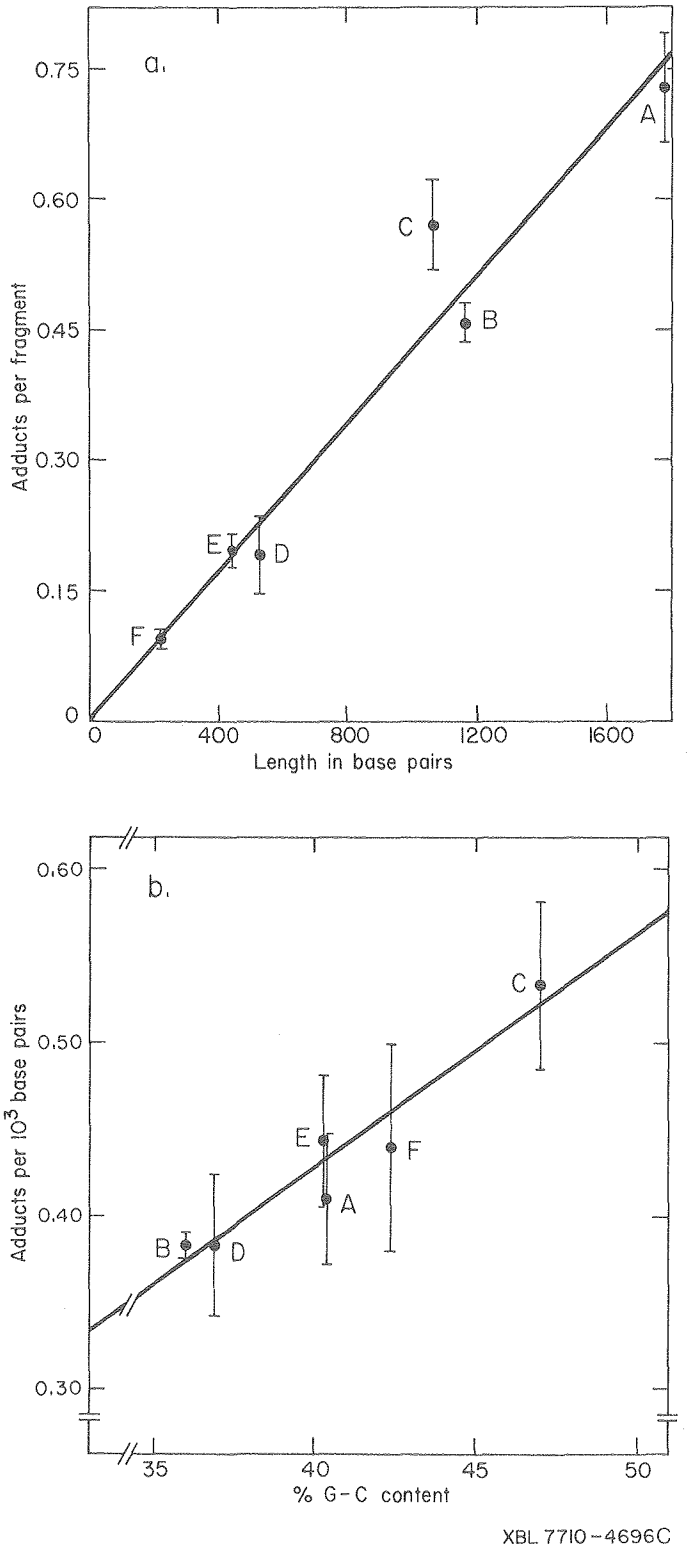

XBL 7710-4696C

Despite the low level of modification, no reaction "hotspots" were detected. The distribution of adducts among the Hind III fragments was solely dependent upon their length and G-C content. This excludes any extended base sequence or secondary structure specificity in the interaction of BaP diol epoxide with DNA and rules out preferential reaction of the hydrocarbon with transiently denatured regions.

A third model, which I have not ruled out, is orientation of the hydrocarbon within the minor groove prior to reaction. While stereoselectivity could be explained by such a model, it is not clear how such external binding would respond to changes in ionic strength and superhelicity. Furthermore, the formation of an external complex is problematical since it would lack both the stacking interactions provided by intercalation and the electrostatic interactions characteristic of external binding.

From the preceding analysis it is likely that BaP diol epoxide intercalates prior to reaction with the exocyclic amino group of guanine, even though that site is relatively exposed in the minor groove. An intercalation model readily explains the stereoselectivity of the reaction and its modulation by nucleosomal histone cores, ionic strength, and superhelicity. Intercalation is accompanied by an unwinding angle of less than 30^{o}, and disruption of base pairing occurs only after covalent linkage. A fluorimetric kinetic analysis of the interaction of BaP diol epoxide with DNA also supports an initial intercalation mode (T. Meehan, J. Becker, K. Straub, unpublished observations). The situation with deoxyadenosine is less clear. Decreased stereoselectivity indicates the hydrocarbon is not as oriented in the helix and suggests that covalent reaction may be preceded by "loose" intercalation or ex-

ternal binding (8).

Chapter 5: Modification of Minichromosomal DNA

Isolation and Characterization of SV40 Minichromosomes. Electron microscopy and nuclease digestion studies have demonstrated that eucaryotic chromatin has a structural repeat unit of approximately 200 base pairs (164-169). Each unit contains a 140 base pair length of DNA coiled around an octamer core consisting of two copies each of the histones H2A, H2B, H3, and H4 (170-172). These structures, referred to as nucleosomes or ν bodies, are joined to one another by relatively exposed spacer DNA. The spacer DNA sections are 40-60 base pairs in length and are complexed with the lysine-rich histone H1 (173,174). The periodic structure of chromatin is reflected in electron micrographs where nucleosomes appear as beads on a thin DNA filament and in staphylococcal nuclease digests where intact nucleosomes are released.

Within the nuclei of infected cells SV40 DNA is associated with cellular histones in a chromatin-like structure called the minichromosome (62,65,175-177). Viral chromatin closely resembles the more complex chromatin of mammalian cells and is replicated and transcribed by the same cellular enzymes (57). Given the physical and genetic simplicity of the SV40 minichromosome, it has proven to be a useful structural as well as functional model for eucaryotic chromatin (62). This chapter describes an investigation of the integrity of BaP diol epoxide modified SV40 minichromosomes and the modulation of DNA alkylation and strand scission by minichromosomal histones.

In low ionic strength solutions ($\mu < 0.1$) the SV40 minichromosome possesses an extended beads-on-a-string morphology (62,65,176,177). Electron micrographs demonstrate a relaxed circular DNA filament containing an average of 24 nucleosomal beads (62). This is exactly the value predicted given the 200 base pair repeat unit length of chromatin, the length of the SV40 genome (5200 base pairs), and the fact that a 400 base pair sequence at the origin of replication in SV40 minichromosomes is exposed (178). Relative to the viral DNA sequence, the nucleosomes occupy a limited number of regularly spaced alternative positions (179). Migration of the nucleosomal histone cores between these positions is believed to occur through a sliding mechanism and is slow (180). Dissociation of the core histones from DNA does not occur at physiological ionic strength (176,180-182). When the minichromosome is deproteinized the resultant form I DNA has 24-26 superhelical turns in 0.2 M NaCl at 37^{o} indicating that, operationally, each nucleosome stabilizes one superhelical turn (110-112).

SV40 minichromosomes containing histone H1 compact dramatically when the ionic strength is raised to 0.1-0.2 (62,78,183). The compaction is accompanied by an increase in sedimentation coefficient from 50-60S to 70-95S relative to form I SV40 DNA (21S). In electron micrographs each minichromosome now appears as a compact spherical particle approximately 300 $\mathring{A}$ in diameter (62,183). Individual nucleosomes can be visualized within the particle. The compact form of the minichromosome, in contrast to its circular beaded form, is totally resistant to staphylococcal nuclease strongly suggesting that the internucleosomal DNA regions are not exposed on the outside (183).

Minichromosomes isolated from lytically infected cells under conditions of low ionic strength and minimal protein degradation contain the entire complement of histones including H1. However, when the same nucleoprotein complex is isolated from purified virions histone H1 is lacking (184,185). There is evidence that this histone is displaced from the minichromosome by viral capsid protein during virion assembly (186). Histone H1 depleted minichromosomes retain the extended beads-on-a-string conformation at physiological ionic strength (62,78,183). This suggests that histone H1 is responsible for formation and maintenance of the compact state of SV40 chromatin and implies a similar role for this histone in cellular chromatin (187).

The viral chromatin employed here was extracted with 0.25% Triton X-100 from nuclei of lytically infected cells at the peak of DNA synthesis approximately 42-44 hr after high multiplicity infection. The yield of minichromosomes was maximized and the loss of histone H1 minimized by extracting the nuclei in the presence of 0.13 M NaCl (66). Enzymatic digestion of the liberated chromatin was inhibited by EDTA and phenylmethylsulfonyl fluoride. After pelleting the cellular chromatin, the nuclear extract was centrifuged through a 5-40% sucrose gradient. The radioactivity and absorbance profiles of a typical gradient are shown in Figure 27A. In this preparation the minichromosomes were labeled with [^{3}H]-thymidine. The peaks of optical density and radioactivity did not coincide, probably reflecting contamination of the viral chromatin with unlabeled ribonucleoprotein particles (188). When fractions in the vicinity of the two peaks were treated with SDS to remove proteins and analyzed by agarose gel electrophoresis (Figure 27B), the ethidium bromide staining bands were attributed to forms I and II SV40 DNA. The

Figure 27A (upper half).

Preparative sucrose density gradient centrifugation of SV40 minichromosomes. [^{3}H]-SV40 chromatin, extracted from lytically infected TC-7 cells as described in Chapter 2, was layered onto a 5-40% sucrose gradient in 10 mM Tris-HCl (pH 7.8)-1 mM EDTA-0.13 M NaCl and centrifuged for 5 hr at 25,000 rpm. The gradient was collected from below into 1.0 ml fractions which were characterized by absorption, radioactivity, and gel electrophoresis.

Figure 27B (lower half).

Agarose slab gel of sucrose density gradient fractions containing SV40 minichromosomes. Aliquots (50 µl) from fractions 11-19 of the above gradient were deproteinized with SDS and electrophoresed as DNA on a 1.4% agarose slab gel. The direction of electrophoresis was downward. Forms I and II DNA refer to superhelical and nicked circular SV40 DNA, respectively.

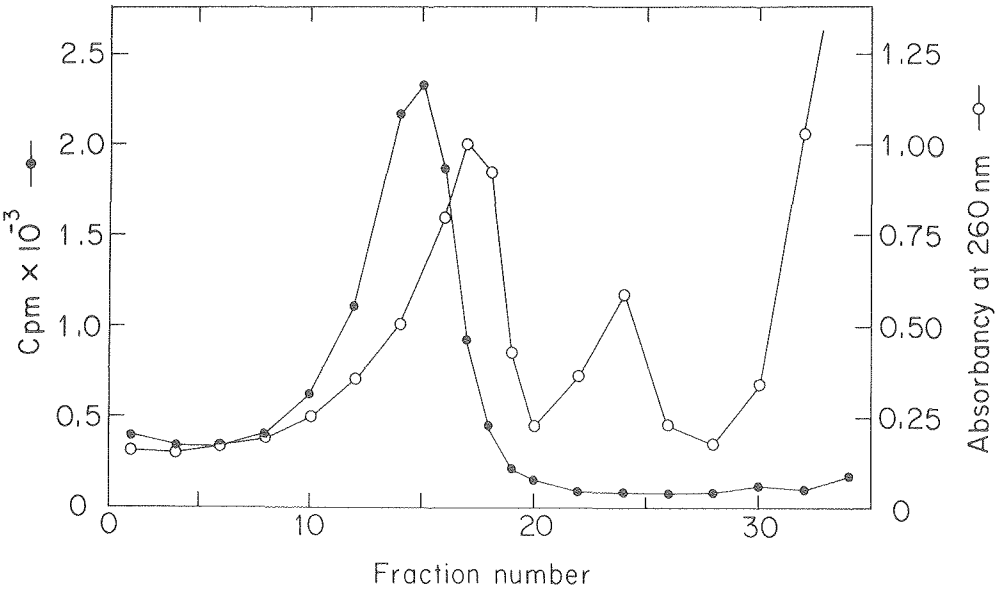

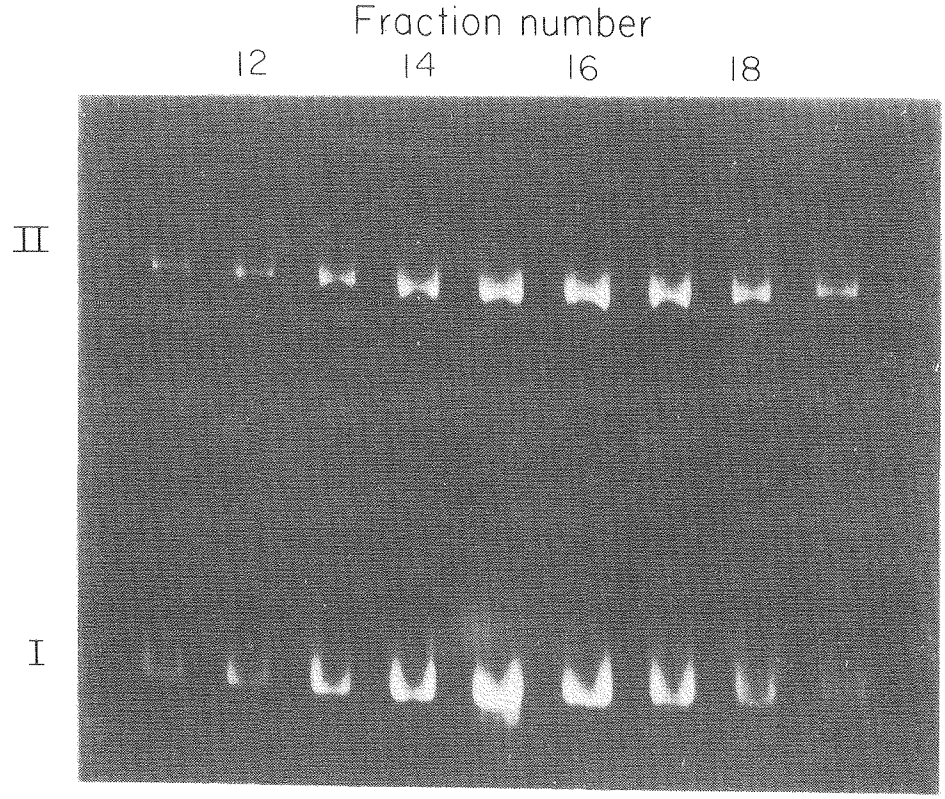

XBB 796-7857A

level of viral DNA correlated with the [^{3}H]-thymidine label. Typically, peak SV40 chromatin fractions were pooled and used within 72 hr.

The SV40 minichromosomes were characterized by standard techniques. In electron micrographs at low ionic strength they exhibited the characteristic beads-on-a-string morphology (A. Tung, unpublished results). The degree of compaction at higher ionic strength was not investigated. SDS-polyacrylamide gel electrophoresis of the minichromosomes gave 4 bands corresponding to the core histones H2A, H2B, H3, and H4 and a less intense band corresponding to histone H1 (S. Treon, unpublished results). In addition, slower moving bands with mobilities similar to the viral capsid proteins were also present. Digestion of the minichromosomes with staphylococcal nuclease liberated 50-60% of the DNA and left the remainder as 140 base pair fragments. This pattern is characteristic of chromatin and will be discussed in detail later.

The absorption spectrum of dialyzed viral chromatin indicated a protein to DNA weight ratio of 2.5. This was higher than the 1:1 ratio commonly accepted for chromatin (65). To obtain a more accurate estimate of this ratio the viral chromatin was fixed with formaldehyde and glutaraldehyde as described by Christiansen and Griffith (78) and analyzed by CsCl density gradient centrifugation (Figure 28). The bouyant density of the minichromosomal complex, 1.41-1.43, was below literature values of 1.45-1.49 (78,186,189). A weight ratio of protein to DNA of 2.0-2.5 was calculated using equation 3 from buoyant density values of

$$(1 + x)\,\rho_{chromatin} = \rho_{DNA} + \rho_{protein} \qquad (3)$$

1.701 (190), 1.295 (191), and 1.41-1.43 for DNA, histones, and chromatin, respectively. The high ratio obtained suggests that the minichro-

Figure 28.

Equilibrium centrifugation of SV40 minichromosomes fixed with formaldehyde and glutataldehyde. [^{3}H]-SV40 chromatin was fixed with formaldehyde and glutaraldehyde and banded to equilibrium in CsCl as described in Chapter 2. Several determinations gave bouyant density values of 1.41-1.43 for the minichromosomal band.

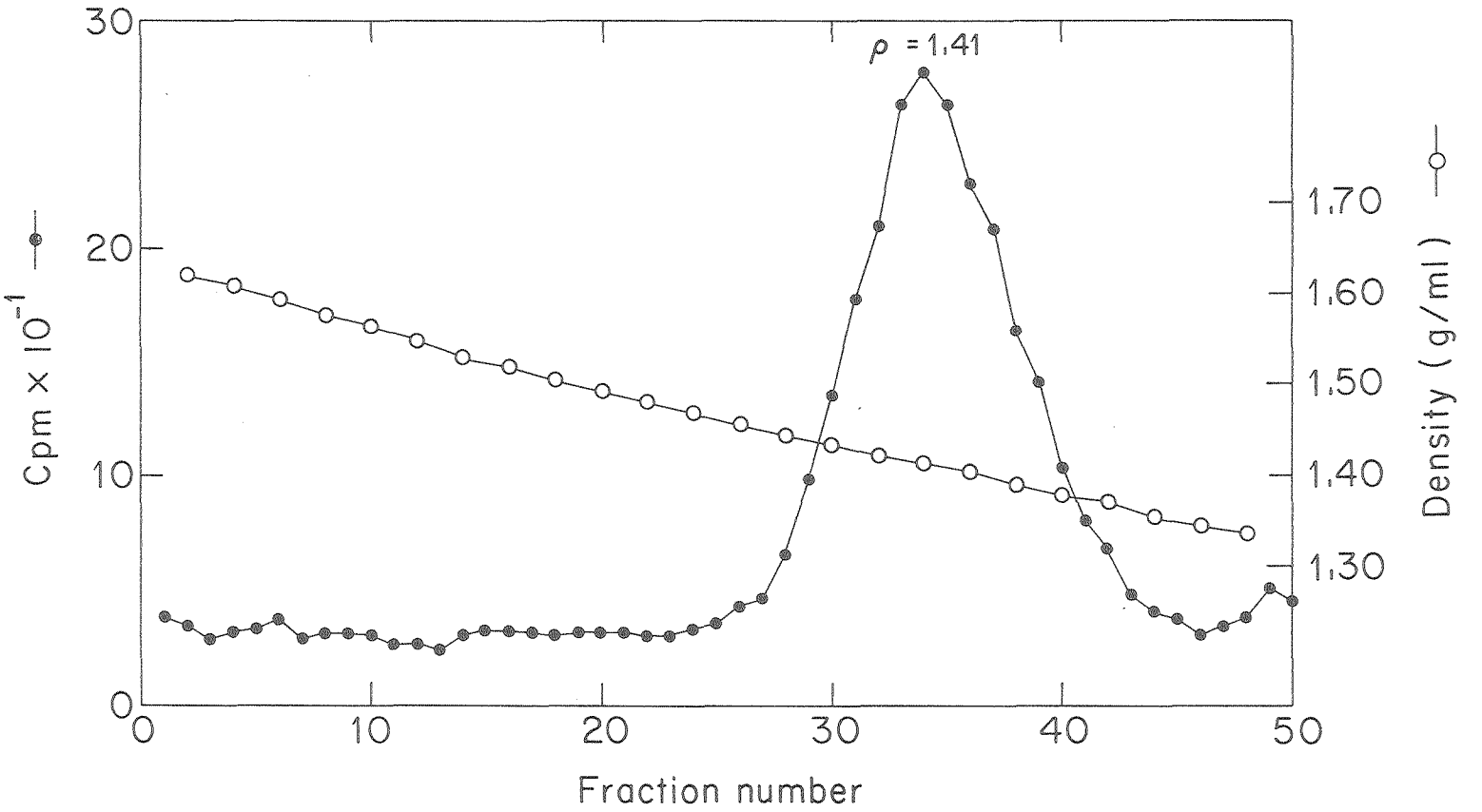

XBL7811-13036

mosomes were contaminated with nonhistone protein, a large fraction of which could be viral capsid protein. Except for the buoyant density, these proteins do not appear to affect the structural properties of the minichromosomes.

The sedimentation coefficient of viral chromatin was 55S in 20 mM Tris-HCl buffer and 63S in the same buffer with 0.13 M NaCl (Figure 29). The minor increase in sedimentation implies only slight compaction of the minichromosomes at physiological ionic strength and is indicative of a histone H1 deficiency. The deficiency was confirmed by the low level of this histone in SDS-polyacrylamide gels of the minichromosomes. Recently, Fernandez-Munoz et al. (186) have reported that a significant fraction of the viral chromatin extracted from nuclei of lytically infected cells with Triton X-100 may be derived from mature virions. With alternative extraction procedures which avoid detergent treatment three distinct viral nucleoprotein complexes are isolated, one of which is the mature virion. Triton X-100 extraction presumably converts all three complexes to one relatively homogeneous minichromosomal complex. It is conceivable that the minichromosomes isolated here are depleted in histone H1 and rich in nonhistone (possibly viral capsid) protein because a large fraction are derived from mature virions.

Reaction of BaP Diol Epoxide with SV40 Minichromosomes. I have shown in Chapters 3 and 4 that a small fraction of the BaP diol epoxide adducts in SV40 DNA rearrange with strand scission and that the remainder induce a strain dependent denaturation of the DNA helix. The SV40 minichromosome is an ideal substrate with which to study how such alterations affect the integrity of chromatin structure. However, since chromatin is by definition a histone-DNA complex, it is important

Figure 29.

Sucrose density gradient centrifugation of compact and extended SV40 minichromosomes. [^{3}H]-SV40 chromatin (ca. 3.3 µg) was centrifuged for 90 min at 50,000 rpm through a 5.0 ml 5-30% sucrose gradient in 20 mM Tris-HCl (pH 8.0)-0.5 mM EDTA in the presence (●) or absence (o) of 0.13 M NaCl. Centrifugation was from right to left. Sedimentation coefficients were determined relative to SV40 form I DNA (■) which was run in a parallel gradient.

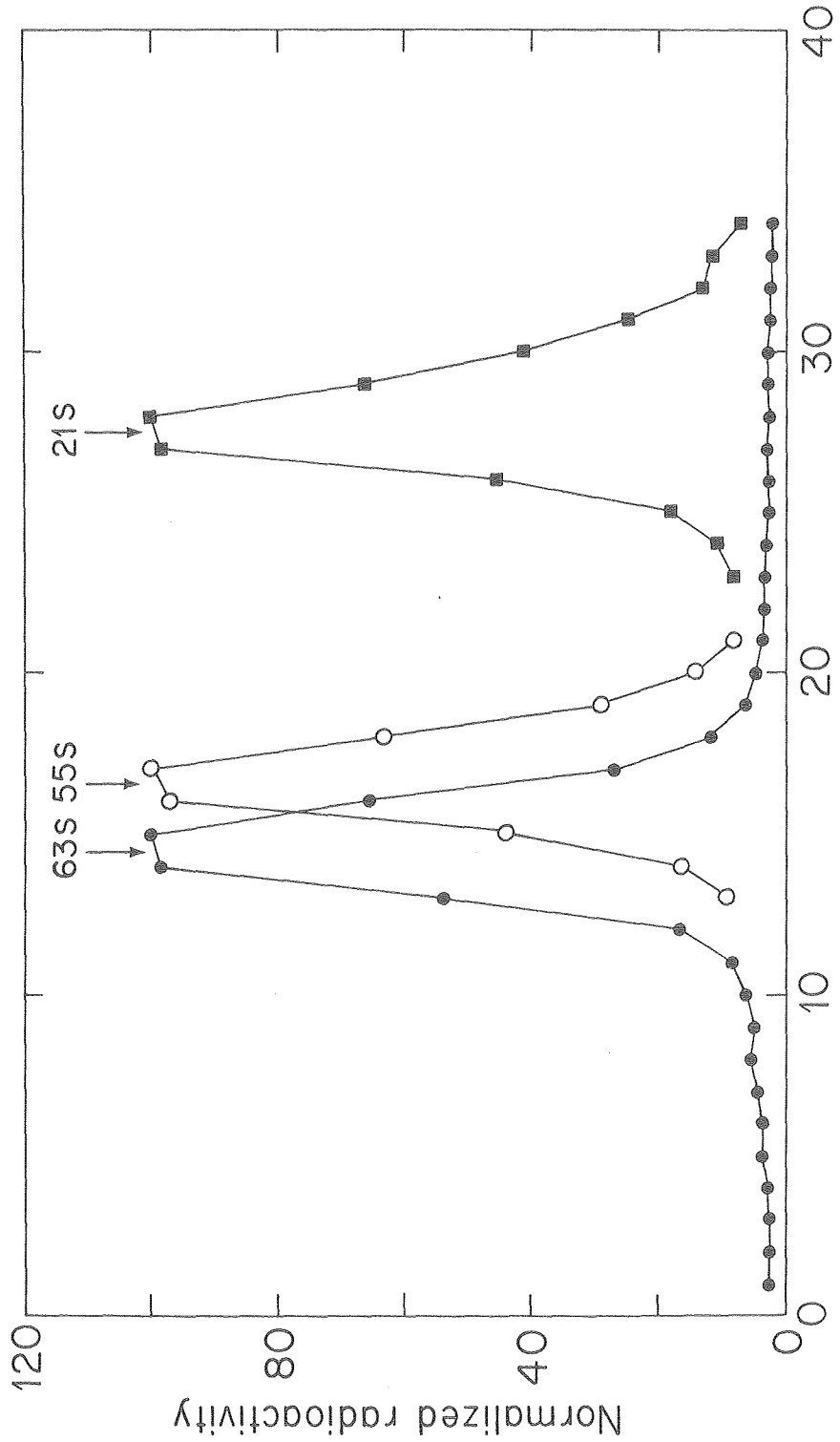

XBL7811-13035

to recognize that changes in minichromosomal structure could also arise from modification of protein. When chromatin is reacted in vitro with BaP diol epoxide, approximately 15% of total alkylation occurs on histone protein (98).

Staphylococcal nuclease is a sensitive probe of chromatin structure. As alluded to earlier, it preferentially digests internucleosomal DNA. When mammalian chromatin is incubated with this enzyme, the deproteinized nucleoprotein complex gives a characteristic time dependent migration pattern in polyacrylamide gels (168). Brief digestion produces a series of discrete DNA bands which are multiples of a monomer 180-200 base pairs in length. The multimers are precursors of the monomer which upon further digestion gives rise to a homogeneous 140 base pair fragment. Prolonged digestion of the chromatin leads to an array of limit digest DNA bands 45-130 base pairs in length. At this stage about 50% of the DNA has become acid soluble. The 180-200 base pair periodicity of partially digested DNA is a direct reflection of the repeat unit length in chromatin, and the relatively nuclease resistant 140 base pair fragment represents nucleosomal core DNA. When circular beaded SV40 chromatin is digested with staphylococcal nuclease a similar DNA banding pattern is obtained, although large multimeric DNA bands are absent at early digestion times (177,189,192). This has been attributed to variability in the length of viral internucleosomal DNA (192).

I have investigated the integrity of BaP diol epoxide modified SV40 minichromosomes containing 3 DNA adducts per genome with staphylococcal nuclease. The viral chromatin, labeled with ^{32}P, was deproteinized and analyzed as a function of digestion time in a 6% polya-

crylamide gel. Figure 30 is an autoradiograph of that gel and shows the DNA fragmentation pattern for (A) control and (B) modified minichromosomes. The gel was calibrated with a Hind II digest of ϕX174 RF DNA, and the percent DNA rendered ethanol soluble is shown at the bottom of each track. A close examination reveals no differences between the two chromatin samples. In both the DNA monomer band had an initial length of circa 200 base pairs which decreased to 140 base pairs at 46-48% digestion. A high background obscures the dimer and trimer bands. The band comigrating with the largest ϕX174 DNA fragment is unidentified. The identical digestion profiles imply that low level BaP diol epoxide binding (< 5 DNA adducts/minichromosome) does not disturb gross nucleosomal structure. A similar conclusion has been reached from chromatin reconstitution experiments employing BaP diol epoxide modified DNA and either untreated or modified histones (98,144).

When more highly modified viral chromatin was analyzed by sucrose density gradient centrifugation, changes in the sedimentation pattern clearly indicated structural alterations (Figure 31). The minichromosomes in this study were alkylated at molar reaction ratios of 0.2-3.0 (BaP diol epoxide/minichromosomal DNA mononucleotide) and are estimated to contain 35-450 DNA adducts and 5-10 fold fewer protein adducts. Their overall structure was not affected by alkylation at molar reaction ratios as high as 0.8. The increased sedimentation coefficient of these samples relative to an unreacted control is probably due to the added mass of physically and covalently bound hydrocarbon although a more compact hydrodynamic configuration cannot be ruled out. At higher molar reaction ratios the minichromosomes were converted to slowly sedimenting heterodisperse fragments; this is attributed to BaP diol epox-

Figure 30.

Time course of staphylococcal nuclease digestion of (A) control and (B) BaP diol epoxide modified SV40 minichromosomes. Autoradiograph of a 6% polyacrylamide gel. Freshly isolated [^{32}P]-SV40 chromatin was incubated with [^{3}H]-BaP diol epoxide (molar reaction ratio = 0 or 0.32) in 10 mM Tris-HCl (pH 7.8)-1 mM EDTA-0.13 M NaCl-4% DMSO-ca. 20% sucrose for 20 min at 37^{o}. The minichromosomal DNA of both samples was immediately digested at 37^{o} with staphylococcal nuclease (1.8 E.U./µg viral DNA). Aliquots, withdrawn over a 20 min period, were quenched with EDTA, treated with RNase and pronase as described in Chapter 2, extracted with chloroform-phenol-isoamyl alcohol (24:25:1) and ethyl acetate, and ethanol precipitated. Approximately 5-10 µg of viral DNA was loaded onto each gel slot. The percentage of DNA, as ^{32}P radioactivity, rendered ethanol soluble at each stage of the digestion is shown at the bottom of the figure and the distribution of ϕX174 Hind II calibration fragments is shown at the sides of the figure. The alkylated chromatin contained 3.0 DNA adducts/minichromosome.

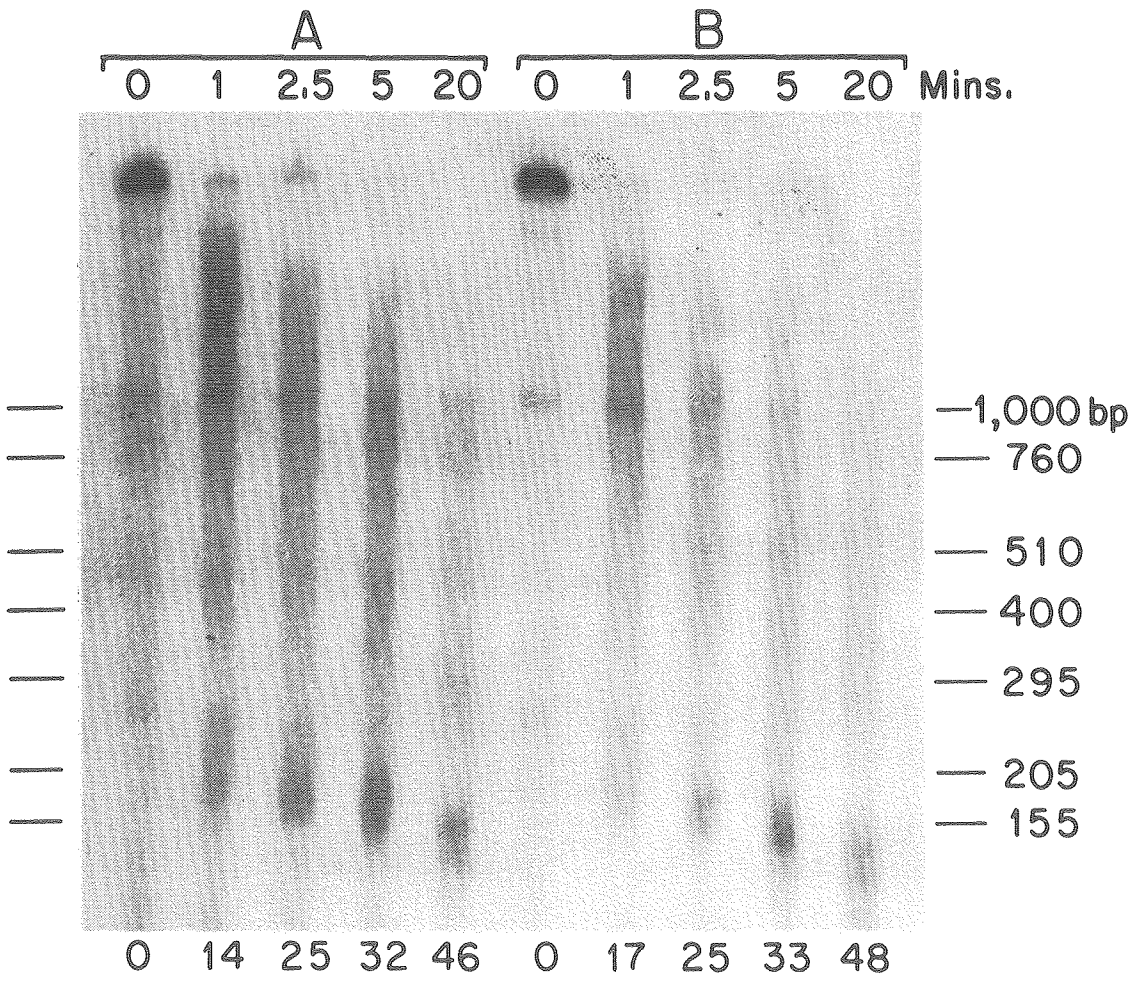

XBB 780-13408

Figure 31.

Sedimentation pattern of SV40 minichromosomes reacted with BaP diol epoxide. [^{3}H]-SV40 chromatin (ca. 1.25 µg) was reacted at 37^{o} for 24 hr with a concentration series of BaP diol epoxide in 105 µl of 20 mM Tris-HCl (pH 8.0)-0.5 mM EDTA-5% DMSO. The modified chromatin was layered onto 5.0 ml 5-30% sucrose gradients prepared in 10 mM Tris-HCl (pH 7.7)-1 mM EDTA-0.13 M NaCl and centrifuged for 90 min at 50,000 rpm. The gradients were collected from the bottom and counted. Molar reaction ratios of BaP diol epoxide to DNA mononucleotide were 0 (●), 0.2 (o), 0.8 (Δ), 1.5 (▲), and 3.0 (◇).

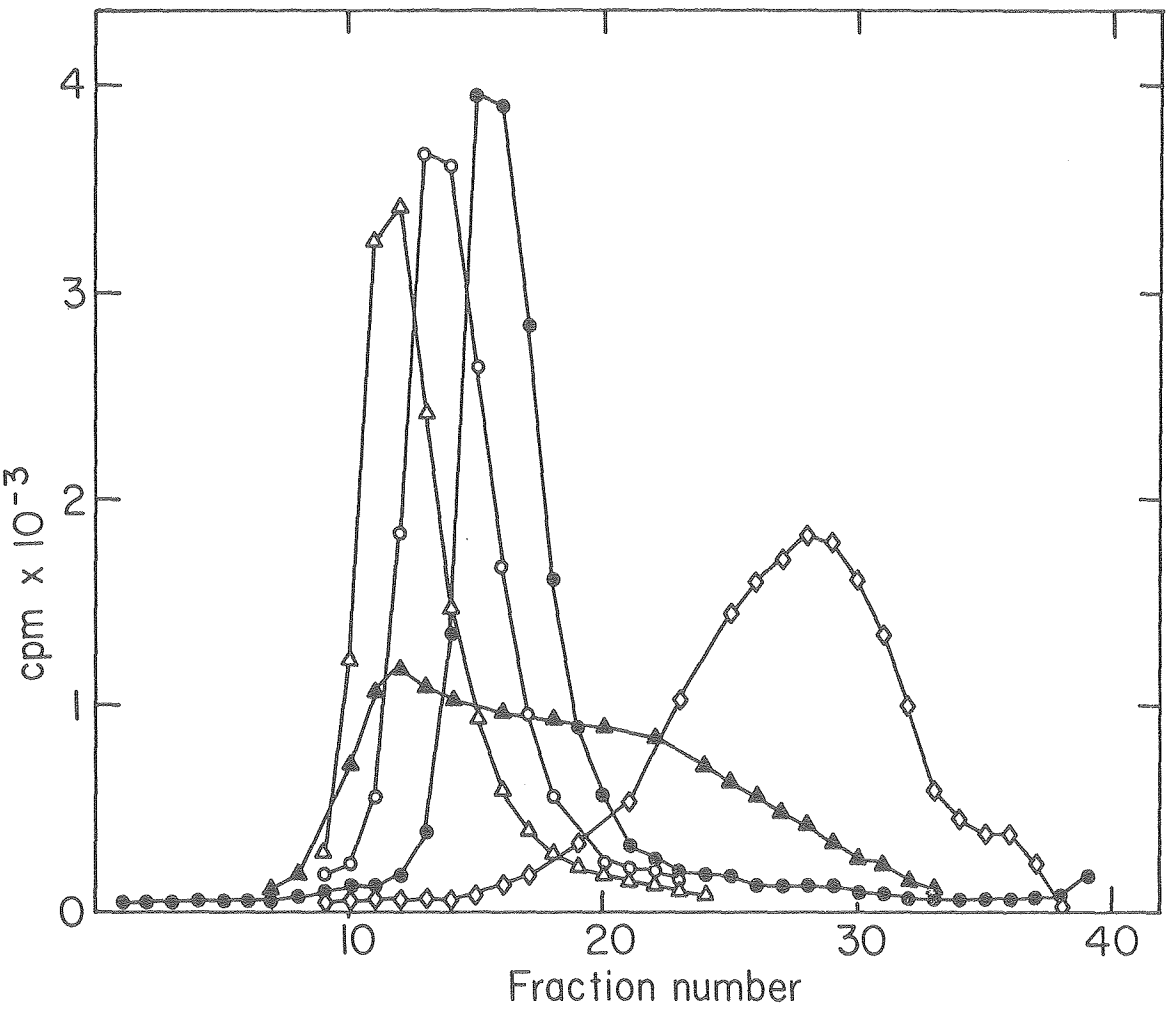

XBL 781-3768

ide induced DNA strand scission.

The modified minichromosomes were also characterized by agarose gel electrophoresis. After alkylation in 20 mM Tris-HCl buffer at molar reaction ratios of 0.05-3.0 the minichromosomes were divided into two sets. One was deproteinized and electrophoresed as DNA (Figure 32A). The other was electrophoresed at low ionic strength as a nucleoprotein complex (Figure 32B). Tracks from left to right corresponded to increasing modification; track a was an unreacted control. The DNA banding pattern was very similar to that obtained with superhelical DNA (see Figure 3). At lower molar reaction ratios alkylation of form I minichromosomal DNA reduced its superhelical density and in turn decreased its electrophoretic mobility. At higher molar reaction ratios extensive strand scission led to full length linear DNA and smaller fragments which ran off the gel. This degradation was probably due to depurination strand scission at minor alkylation sites (see Chapter 3).

In the corresponding nucleoprotein gel the minichromosomes electrophoresed as a fairly sharp band with slight high molecular weight trailing. At intermediate reaction ratios, where the viral DNA contained up to several single strand nicks, the minichromosomes continued to migrate as a discrete band. Since the minichromosomes contain little or no torsional strain, occasional DNA nicks did not significantly alter their configuration. The slight decrease in band mobility at intermediate reaction ratios is probably equivalent to the enhancement of sedimentation seen in sucrose gradients. Taken together, these effects are consistent with a molecular weight increase of the modified minichromosomes due to the presence of physically and covalently bound hydrocarbon. At the highest molar reaction ratios, where the viral DNA

Figure 32.

Electrophoretic pattern of SV40 minichromosomes reacted with BaP diol epoxide and analyzed as (A) DNA and (B) chromatin. SV40 chromatin (ca. 1.5 µg) was reacted with a concentration series of BaP diol epoxide in 210 µl of 20 mM Tris-HCl (pH 8.0)-0.5 mM EDTA-5% DMSO. After 24 hr at 37^{o} the reaction mixtures were divided into two sets. One set was deproteinized as described in Chapter 2 and electrophoresed as DNA for 12 hr at 50 V on a 1.4% agarose slab gel. The other set was electrophoresed as chromatin for 6 hr at 50 V on a 1% low ionic strength slab gel. In both gels the direction of electrophoresis was downward. The molar reaction ratios of BaP diol epoxide to DNA mononucleotide were (a) 0, (b) 0.05, (c) 0.10, (d) 0.15, (e) 0.20, (f) 0.30, (g) 0.40, (h) 0.60, (i) 0.80, (j) 1.0, (k) 1.5, and (l) 3.0.

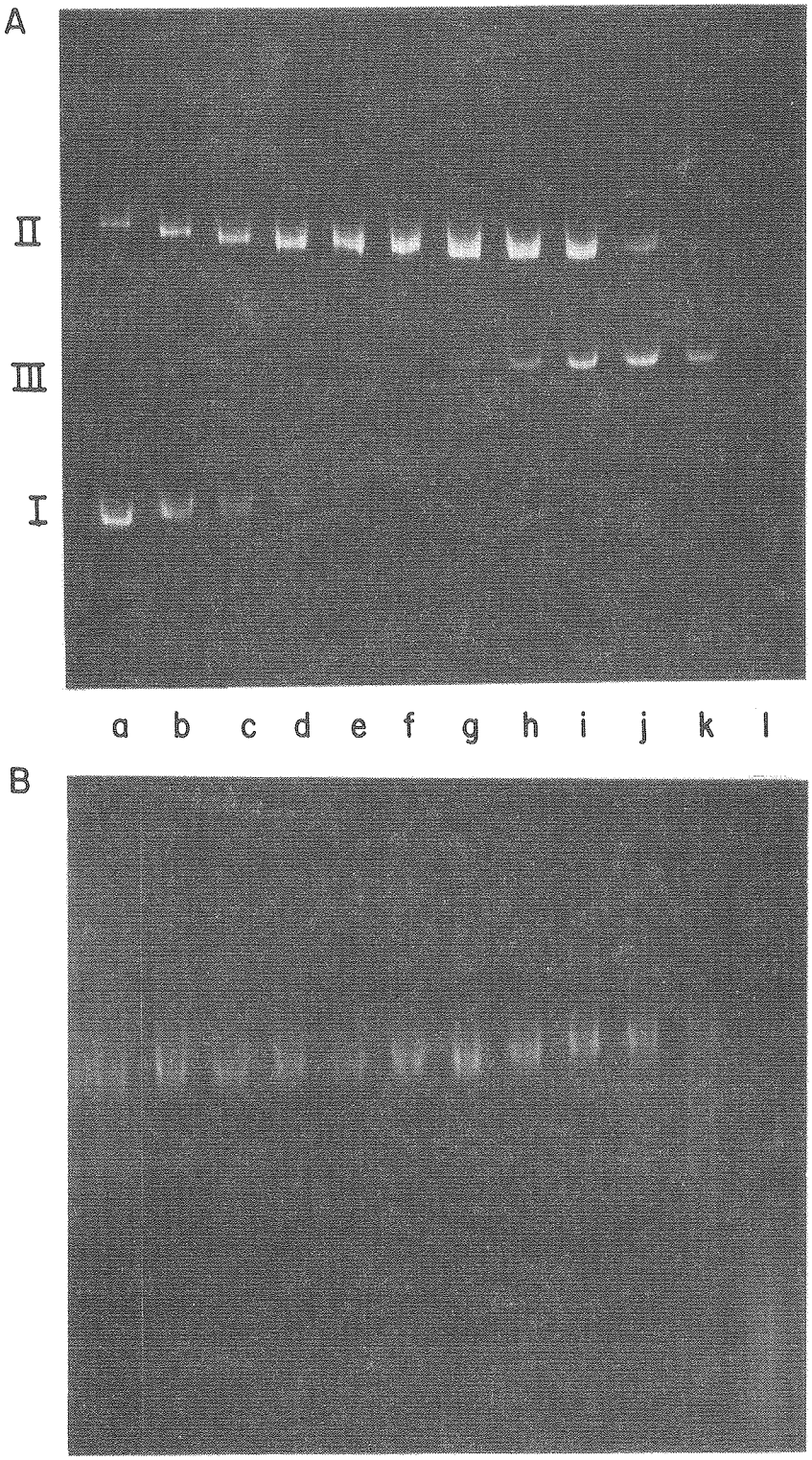

XBB 781-1007

was extensively fragmented, the minichromosomes were degraded and ran as a low molecular weight heterodisperse band.

Just as chromatin structure was altered by BaP diol epoxide adducts, DNA alkylation and strand scission by the hydrocarbon might be modulated by the repeat structure of the nucleoprotein complex. An indication of such a modulation is shown in Figure 33, where the loss of superhelical DNA was plotted as a function of BaP diol epoxide molar reaction ratio for both naked and minichromosomal SV40 DNA. The topological DNA forms were separated by gel electrophoresis after first removing protein from the minichromosome samples and quantified by fluorimetric densitometry. No correction was made for the differential staining of the DNA bands by ethidium bromide (193), and so the percent form I DNA was underestimated especially at higher molar reaction ratios. Nonetheless, a comparison of the curves suggests that strand scission was favored in minichromosomal DNA.

The question of modulation was carefully studied by reacting ^{3}H-labeled BaP diol epoxide with ^{14}C-labeled SV40 minichromosomes or superhelical DNA. The reactions were conducted in 20 mM Tris-HCl, pH 8.0, buffer containing 0.5 mM EDTA and 10% DMSO. To ascertain the effect of minichromosome compaction on DNA alkylation and strand scission, a duplicate set of reactions were conducted in the same buffer containing 0.13 M NaCl. After 2-4 hr incubation at 37^{o} the viral DNA was isolated and assayed for covalent binding. Separate samples were incubated 24 hr prior to analysis for strand scission. The minichromosomes were deproteinized by pronase digestion followed by chloroform-phenol-isoamyl alcohol extraction. Unreacted hydrocarbon was removed by ethyl acetate extraction and ethanol precipitation of the DNA.

Figure 33.

DNA strand scission by BaP diol epoxide in SV40 DNA and SV40 minichromosomes. SV40 form I DNA and SV40 chromatin were reacted with a concentration series of BaP diol epoxide for 24 hr at 37^{o} in 20 mM Tris-HCl (pH 8.0)-0.5 mM EDTA-5% DMSO. The DNA of both substrates was electrophoresed on 1.4% agarose slab gels. After staining with ethidium bromide the fluorescent DNA bands were traced and the % form I DNA present in each track determined. No correction was made for the differential fluorescence of forms I and II DNA. (●), protein-free DNA; (○), minichromosomal DNA.

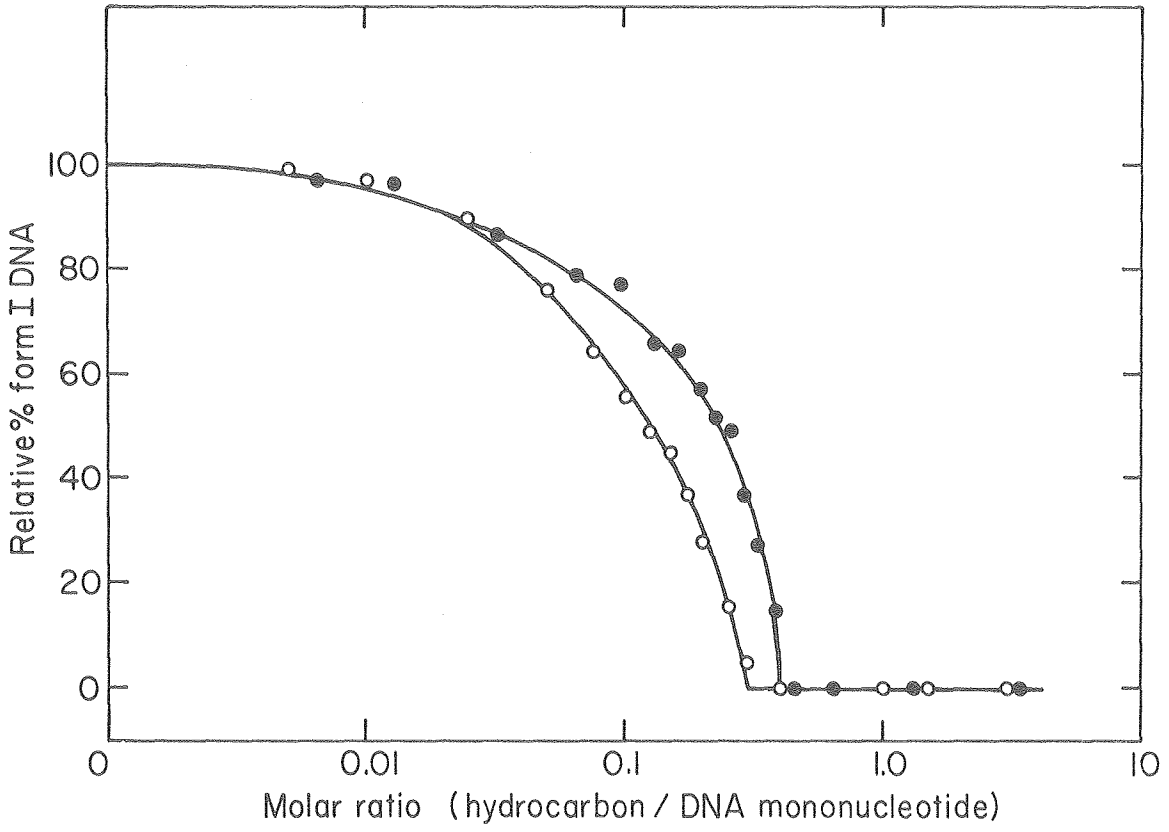
Relative % form I DNA
100
80
60
40
20
0
0
0.01
0.1
1.0
10
Molar ratio (hydrocarbon / DNA mononucleotide)

XBL 781-3770

Strand scission, expressed as nicks per genome, was determined by counting the radioactivity of the DNA bands after agarose gel electrophoresis.

The results in Figure 34 demonstrate that DNA alkylation and nicking were modulated by the minichromosome structure. In low ionic strength buffer minichromosomal DNA exhibited enhanced nicking and reduced binding relative to superhelical DNA. In the presence of 0.13 M NaCl both nicking and binding were reduced 10 fold for the two DNA substrates. Although higher binding was still observed with superhelical DNA, both substrates exhibited comparable strand scission in physiological salt. The ratio of adducts per nick and the percent inhibition of binding and nicking by 0.13 M NaCl are summarized for the two DNAs in Table 5.

The dramatic inhibition by NaCl of form I SV40 DNA binding and nicking has been discussed in the two preceding chapters. NaCl evidently has a similar effect on minichromosomes. By acting as a counterion, Na^+ reduces the repulsion of negatively charged DNA phosphates and stabilizes the helix (102). In so doing it reduces the physical, possibly intercalative, association which precedes covalent reaction of BaP diol epoxide with DNA. Nicking requires an initial alkylation event and is inhibited by the same mechanism or by direct masking of the DNA reaction sites by bound Na^+ (100,101). An additional factor which may reduce BaP diol epoxide alkylation and nicking of minichomosomal DNA in 0.13 M NaCl is physical compaction of the minichromosomes. However, the viral chromatin employed here is depleted in histone H1 and only undergoes minor compaction in 0.13 M NaCl. Even so, a comparison of the percent inhibition values for naked and minichromosomal DNA

Figure 34.

Comparison of BaP diol epoxide dependent DNA alkylation and strand scission in SV40 DNA and SV40 chromatin in the presence and absence of 0.13 M NaCl. [^{14}C]-SV40 form I DNA (1.88 μg) and [^{14}C]-SV40 minichromosomes (ca. 13.5 μg) were modified with a concentration series of [^{3}H]-BaP diol epoxide in 20 mM Tris-HCl (pH 8.0)-0.5 mM EDTA-10% DMSO both in the presence and absence of 0.13 M NaCl. After 2-4 hr at 37^{o} aliquots were removed for determination of DNA alkylation; after 24 hr additional aliquots were analyzed for DNA strand scission. Details of the experimental protocol are in Chapter 2. (●—●), protein-free DNA in 0 M NaCl; (o—o), minichromosomal DNA in 0 M NaCl; (●---●), protein-free DNA in 0.13 M NaCl; (o---o), minichromosomal DNA in 0.13 M NaCl.

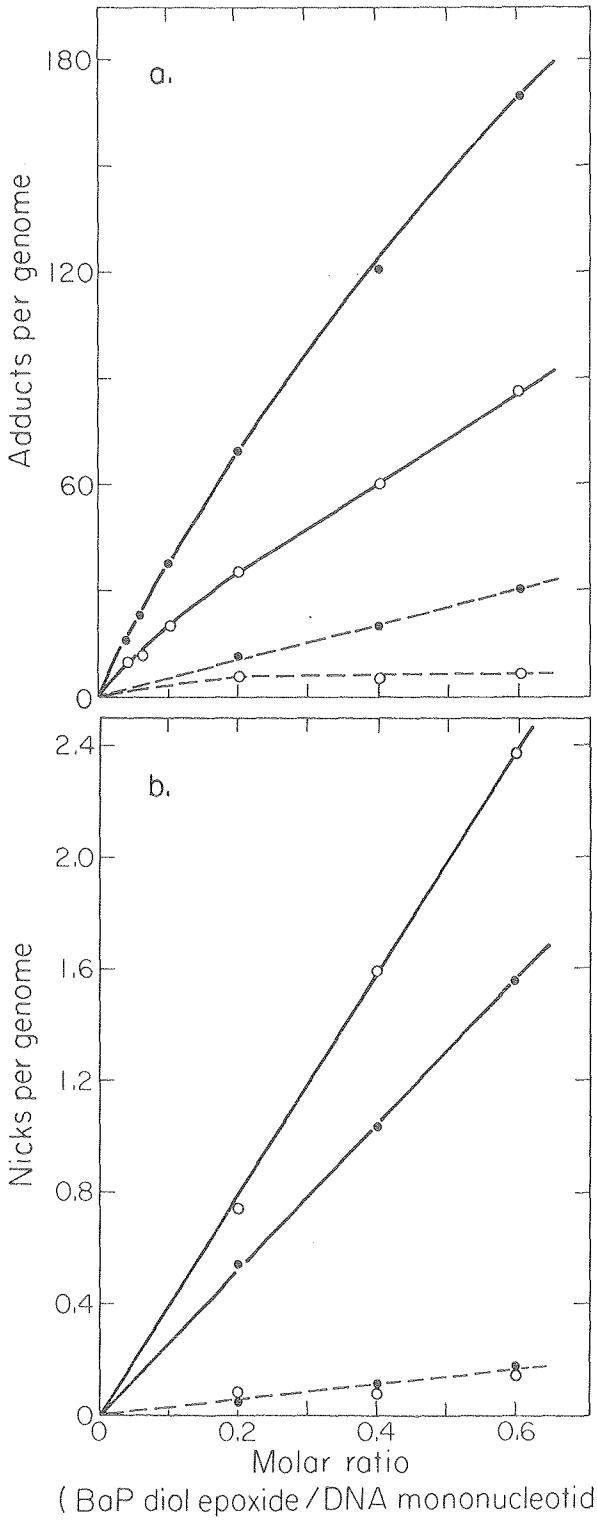
a.
b.
Adducts per genome
Nicks per genome
180
120
60
0
2.4
2.0
1.6
1.2
0.8
0.4
0
0.2
0.4
0.6
Molar ratio
(BaP diol epoxide / DNA mononucleotide)

XBL796-4813

Table 5.

Inhibition of BaP Diol Epoxide Modification of SV40 DNA by NaCl*

[NaCl]	Adducts/Nick	% Inhibition	
		Binding	Nicking
Naked DNA			
0 mM	117 ± 9	0	0
130 mM	197 ± 23	82.7	89.8
Minichromosomal DNA			
0 mM	40 ± 5	0	0
130 mM	60 ± 12	89.1	92.6

* The data are average values obtained from the curves in Figure 34.

in Table 5 indicates that this compaction slightly reduces the accessibility of DNA to nicking and binding.

The enhancement of strand scission in minichromosomal relative to naked DNA was unexpected but has several possible explanations: Firstly, the chromatin preparation may contain an endogenous endonuclease which nicks adjacent to BaP diol epoxide adducts. Secondly, the minichromosomal histones may slightly alter the distribution of DNA adducts favoring those which rearrange with strand scission. Thirdly, the histones may catalyze the rearrangement leading to strand scission. This explanation is the most likely as I have previously shown that the primary mechanism of nicking is depurination strand scission; rearrangement of deoxyribose at apurinic sites is known to be catalyzed by lysine, arginine, and histidine and by basic proteins which contain these amino acids (88).

The two fold reduction in alkylation of viral DNA when it was reacted as a nucleoprotein complex can be attributed to minichromosomal protein which competes with the viral DNA for BaP diol epoxide. Furthermore, studies with cellular chromatin indicate that the histone cores can reduce the availability of nucleosomal DNA to the epoxide (98,144,156,194). The distribution of BaP diol epoxide adducts in minichromosomal linker and core DNA will be described below.

The microenvironment of BaP diol epoxide DNA adducts in the SV40 minichromosome was probed by isopycnic centrifugation. It has been shown in Chapter 4 that the physical structure of BaP diol epoxide alkylation sites is dependent upon the torsional strain in the molecule. In superhelical DNA the sites are extensively denatured while in relaxed DNA the same sites have an ordered structure with only slight de-

naturation. In SV40 minichromosomes the superhelical turns of the DNA are stabilized within the nucleosomes, and it is expected that the alkylation sites resemble those of relaxed DNA. To test this assumption minichromosomes containing approximately 60 DNA adducts per genome were fixed by the method of Christiansen and Griffith (78) and centrifuged to equilibrium in a CsCl gradient. The buoyant density of the modified chromatin was identical to an untreated control indicating no substantial denaturation at the alkylation sites.

Alkylation of Nucleosomal Versus Internucleosomal DNA. With the recent availability of enzymes such as staphylococcal nuclease and pancreatic DNase (DNase I) which only partially digest the DNA in a nucleoprotein complex, it has become possible to map the distribution of alkylation sites within the repeat unit of chromatin. Staphylococcal nuclease preferentially attacks linker DNA while DNase I is less specific and attacks both inter- and intranucleosomal DNA stretches (168, 195,196). Most carcinogens when investigated exhibit nonrandom binding to chromatin. Some preferentially alkylate nucleosomal core DNA and are selectively released by DNase I while others preferentially alkylate internucleosomal spacer DNA and are selectively released by staphylococcal nuclease (197-203). Reduced binding of BaP diol epoxide to minichromosomal DNA suggested the existence of a nonrandom binding pattern; this was investigated with staphylococcal nuclease.

Viral chromatin was reacted with BaP diol epoxide and digested with staphylococcal nuclease immediately after isolation. The digestion of bulk DNA and BaP diol epoxide modified nucleotides was followed by counting ethanol precipitable ^{32}P and ^{3}H radioactivity, respectively, after removal of RNA, protein, and unreacted hydrocarbon. By labeling

the DNA with ^{32}P the release of all four nucleotides could be monitored thereby avoiding problems associated with the preferential release of radioactive thymidine by staphylococcal nuclease (204). Control experiments indicated that low modification levels (< 5 DNA adducts/genome) did not affect the fragmentation pattern or the digestion kinetics of minichromosomal DNA (Figure 30). Approximately 50% of the DNA was rendered ethanol soluble, a value characteristic of the nucleoprotein complex. Modified protein-free viral DNA was almost completely digested by staphylococcal nuclease (Figure 35). However, the covalently bound BaP diol epoxide was less completely solubilized and suggested that certain alkylation sites were resistant to digestion.

When BaP diol epoxide modified minichromosomes were incubated with staphylococcal nuclease, bulk DNA and covalently bound hydrocarbon were digested with the kinetics shown in Figure 36. After 20 min of incubation 60% of the DNA and 56% of the adducts were released, clearly indicative of a uniform distribution of adducts at the time of digestion. Following deproteinization the residual nuclease-resistant ^{32}P and ^{3}H radioactivity was almost totally solubilized by the enzyme, discounting the possibility that hydrocarbon modified macromolecules other than DNA were present in the ethanol pellet. The ratio of ^{32}P to ^{3}H was also determined for total DNA prior to digestion and for nucleosomal core DNA generated by the nuclease and isolated by gel electrophoresis. Digestion of the minichromosomes increased the ratio from 0.15 ± 0.02 to 0.18 ± 0.02, again indicative of random alkylation. The slight rise in the ratio is attributed to resistance of some modified sites to nuclease digestion.

Figure 35.

Staphylococcal nuclease digestion of SV40 DNA after prior reaction with BaP diol epoxide. [^{32}P]-SV40 form I DNA containing 2.2 [^{3}H]-BaP diol epoxide adducts/genome was digested at 37^{o} with 0.9 E.U. staphylococcal nuclease/μg DNA in 20 mM Tris-HCl (pH 8.0)-0.5 mM EDTA-0.2 M NaCl-3 mM $CaCl_2$-3 mM $MgCl_2$-4% DMSO. Aliquots were taken into EDTA, extracted with ethyl acetate, precipitated in 67% ethanol and collected on 0.45 μ Millipore HAWP filters for counting. (●), DNA; (o), BaP diol epoxide adducts. 100% = 3,200 cpm ^{32}P and 350 cpm ^{3}H.

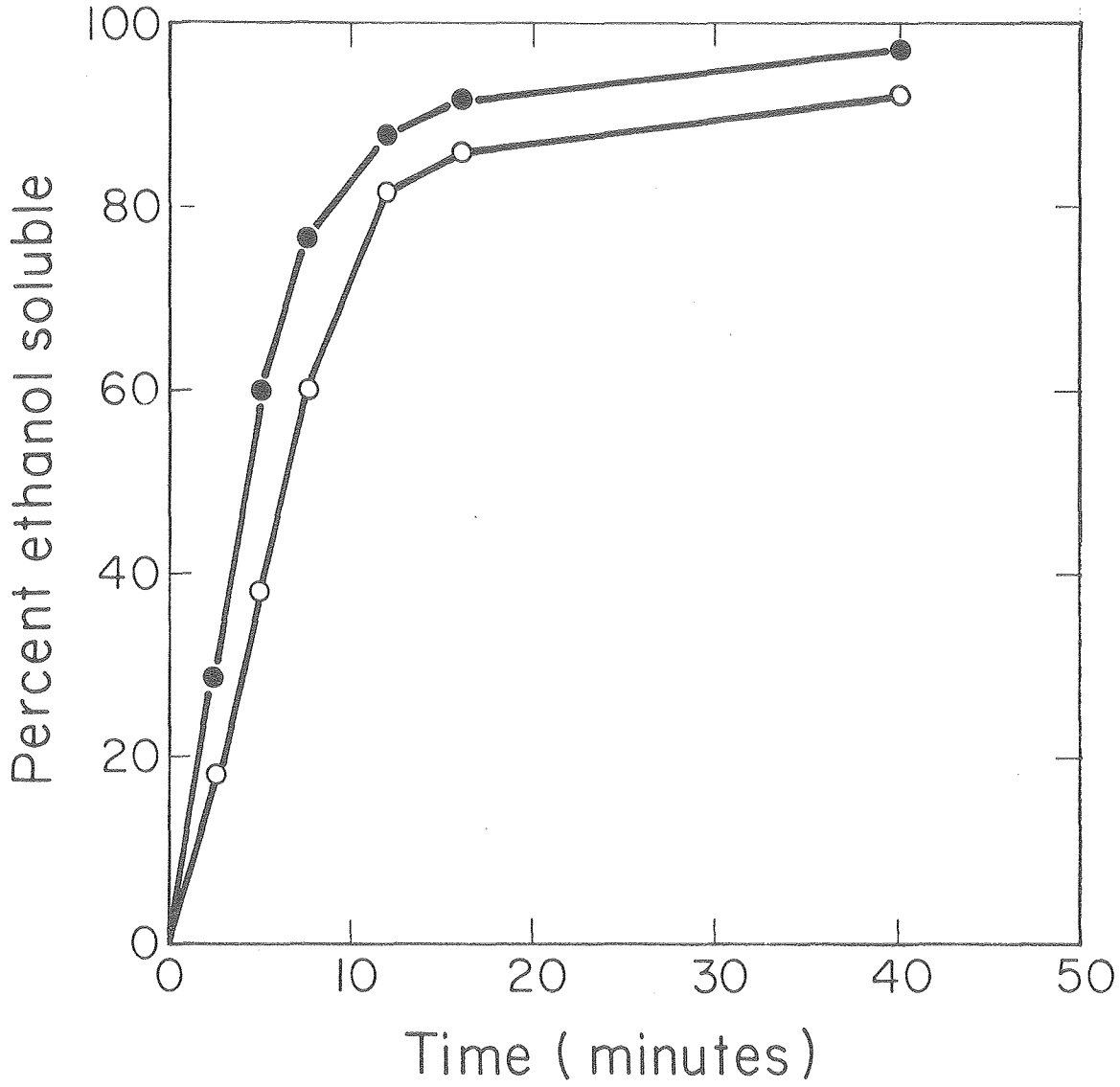

XBL 7810-4314

Figure 36.

Staphylococcal nuclease digestion of "compact" SV40 minichromosomes after prior reaction with BaP diol epoxide. [^{32}P]-SV40 chromatin (ca. 90 µg) was incubated 20 min at 37^{o} with [^{3}H]-BaP diol epoxide (molar reaction ratio = 0.55) in 10 mM Tris-HCl (pH 7.8)-1 mM EDTA-0.13 M NaCl-3% DMSO-circa 20% sucrose. The alkylated chromatin (0.74 DNA adducts/minichromosome) was immediately digested at 37^{o} with 4.3 E.U. staphylococcal nuclease/µg viral DNA. Aliquots were taken over a 20 min period into EDTA. Ethanol precipitable radioactivity was determined after deproteinization, ethyl acetate extraction and ethanol precipitation as described in Chapter 2. (●), minichromosomal DNA; (o), BaP diol epoxide DNA adducts. 100% = 12,800 cpm ^{32}P and 650 cpm ^{3}H.

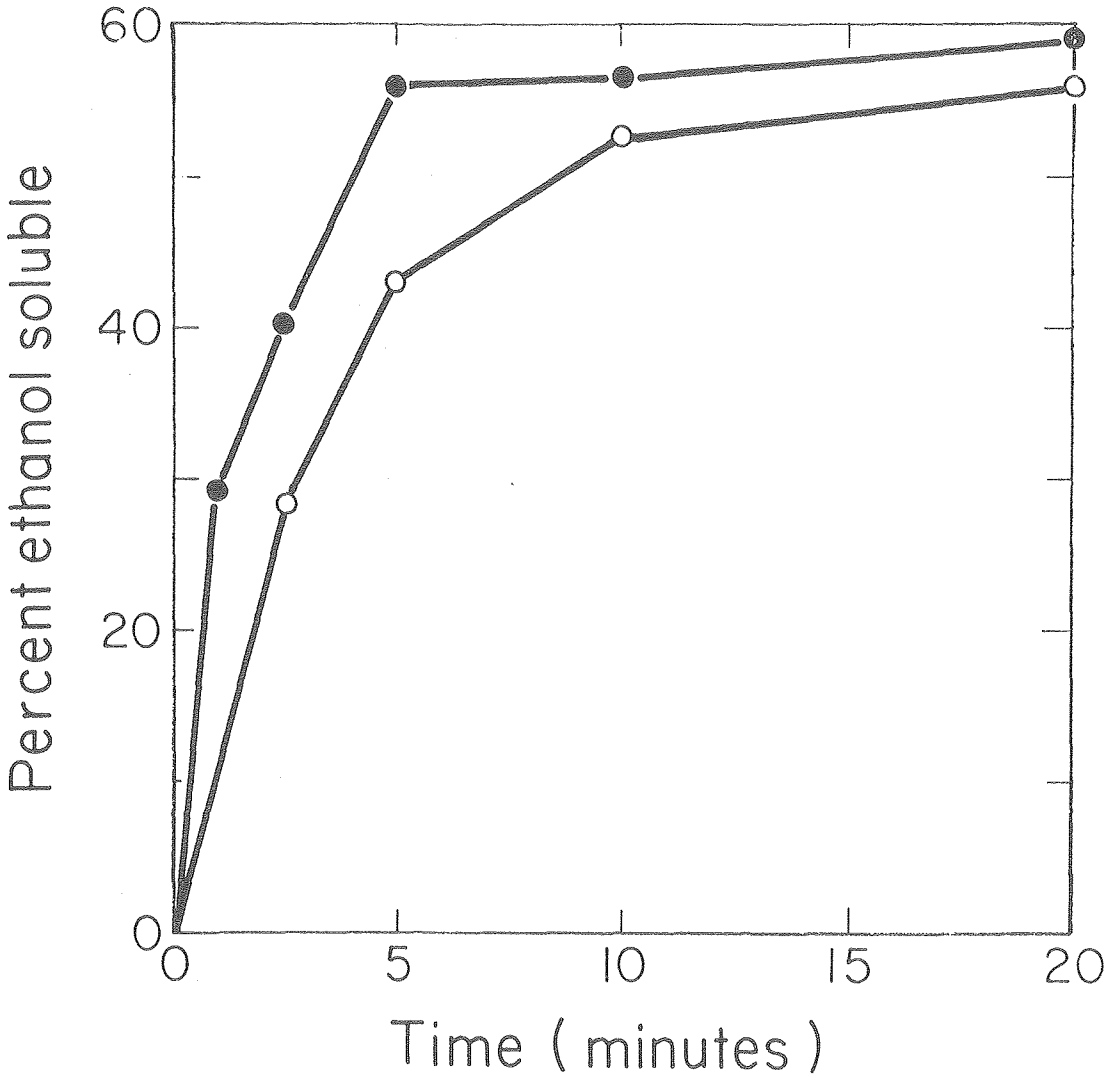

XBL7810-4315

The staphylococcal nuclease digestion described above was carried out in 0.13 M NaCl. Had the minichromosomes contained a normal complement of histone H1 they would have been refractile to the enzyme (183). When the same incubation was carried out in the absence of salt, the kinetics in Figure 37 were obtained. The two digestions are not strictly comparable since modification at low ionic strength generated 35 fold more DNA adducts. The extensive DNA digestion may reflect a perturbation of basic nucleosomal structure by the high modification. In any case, the release of covalently bound BaP diol epoxide paralleled the digestion of DNA albeit at a lower level.

The random distribution of BaP diol epoxide DNA adducts which I have found in the SV40 minichromosome implies a rather uniform decrease in the accessibility of all regions of minichromosomal DNA and was unexpected in light of several recently published studies with cellular chromatin which indicate that both BaP diol epoxide and metabolically activated BaP preferentially alkylate internucleosomal DNA (98,144,156, 201). SV40 minichromosomes resemble transcriptionally active chromatin (205). The nucleosomal core histones H3 and H4 are highly acetylated and phosphorylated (186,206,207). Weintraub and Groudine (208) have shown that transcriptionally active genes are readily digested by DNase I and have postulated that such genes have a conformation different from inactive chromatin. It is tempting to speculate that the acetylation and phosphorylation of core histones which renders DNA more susceptible to DNase I also makes it more accessible to BaP diol epoxide.

The viral minichromosomes also differ from cellular chromatin in their low content of histone H1. Loss of this histone from chromatin eliminates a very high affinity binding site for ethidium bromide

Figure 37.

Staphylococcal nuclease digestion of "extended" SV40 minichromosomes after prior reaction with BaP diol epoxide. [^{32}P]-SV40 chromatin (ca. 80 µg) was incubated 20 min at 37^{o} with [^{3}H]-BaP diol epoxide (molar reaction ratio = 0.44) in 20 mM Tris-HCl (pH 8.0)-0.5 mM EDTA-3% DMSO. The alkylated chromatin (27.5 adducts/minichromosome) was immediately digested at 37^{o} with 9.5 E.U. staphylococcal nuclease/µg viral DNA. Aliquots were analyzed as outlined in Figure 36. (●), minichromosomal DNA; (o), BaP diol epoxide DNA adducts. 100% = 6,000 cpm ^{32}P and 5,100 cpm ^{3}H.

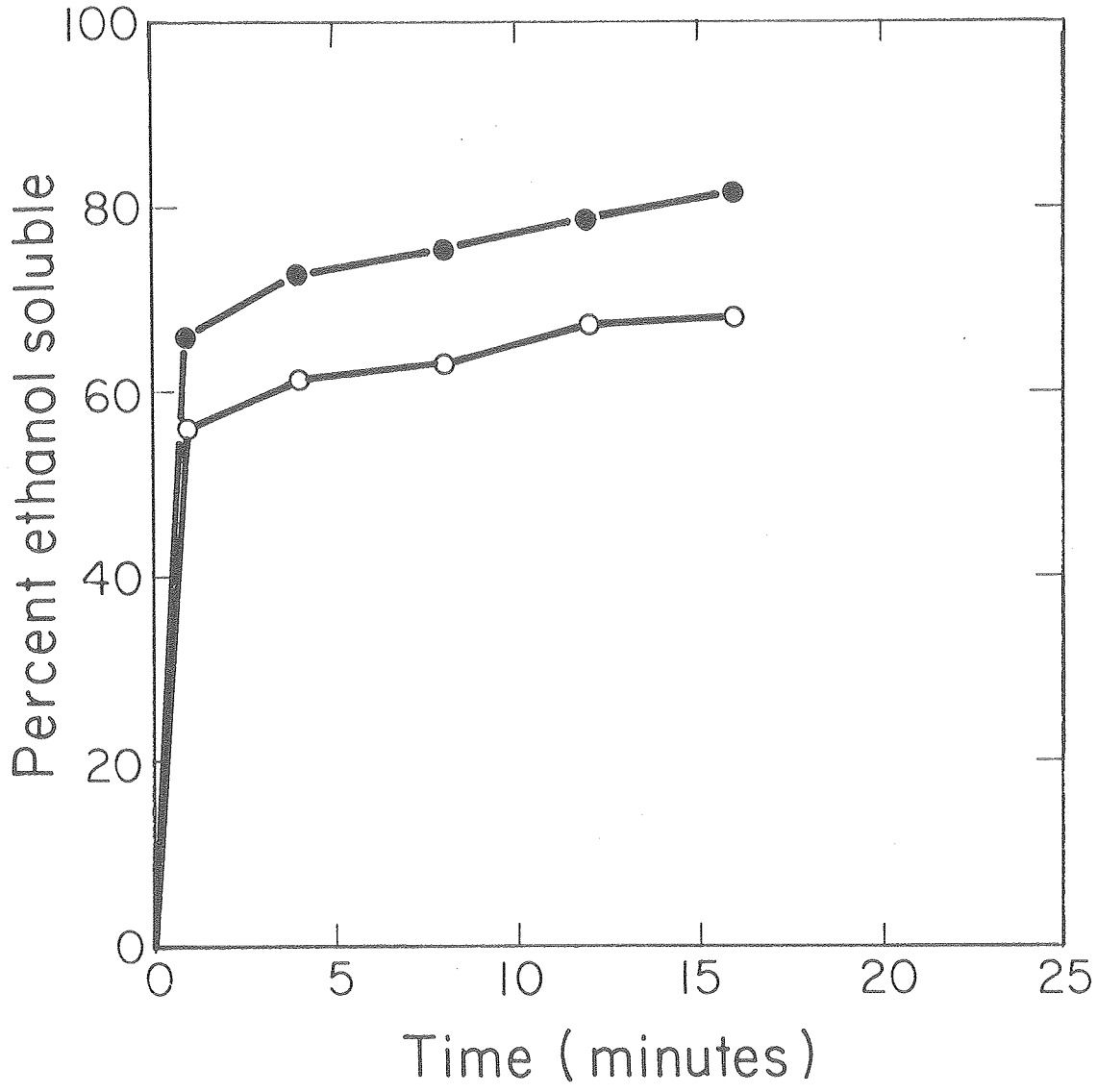

XBL 7810-4316

(209). If BaP diol epoxide intercalates prior to reaction, preferential alkylation of linker DNA may be reduced in the histone H1 depleted minichromosomes. It should be noted, however, that when these same minichromosomes were photoreacted with psoralen, the reaction was highly specific for linker DNA (158).

A third possibility which may explain the equal accessibility of nucleosomal and linker DNA involves migration of the nucleosomal histone cores along the DNA effectively randomizing the sites of alkylation. Beard (180) has found that histone cores can slowly migrate in H1 depleted minichromosomes but was unable to measure the rate. It is conceivable that sufficient migration may occur, possibly facilitated by BaP diol epoxide adducts or physically bound BaP tetraol, to randomize the DNA alkylation sites. The effect of nonhistone proteins present in the minichromosome preparation on DNA accessibility or histone migration is unknown.

Chapter 6: Conclusions

I have shown in Chapter 3 that BaP diol epoxide nicks DNA through a rearrangement of one or more minor alkylation sites. The low level of strand scission (1-2 nicks/100 adducts) mirrors the frequency of these particular adducts. I have conducted experiments aimed at elucidating the mechanism of strand scission. Evidence for a phosphotriester mechanism was not obtained. In fact, the inability of BaP diol epoxide to nick TMV RNA and poly(dT) or to form a reaction product with dibutyl phosphate strongly argues against that mechanism. If triesters are formed in DNA they hydrolyze with exclusive loss of the hydrocarbon. In contrast, substantial evidence supports a depurination strand scission mechanism. The susceptibility of BaP diol epoxide modified DNA to apurinic endonuclease clearly demonstrates the presence of apurinic sites and the identification of a labile N-7 guanine adduct (16,17) provides an explanation for the rapid appearance of these sites. The rate of spontaneous strand scission was consistent with the half-lives for depurination of the N-7 guanine adduct (17) and β-elimination at the resultant apurinic site.

In the study of strand scission it became apparent that an as yet unidentified BaP diol epoxide adduct slowly rearranged to an alkali labile derivative which at high pH spontaneously broke the DNA backbone. After 24 hr incubation at 37^{o} and pH 8.0 approximately 4% of the alkylation sites were rendered alkali labile. This rearrangement may be identical to that observed by Mizusawa and Kakefuda (56) who found that

BaP diol epoxide adducts elicit strand scission after sequential exposure to heat and alkali. A future investigation of the stability of BaP diol epoxide exocyclic amino group adducts in SV40 DNA is contemplated.

The results in Chapter 4 demonstrated that BaP diol epoxide alkylation of the N^2 amino group of guanine disrupted hydrogen bonding and destabilized the double helix. The unwinding angle of this adduct ranged from 328^o in superhelical SV40 DNA to 30^o in the same partially relaxed DNA. Its presence in DNA induced a strain dependent denaturation of 1-10 base pairs. The extensive unwinding observed with superhelical DNA suggests that any modification which interferes with base pairing (i.e., alkylation of a hydrogen bonding position or formation of an apurinic/apyrimidinic site) will exhibit an equally large unwinding angle in the presence of torsional strain. The electrophoretic determination of unwinding angles described here was originated by Wiesehahn and Hearst (120) and is readily applicable to any radiolabeled chemical which covalently binds to DNA. It would be interesting to determine the unwinding angles of a variety of structurally diverse ultimate carcinogens in both superhelical and covalently closed relaxed DNA. Such a study might extend the limited correlation between unwinding ability and mutagenicity published by Drinkwater et al. (50).

When my unwinding data is combined with the electric linear dichroism and fluorescence studies of Geacintov et al. (151,152), a model for the microenvironment of the major deoxyguanosine adduct emerges. In the absence of superhelical or other strain, the modified G-C base pair is probably disrupted with the attached hydrocarbon residing in the minor or major groove. Orientation of the hydrocarbon within the major groove requires a 180^o rotation of the modified guanine base about its glyco-

sidic linkage. Although data presented in this thesis is consistent with intercalation of BaP diol epoxide prior to covalent reaction, the covalently bound hydrocarbon is not intercalated.

The interaction of BaP diol epoxide with SV40 minichromosomes was described in Chapter 5. Low levels of modification did not detectably alter the structure of the minichromosomes. Relative to naked SV40 DNA alkylation and strand scission of minichromosomal DNA was reduced or enhanced by factors of 1.5 and 2.0, respectively. The reduction in covalent binding was attributed to the presence of histones, which competed with DNA for the hydrocarbon and reduced the probability of BaP diol epoxide intercalation by tightening the helix. The enhancement of strand scission was due to the catalytic effect of histones on the rate of β-elimination at apurinic sites although an altered adduct profile was not excluded. Staphylococcal nuclease digestion indicated that BaP diol epoxide randomly alkylated the minichromosomal DNA. This was in contrast to cellular chromatin where internucleosomal DNA is preferentially modified (98,144,156). Differences in the minichromosomal protein complement were responsible for this altered susceptibility.

With the close of the 1970's we possess a good understanding of the DNA alkylation sites of BaP diol epoxide and their effects on the conformation of the double helix. During the next decade the emphasis of research will switch to the molecular mechanisms by which these aberrant structures alter the normal functioning of DNA. Inactivation of DNA template function (53-56,210) and mutagenesis of DNA (39-43) are two such areas of expanding research. BaP diol epoxide modified DNA exhibits reduced replicational (53-56) and transcriptional (210) activities.

A single hydrocarbon adduct can apparently block chain elongation (53). Yet this same DNA exhibits a high frequency of mutation. The latter event may occur on rare occasions when DNA polymerase bypasses an alkylation site by omitting one or more bases in the daughter strand (frameshift mutation) or by randomly inserting noncomplementary bases (missence mutation). It is also possible that error-prone repair could play a role in this process.

One possible approach to the study of site-directed BaP diol epoxide mutagenesis is suggested by the work of Shortle and Nathans (211). It would utilize the SV40 virus system and take advantage of the localized denaturation induced by BaP diol epoxide adducts in superhelical DNA. Such sites should be resistant to restriction endonucleases and thereby permit the isolation of superhelical DNA molecules containing one BaP diol epoxide adduct at or near a unique single-cut restriction enzyme site. With these molecules one could estimate mutation frequencies as well as investigate the effect of alkylation on eucaryotic gene expression. By proper selection of the restriction enzyme, DNA with a modified site located outside of known gene sequences could be isolated. Mutant clones, resistant to the restriction enzyme, should be recoverable from that DNA. Sequence analysis of the cloned DNA would elucidate the base pair changes associated with forward BaP diol epoxide induced mutation.

References

1. J. Higginson in "Environment and Cancer," 24th Symposium Fundam. Cancer Res. (Williams and Wilkins: Baltimore, 1972), pp. 69-92.
2. B. Pullman in "Polycyclic Hydrocarbons and Cancer," Vol. 2, eds. H. V. Gelboin and P. O. P. Ts'O (Academic Press: New York, 1972), pp. 419-426.
3. P. Brookes and P. D. Lawley, Nature 202, 781-784 (1964).
4. J. McCann and B. N. Ames, Proc. Natl. Acad. Sci. USA 73, 950-954 (1976).
5. E. Huberman, Mutation Res. 29, 285-291 (1975).
6. T. Meehan, K. Straub, and M. Calvin, Nature 269, 725-727 (1977).
7. K. M. Straub, T. Meehan, A. L. Burlingame, and M. Calvin, Proc. Natl. Acad. Sci. USA 74, 5285-5289 (1977).
8. T. Meehan and K. Straub, Nature 277, 410-412 (1979).
9. I. B. Weinstein, A. M. Jeffrey, K. W. Jennette, S. H. Blobstein, R. G. Harvey, C. Harris, H. Autrup, H. Kasai, and K. Nakanishi, Science 193, 592-595 (1976).
10. K. W. Jennette, A. M. Jeffrey, S. H. Blobstein, F. A. Beland, R. G. Harvey, and I. B. Weinstein, Biochemistry 16, 932-938 (1977).
11. A. M. Jeffrey, I. B. Weinstein, K. W. Jennette, K. Grzeskowiak, R. G. Harvey, H. Autrup, and C. Harris, Nature 269, 348-350 (1977).
12. M. Koreeda, P. D. Moore, H. Yagi, H. J. C. Yeh, and D. M. Jerina, J. Am. Chem. Soc. 98, 6720-6722 (1976).
13. J. Remsen, D. Jerina, H. Yagi, and P. Cerutti, Biochem. Biophys. Res. Commun. 74, 934-940 (1977).
14. M. Koreeda, P. D. Moore, P. G. Wislocki, W. Levin, A. H. Conney, H. Yagi, and D. M. Jerina, Science 199, 778-781 (1978).

15. M. R. Osborne, F. A. Beland, R. G. Harvey, and P. Brookes, Int. J. Cancer 18, 362-368 (1976).

16. M. R. Osborne, R. G. Harvey, and P. Brookes, Chem.-Biol. Interactions 20, 123-130 (1978).

17. H. W. S. King, M. R. Osborne, and P. Brookes, Chem.-Biol. Interactions 24, 345-353 (1979).

18. E. J. Baum in "Polycyclic Hydrocarbons and Cancer," Vol. 1, eds. H. V. Gelboin and P. O. P. Ts'O (Academic Press: New York, 1978), pp. 45-70.

19. J. C. Arcos and M. F. Argus, "Chemical Induction of Cancer," Vol. IIA (Academic Press: New York, 1974), pp. 302-337.

20. A. Pullman and B. Pullman, Advan. Cancer Res. 3, 117-169 (1955).

21. J. A. Miller, Cancer Res. 30, 559-576 (1970).

22. P. Sims and P. L. Grover, Advan. Cancer Res. 20, 165-274 (1974).

23. J. R. Gillette, D. C. Davis, and H. Sesame, Ann. Rev. Pharmacol. 12, 47-80 (1972).

24. J. Deutsch, J. C. Leutz, S. K. Yang, H. V. Gelboin, Y. L. Chiang, K. P. Vatsis, and M. J. Coon, Proc. Natl. Acad. Sci. USA 75, 3123-3127 (1978).

25. M. T. Huang, S. B. West, and A. Y. H. Lu, J. Biol. Chem. 251, 4659-4665 (1976).

26. F. Oesch, Xenobiotica 3, 305-340 (1973).

27. N. Nemoto and H. V. Gelboin, Biochem. Pharmacol. 25, 1221-1226 (1976).

28. G. M. Cohen, B. P. Moore, and J. W. Bridges, Biochem. Pharmacol. 26, 551-553 (1977).

29. A. Y. H. Lu, D. Ryan, D. M. Jerina, J. W. Daly, and W. Levin, J. Biol. Chem. 250, 8283-8288 (1975).

30. E. Boyland, Biochem. Soc. Symp. 5, 40 (1950).

31. D. M. Jerina, D. R. Thakker, H. Yagi, W. Levin, A. W. Wood, and A. H. Conney, Pure Appl. Chem. 50, 1033-1044 (1978).

32. Committee on Biologic Effects of Atmospheric Pollutants, "Particulate Polycyclic Organic Matter" (Natl. Acad. Sci., Washington D. C., 1972) p. 30.

33. C. Heidelberger, Ann. Rev. Biochem. 44, 79-121 (1975).

34. K. Vahakangas, D. W. Nebert, and O. Pelkonen, Chem.-Biol. Interactions 24, 167-176 (1979).

35. A. Borgen, H. Darvey, N. Castagnoli, T. T. Crocker, R. E. Rasmussen, and I. Y. Wang, J. Med. Chem. 16, 502-506 (1973).

36. P. Sims, P. L. Grover, A. Swaisland, K. Pal, and A. Hewer, Nature 252, 326-328 (1974).

37. S. K. Yang, D. W. McCourt, P. P. Roller, and H. V. Gelboin, Proc. Natl. Acad. Sci. USA 73, 2594-2598 (1976).

38. J. R. Landolph, J. F. Becker, H. Gamper, J. C. Bartholomew, and M. Calvin, Chem.-Biol. Interactions 23, 331-334 (1978).

39. C. Malaveille, H. Bartsch, P. L. Grover, and P. Sims, Biochem. Biophys. Res. Commun. 66, 693-700 (1975).

40. A. W. Wood, W. Levin, A. Y. H. Lu, H. Yagi, D. Hernandez, D. M. Jerina, and A. H. Conney, J. Biol. Chem. 251, 4882-4890 (1976).

41. E. Huberman, L. Sachs, S. K. Yang, and H. V. Gelboin, Proc. Natl. Acad. Sci. USA 73, 607-611 (1976).

42. R. F. Newbold and P. Brookes, Nature 261, 52-54 (1976).

43. C. Malaveille, T. Kuroki, P. Sims, P. L. Grover, and H. Bartsch, Mutation Res. 44, 313-326 (1977).

44. J. Kapitulnik, W. Levin, A. H. Conney, H. Yagi, and D. M. Jerina, Nature 266, 378-380 (1977).

45. W. Levin, A. W. Wood, H. Yagi, D. M. Jerina, and A. H. Conney, Proc. Natl. Acad. Sci. USA 73, 3867-3871 (1976).

46. H. Marquardt, P. L. Grover, and P. Sims, Cancer Res. 36, 2059-2064 (1976).

47. R. Mager, E. Huberman, S. K. Yang, H. V. Gelboin, and L. Sachs, Int. J. Cancer 19, 814-817 (1977).

48. D. R. Thakker, H. Yagi, A. Y. H. Lu, W. Levin, A. H. Conney, and D. M. Jerina, Proc. Natl. Acad. Sci. USA 73, 3381-3385 (1976).

49. H. B. Gamper, A. S.-C. Tung, K. Straub, J. C. Bartholomew, and M. Calvin, Science 197, 671-674 (1977).

50. N. R. Drinkwater, J. A. Miller, E. C. Miller, and N.-C. Yang, Cancer Res. 38, 3247-3255 (1978).

51. B. Jernstrom, S. Orrenius, O. Undeman, A. Graslund, and A. Ehrenberg, Cancer Res. 38, 2600-2607 (1978).

52. D. Sagher, R. G. Harvey, W.-T. Hsu, and S. B. Weiss, Proc. Natl. Acad. Sci. USA 76, 620-624 (1979).

53. W.-T. Hsu, E. J. S. Lin, R. G. Harvey, and S. B. Weiss, Proc. Natl. Acad. Sci. USA 74, 3335-3339 (1977).

54. I. Yamaura, H. Marquardt, and L. F. Cavaliere, Chem.-Biol. Interactions 23, 399-407 (1978).

55. P. Moore and B. S. Strauss, Nature 278, 664-666 (1979).

56. H. Mizusawa and T. Kakefuda, Nature 279, 75-78 (1979).

57. J. Tooze ed., "The Molecular Biology of Tumour Viruses" (Cold Spring Harbor Laboratory, Cold Spring Harbor, N. Y., 1973) pp. 269-419.

58. B. Hirt, J. Mol. Biol. 26, 365-369 (1967).

59. M. H. Green, H. I. Miller, and S. Hendler, Proc. Natl. Acad. Sci. USA 68, 1032-1036 (1971).

60. W. Fiers, R. Contreras, G. Haegeman, R. Rogiers, A. Van de Voorde, M. Van Heuverswyn, J. Van Herrewegle, G. Volckaert, and M. Ysebaert, Nature 273, 113-119 (1978).

61. V. B. Reddy, B. Thimmappaya, R. Dhar, K. N. Subramanian, S. Zain, J. Pan, P. K. Ghosh, M. L. Celma, and S. M. Weissman, Science 200, 494-502 (1978).

62. U. Muller, H. Zentgraft, I. Eicken, and W. Keller, Science 201, 406-415 (1978).

63. A. R. Peacocke and I. O. Walker, J. Mol. Biol. 5, 550-559 (1962).

64. W. Meinke, M. R. Hall, and D. A. Goldstein, J. Virol. 15, 439-448 (1975).

65. J. D. Griffith, Science 187, 1202-1203 (1975).

66. A. J. Varshavsky, V. V. Bakayev, P. M. Chumackov, and G. P. Georgiev, Nucleic Acids Res. 3, 2101-2113 (1976).

67. R. T. Su and M. L. DePamphilis, Proc. Natl. Acad. Sci. USA 73, 3466-3470 (1976).

68. O. Warburg and W. Christian, Biochem. Z. 310, 384-421 (1942).

69. D. J. McCaustland and J. F. Engel, Tet. Lett. 30, 2549-2552 (1975).

70. D. J. McCaustland, D. L. Fischer, W. P. Duncan, E. J. Ogilvie, and J. F. Engel, J. Lab. Comp. and Radiopharm. 12, 583-589 (1976).

71. R. W. Davis, M. Simon, and N. Davidson, Methods Enzymol. 21, 413-428 (1971).

72. A. K. Kleinschmidt, Methods Enzymol. 12B, 361-377 (1968).

73. F. W. Studier, J. Mol. Biol. 79, 237-248 (1973).

74. J. E. Germond, B. Hirt, P. Oudet, M. Gross-Bellard, and P. Chambon, Proc. Natl. Acad. Sci. USA 72, 1843-1847 (1975).

75. A. C. Peacock and C. W. Dingman, Biochemistry 7, 668-674 (1968).

76. D. Z. Staynov, J. C. Pinder, and W. B. Gratzer, Nature New Biol. 235, 108-110 (1972).

77. G. K. McMaster and G. G. Carmichael, Proc. Natl. Acad. Sci. USA 74, 4835-4838 (1977).

78. G. Christiansen and J. Griffith, Nucleic Acids Res. 4, 1837-1851 (1977).

79. U. Kuhnlein, E. E. Penhoet, and S. Linn, Proc. Natl. Acad. Sci. USA 73, 1169-1173 (1976).

80. K. M. Kirtikar, G. R. Cathcart, and D. A. Goldthwait, Proc. Natl. Acad. Sci. USA 73, 4324-4328 (1976).

81. S. L. Ross and R. E. Moses, Biochemistry 17, 581-586 (1978).

82. G. Zweig and J. Sherma eds., "CRC Handbook of Chromatography" (CRC Press, Cleveland, Ohio, 1972) p. 162.

83. L. F. Povirk, W. Wubker, W. Kohnlein, and F. Hutchinson, Nucleic Acids Res. 4, 3573-3580 (1977).

84. V. Ivanovic, N. E. Geacintov, and I. B. Weinstein, Biochem. Biophys. Res. Commun. 70, 1172-1179 (1976).

85. H.-J. Rhaese and E. Freese, Biochim. Biophys. Acta 190, 418-433 (1969).

86. B. Singer, Progr. Nucl. Acids Res. Molec. Biol. 15, 219-284 (1975).

87. B. Singer, Nature 264, 333-339 (1976).

88. T. Lindahl and A. Andersson, Biochemistry 11, 3618-3623 (1972).

89. K. V. Shooter, Chem.-Biol. Interactions 11, 575-588 (1975).

90. P. Bannon and W. Verly, Eur. J. Biochem. 31, 103-111 (1972).

91. K. V. Shooter, Chem.-Biol. Interactions 13, 151-163 (1976).

92. K. V. Shooter and R. K. Merrifield, Chem.-Biol. Interactions 13, 223-236 (1976).

93. S. Walles and L. Ehrenberg, Acta Chem. Scand. 22, 2727-2729 (1968).

94. K. V. Shooter, R. Howse, S. A. Shah, and P. D. Lawley, Biochem. J. 137, 303-312 (1974).

95. K. V. Shooter, R. Howse, and R. K. Merrifield, Biochem. J. 137, 313-317 (1974).

96. D. M. Brown, D. I. Magrath, A. R. Todd, J. Chem. Soc., 4396-4401 (1955).

97. K. V. Shooter, M. R. Osborne, and R. G. Harvey, Chem.-Biol. Interactions 19, 215-223 (1977).

98. A. Kootstra, T. J. Slaga, and D. E. Olins, "Studies on the Binding of BaP Diol Epoxide to DNA and Chromatin," in 3rd International Symposium on Polycyclic Aromatic Hydrocarbons (Oct. 1978) In press.

99. W. Dove and N. Davidson, J. Mol. Biol. 5, 467-478 (1962).

100. E. Kriek and P. Emmelot, Biochemistry 2, 733-740 (1963).

101. S. Rajalakshmi, P. M. Rao, and D. S. R. Sarma, Biochem. Biophys. Res. Commun. 81, 936-940 (1978).

102. J. E. Hyde and J. E. Hearst, Biochemistry 17, 1251-1257 (1978).

103. A. Eastman, J. Sweetenham, and E. Bresnick, Chem.-Biol. Interactions 23, 345-353 (1978).

104. M. Riley, B. Maling, and M. J. Chamberlin, J. Mol. Biol. 20, 359-389 (1966).

105. G. D. Fasman, C. Lindblow, and L. Grossman, Biochemistry 3, 1015-1021 (1964).

106. M. J. Chamberlin and D. L. Patterson, J. Mol. Biol. 12, 410-428 (1965).

107. S. B. Zimmerman, G. H. Cohen, and D. R. Davies, J. Mol. Biol. 92, 181-192 (1975).

108. J. Vinograd, J. Lebowitz, and R. Watson, J. Mol. Biol. 33, 173-197 (1968).

109. D. Glaubiger and J. E. Hearst, Biopolymers 5, 691-696 (1967).

110. D. R. Davies and R. L. Baldwin, J. Mol. Biol. 6, 251-255 (1963).

111. W. Keller, Proc. Natl. Acad. Sci. USA 72, 4876-4880 (1975).

112. M. Shure and J. Vinograd, Cell 8, 215-226 (1976).

113. L. S. Lerman, V. Luzzati, and F. Mason, J. Mol. Biol. 3, 634-639 (1961).

114. C. Tsai, S. C. Jain, and H. M. Sobell, J. Mol. Biol. 114, 301-315 (1977).

115. S. C. Jain, C. Tsai, and H. M. Sobell, J. Mol. Biol. 114, 317-331 (1977).

116. S. Neidel, A. Achari, G. L. Taylor, H. M. Berman, H. L. Carrol, J. P. Glusker, and W. C. Stallings, Nature 269, 304-307 (1977).

117. T. D. Sakore, S. C. Jain, C. Tsai, and H. Sobell, Proc. Natl. Acad. Sci. USA 74, 188-192 (1977).

118. H. Sobell and S. C. Jain, J. Mol. Biol. 68, 21-34 (1972).

119. N. E. Geacintov, T. Prusik, and J. M. Khosrofian, J. Am. Chem. Soc. 98, 6444-6452 (1976).

120. G. Wiesehahn and J. E. Hearst, Proc. Natl. Acad. Sci. USA 75, 2703-2707 (1978).

121. M. Waring, J. Mol. Biol. 54, 247-279 (1970).

122. L. F. Povirk, M. Hogan, and N. Dattagupta, Biochemistry 18, 96-101 (1979).

123. J. C. Wang, J. Mol. Biol. 89, 783-801 (1974).

124. C. C. Tsai, S. C. Jain, H. M. Sobell, Proc. Natl. Acad. Sci. USA 72, 628-632 (1975).

125. M. Hogan, N. Dattagupta, and D. M. Crothers, Biochemistry 18, 280-288 (1979).

126. L. V. Crawford and M. J. Waring, J. Mol. Biol. 25, 23-30 (1967).

127. H. M. Sobell, C. C. Tsai, S. C. Jain, and S. G. Gilbert, J. Mol. Biol. 114, 333-365 (1977).

128. M. Levitt, Proc. Natl. Acad. Sci. USA 75, 640-644 (1978).

129. W. Dean and J. Lebowitz, Nature New Biol. 231, 5-8 (1971).

130. J. Lebowitz, A. K. Chaudhuri, A. Gonenne, and G. Kitos, Nucleic Acids Res. 4, 1695-1711 (1977).

131. G. L. Cohen, W. R. Bauer, J. K. Barton, and S. J. Lippard, Science 203, 1014-1016 (1979).

132. A. F. Levine, L. M. Fink, I. B. Weinstein, and D. Grunberger, Cancer Res. 34, 319-327 (1974).

133. M. J. Waring and S. M. Henley, Nucleic Acids Res. 2, 567-586 (1975).

134. F. Pochon and A. M. Michelson, Biochim. Biophys. Acta 182, 17-23 (1969).

135. M. Ikehara and M. Hattori, Biochemistry 10, 3585-3590 (1971).

136. L. Mengle, H. Gamper, and J. Bartholomew, Cancer Letters 5, 131-137 (1978).

137. T. Hsieh and J. C. Wang, Biochemistry 14, 527-535 (1975).

138. J.-M. Saucier and J. C. Wang, Biochemistry 12, 2755-2758 (1973).

139. H. Boedtker, J. Mol. Biol. 2, 171-188 (1960).

140. F. Traganos, Z. Darzynkiewicz, T. Sharpless, and M. E. Melamed, J. Histochem. Cytochem. 25, 46-56 (1977).

141. P. Pulkrabek, S. Leffler, I. B. Weinstein, and D. Grunberger, Biochemistry 16, 3127-3132 (1977).

142. R. H. Heflich, D. J. Dorney, V. M. Maher, and J. J. McCormick, Biochem. Biophys. Res. Commun. 77, 634-641 (1977).

143. T. Kakefuda and H. Yamamoto, Proc. Natl. Acad. Sci. USA 75, 415-419 (1978).

144. H. Yamasaki, T. W. Roush, and I. B. Weinstein, Chem.-Biol. Interactions 23, 201-213 (1978).

145. F. Frenkel, D. Grunberger, M. Boublik, and I. B. Weinstein, Biochemistry 17, 1278-1282 (1978).

146. R. Fuchs and M. Daune, Biochemistry 11, 2659-2666 (1972).

147. R. P. P. Fuchs and M. P. Daune, Biochemistry 13, 4435-4440 (1974).

148. R. P. P. Fuchs, Nature 257, 151-152 (1975).

149. R. P. P. Fuchs, J.-F. Lefevre, J. Pouyet, and M. P. Daune, Biochemistry 15, 3347-3351 (1976).

150. I. B. Weinstein, A. M. Jeffrey, S. Leffler, P. Pulkrabek, H. Yamasaki, and D. Grunberger in "Polycyclic Hydrocarbons and Cancer," Vol. 2, eds. H. V. Gelboin and P. O. P. Ts'O (Academic Press: New York, 1978), pp. 3-36.

183. A. J. Varshavsky, S. A. Nedospasov, V. V. Schmatchenko, V. V. Bakayev, P. M. Chumackov, and G. P. Georgiev, Nucleic Acids Res. 4, 3303-3325 (1977).

184. R. S. Lake, S. Barban, and N. P. Salzman, Biochem. Biophys. Res. Commun. 54, 640-647 (1973).

185. D. M. Pett, M. K. Estes, and J. S. Pagano, J. Virol. 15, 379-385 (1975).

186. R. Fernandez-Munoz, M. Coca-Prados, and M.-T. Hsu, J. Virol. 29, 612-623 (1979).

187. F. Thoma and T. Koller, Cell 12, 101-107 (1977).

188. Y. Tsubota, M. A. Waqar, J. F. Burke, B. I. Milavetz, M. J. Evans, D. Kowalski, and J. A. Huberman, "Association of Enzymes with Replicating and Nonreplicating SV40 Chromosomes," in XLIII Cold Spring Harbor Symposium on Quantitative Biology (1978) In press.

189. M. Persico-DiLauro, R. G. Martin, and D. M. Livingston, J. Virol. 24, 451-460 (1977).

190. J. M. Morrison, H. M. Keir, H. Sulak-Sharpe, and L. V. Crawford, J. Gen. Virol. 1, 101-108 (1967).

191. P. H. Black, E. M. Crawford, and L. V. Crawford, Virol. 24, 381-387 (1964).

192. B. A. J. Ponder, F. Crew, and L. V. Crawford, J. Virol. 25, 175-186 (1978).

193. R. S. Lloyd, C. W. Haidle, and R. R. Hewitt, Cancer Res. 38, 3191-3196 (1978).

194. J. P. Whitlock, Jr. in "Polycyclic Hydrocarbons and Cancer," Vol. 2, eds. H. V. Gelboin and P. O. P. Ts'O (Academic Press: New York, 1978), pp. 75-96.

195. M. Noll, Nucleic Acids Res. 1, 1573-1578 (1974).

196. R. Axel, Biochemistry 14, 2921-2925 (1975).

197. R. Ramanathan, S. Rajalakshmi, and D. S. R. Sarma, Chem.-Biol. Interactions 14, 375-377 (1976).

198. G. Metzger, F. X. Wilhelm, and M. L. Wilhelm, Chem.-Biol. Interactions 15, 257-265 (1976).

199. R. Ramanathan, S. Rajalakshmi, D. S. R. Sarma, and E. Farber, Cancer Res. 36, 2073-2079 (1976).

200. G. Metzger, F. X. Wilhelm, and M. L. Wilhelm, Biochem. Biophys. Res. Commun. 75, 703-710 (1977).

201. C. L. Jahn and G. W. Litman, Biochem. Biophys. Res. Commun. 76, 534-540 (1977).

202. K. D. Tew, S. Sudhakar, P. S. Schein, and M. E. Smulson, Cancer Res. 38, 3371-3378 (1978).

203. S. Sudhakar, K. D. Tew, P. S. Schein, P. V. Woolley, and M. E. Smulson, Cancer Res. 39, 1411-1417 (1979).

204. W. K. Roberts, C. A. Dekker, G. W. Rushizky, and C. A. Knight, Biochim. Biophys. Acta 55, 664-673 (1962).

205. R. T. Simpson, Cell 13, 691-699 (1978).

206. B. S. Schaffhausen and T. L. Benjamin, Proc. Natl. Acad. Sci. USA 73, 1092-1096 (1976).

207. A. Chester and M. Yaniv, Proc. Natl. Acad. Sci. USA 76, 46-50 (1979).

208. H. Weintraub and M. Groudine, Science 193, 848-856 (1976).

209. J.-J. Lawrence and M. Daune, Biochemistry 15, 3301-3307 (1976).

210. S. Leffler, P. Pulkrabek, D. Grunberger, and I. B. Weinstein, Biochemistry 16, 3133-3136 (1977).

211. D. Shortle and D. Nathans, Proc. Natl. Acad. Sci. USA 75, 2170-2174 (1978).